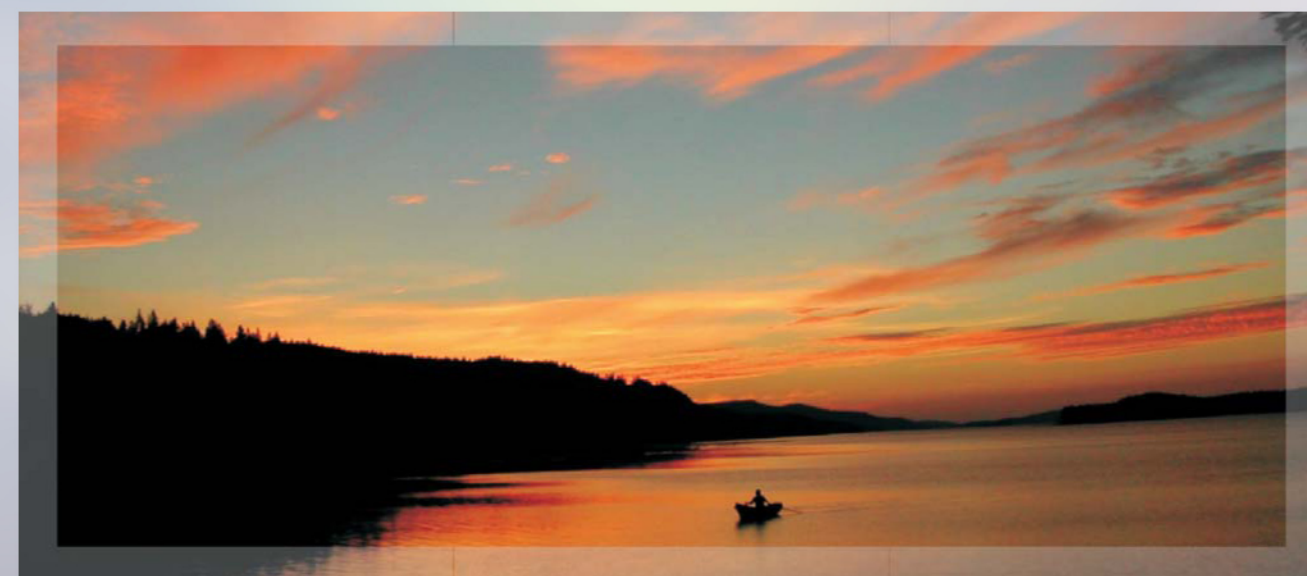


# Proceedings



## Seventh International Workshop **Nanocarbon Photonics and Optoelectronics**

6 - 11 August 2018, Spa Hotel Casino,  
Savonlinna, Finland



University of Eastern Finland  
Institute of Photonics

# Proceedings

## Seventh International Workshop Nanocarbon Photonics and Optoelectronics

Spa Hotel Casino, Savonlinna, Finland

Editors:  
Esko Kauppinen  
Alexander Obraztsov  
Yuri Svirko

Joensuu, Finland

2018



## NPO2018 Schedule-at-a-Glance

		Monday August 6	Tuesday August 7	Wednesday August 8	Thursday August 9	Friday August 10	Saturday August 11
			Graphene & 2D materials	Photonics & Optoelectronics	Photonics & Optoelectronics	Synthesis & Applications	DEPARTURE
09:	00-15		Opening	Eugenius Ivchenko	Feodor Jelezko	Jin Zhang	
	15-30		Kaustav Banerjee				
	30-45						
	45-00						
10:	00-15		Emmanuel Flahaut	Olivia Pulci	Angela Vella	Simone Taioli	
	15-30			Timofei Eremin	Sergey Malykhin	Olga Sedelnikova	
10:30-11:00			Coffee Break				
11:	00-15		Lei Shi	Ping-Heng Tan	Dong-Min Sun	Polina Kuzhir	
	15-30						
	30-45		Tomas Wood	Kimmo Mustanen	Yutaka Ohno	Harri Lipsanen	
	45-00						
12:	00-15		Xiaoxia Yang	Fei Wei	Valentina Eremina	Tommi Kaplas	
	15-30		Yunyun Dai		Nan Wei		
12:30-14:30			Lunch				
14:	30-45	ARRIVAL	Mikhail Portnoi	Shinji Yamashita	Yuichiro Kato	Kaihui Liu	
	45-00						
15:	00-15		Sergey Tarasenko	Zhipei Sun	Qing Dai	Hua Jiang	
	15-30						
	30-45		Wei-Tao Liu	Shi-Wei Wu	Yutaka Matsuo	Simona Moldovan	
	45-00					Yuriy Gladush	
16:00-16:30			Coffee Break				
16:	30-45		Young Hee Lee	Shigeo Maruyama	Albert Nasibulin	Alexander Okotrub	
	45-00						
17:	00-15		Mikhail Glazov	Yan Li	Andreas Johansson	Lubov Bulusheva	
	15-30						
	30-45		Nathalie Arutyunyan	Marina Avramenko	Junji Yumoto	Mohammad Tavakkoli	
	45-00						
18:00-19:30			Dinner		Dinner	Dinner	NPO reception
19:30-22:00				Welcome Dinner	Poster Session I	Poster Session II	and Saimaa sunset steam boat cruise

## Workshop Co-Chairs

Esko Kauppinen, Aalto University, Finland

Alexander Obraztsov, M.V. Lomonosov Moscow State University, Russia

Yuri Svirko, University of Eastern Finland, Finland

## Program Committee

Esko Kauppinen, Aalto University, Finland

Alexander Obraztsov, M.V. Lomonosov Moscow State University, Russia

Elena Obraztsova, A. M. Prokhorov General Physics Institute, Russia

Yuri Svirko, University of Eastern Finland, Finland

## Organizing Committee

Hannele Karppinen, University of Eastern Finland, Finland

Dmitry Lyashenko, Texas State University, USA

Yuri Svirko, University of Eastern Finland, Finland

## NPO2018 Sponsor Organisations



## Welcome to NPO2018

We are pleased to welcome you to the 7<sup>th</sup> International Workshop on Nanocarbon Photonics and Optoelectronics (NPO2018) that continues a series of meetings organized by the University of Eastern Finland in collaboration with the Aalto University. Since 2008, NPO Workshops bring together research leaders from both academia and industry to discuss the latest achievements in this rapidly developing area of modern physics and nanotechnology, with strong focus on new carbon nanomaterials. The Workshops are also of strong educational importance allowing young researchers and students to attend lectures given by senior scientists and to be involved in intensive ideas exchange and networking. We hope that you will enjoy both scientific and social program of NPO2018.

The NPO2018 has attracted about one hundred researchers and students from around the globe. The Proceedings of the Workshop will be published in the special issue of *Physica Status Solidi B*.

We are grateful to our sponsors for their financial backing, which has allowed us to reduce participation fee and to support our lecturers and students. The Workshop venue is at the Best Western Spa Hotel Casino in Savonlinna, Finland, offering magnificent scenery. We hope that the NPO2018 will expand on the success of previous Workshops and will provide its participants with the opportunity to enjoy the beauty of Finnish Lakeland.

Esko Kauppinen

Alexander Obraztsov

Yuri Svirko

*NPO2018 Co-Chairs*

# Contents

<b>Tuesday, August 7</b>	<b>1</b>
9:15-10:00 <b>2D materials for smart life</b>	
Kaustav Banerjee, <i>Department of Electrical and Computer Engineering, University of California, Santa Barbara, CA, USA</i> . . . . .	3
10:00-10:30 <b>Safety of carbon nanomaterials towards the environment</b>	
E. Flahaut <sup>1</sup> , F. Mouchet <sup>1</sup> , C. Line <sup>1,2</sup> , M. Garacci <sup>2</sup> , L. Lagier <sup>2</sup> , L. Evariste <sup>2</sup> , A. Mottier <sup>2</sup> , C. Sarrieu <sup>1</sup> , A-M. Galibert <sup>1</sup> , L. Verneuil <sup>2</sup> , C. Matei Ghimbeu <sup>3</sup> , C. Larue <sup>2</sup> , E. Pinelli <sup>2</sup> , L. Gauthier <sup>2</sup> , <sup>1</sup> <i>CIRIMAT, Université de Toulouse, UMR CNRS-UPS-INP N°5085, Toulouse, France</i> , <sup>2</sup> <i>EcoLab, Université de Toulouse, UMR CNRS-UPS-INP N°5245, Toulouse, France</i> <sup>3</sup> <i>IS2M, Université de Haute Alsace, UMR CNRS-UHA N°7360, Mulhouse, France</i> . . . . .	4
10:30-11:00 <b>Dynamical tuning of graphene plasmonic resonances by ultraviolet illuminations</b>	
Yunyun Dai, Yuyu Xia, Tao Jiang, Ang Chen, Yiwen Zhang, Yujie Bai, Fang Guan, Shiwei Wu, Xiaohan Liu, Lei Shi and Jian Zi, <i>Department of Physics, Key Laboratory of Micro- and Nano-Photonic Structures (Ministry of Education), and State Key Laboratory of Surface Physics, Fudan University, Shanghai 200433, China</i> . . . . .	5
11:30-12:00 <b>Towards optical modulators based on graphene surface plasmons</b>	
T. Wood, M. Kemiche, J. Lhuillier, P. Demongodin, S. Callard, B. Vilquin, P. Rojo-Romeo, C. Monat, <i>University of Lyon, Institut des Nanotechnologies de Lyon, Ecole Centrale de Lyon / INSA de Lyon</i> . . . . .	6
12:00-12:15 <b>Surface-enhanced infrared spectroscopy with graphene plasmon</b>	
Xiaoxia Yang, Hai Hu, Xiangdong Guo, Qing Dai, <i>Division of Nanophotonics, National Center for Nanoscience and Technology, Beijing, China</i> . . . . .	7
12:15-12:30 <b>Systematical investigation of two orthogonal plasmonic modes of graphene ellipse array</b>	
Yuyu Xia <sup>1</sup> , Yunyun Dai <sup>1,2</sup> , Ang Chen <sup>1</sup> , Yanbin Zhang <sup>1</sup> , Bo Wang <sup>1</sup> , Yiwen Zhang <sup>1</sup> , Fang Guan <sup>1</sup> , Xiaohan Liu <sup>1</sup> , Lei Shi <sup>1</sup> and Jian Zi <sup>1</sup> , <sup>1</sup> <i>Department of Physics, Key Laboratory of Micro- and Nano-Photonic Structures (Ministry of Education), and State Key Laboratory of Surface Physics, Fudan University, Shanghai 200433, China</i> , <sup>2</sup> <i>Department of Electronics and Nano-engineering, School of Electric Engineering, Aalto University, FI-00076 Aalto, Finland</i> . . . . .	8
14:30-15:00 <b>Zero-energy vortices in graphene</b>	
C. A. Downing <sup>1</sup> and M. E. Portnoi <sup>2,3</sup> , <sup>1</sup> <i>Departamento de Física Teórica de la Materia Condensada, Universidad Autónoma de Madrid, 28049 Madrid, Spain</i> , <sup>2</sup> <i>School of Physics, University of Exeter, Stocker Road, Exeter EX4 4QL, United Kingdom</i> , <sup>3</sup> <i>ITMO University, St. Petersburg 197101, Russia</i> . . . . .	9
15:00-15:30 <b>Topological edge photocurrents in graphene in the quantum Hall effect regime</b>	
S.A. Tarasenko <sup>1</sup> , M.V. Durnev <sup>1</sup> , H. Plank <sup>2</sup> , and S.D. Ganichev <sup>2</sup> , <sup>1</sup> <i>Ioffe Institute, 194021 St. Petersburg, Russia</i> , <sup>2</sup> <i>University of Regensburg, Terahertz Center, 93040 Regensburg, Germany</i> . . . . .	10
15:30-16:00 <b>SHG studies on surface states of 3D topological insulators and TMDCs</b>	
Wei-Tao Liu, <i>Department of Physics, Fudan University, Shanghai, China</i> . . . . .	11
16:30-17:15 <b>Femtosecond dynamics of exciton and structure in 2H-MoTe<sub>2</sub></b>	
Ji-Hee Kim and Young Hee Lee, <i>Center for Integrated Nanostructure Physics, Institute for Basic Science (IBS), Sungkyunkwan University, Suwon 16419, South Korea</i> . . . . .	12
17:15-17:45 <b>Nonlinear optics and transport of excitons in two-dimensional crystals</b>	
M.M. Glazov, <i>Ioffe Institute, 194021, St.-Petersburg, Russia</i> . . . . .	13

17:45-18:00	<b>Tuning of optical gap in layered gallium selenide</b> N. R. Arutyunyan <sup>1</sup> , E. A. Obraztsova <sup>2</sup> , D. V. Rybkovsky <sup>1,3</sup> , E. D. Obraztsova <sup>1</sup> , <sup>1</sup> A. M. Prokhorov General Physics Institute, Russian Academy of Sciences, 38 Vavilov Street, Moscow, 119991, Russia, <sup>2</sup> M.M. Shemyakin and Yu.A. Ovchinnikov Institute of Bioorganic Chemistry RAS, Miklukho Maklaya st. 16/10, Moscow 117997, Russia, <sup>3</sup> Skolkovo Institute of Science and Technology (Skoltech), Nobelya Ulitsa 3, Moscow 121205, Russia . . . . .	14
<b>Wednesday, August 8</b>		<b>15</b>
9:00-9:45	<b>Photocurrents in Weyl semimetals of gyrotropic classes</b> E.L. Ivchenko, <i>Ioffe Institute of RAS, 26 Politekhnikeskaya, 194021 Saint-Petersburg, Russia</i>	17
9:45-10:15	<b>Validity of Dirac and Weyl fermion picture for Cd<sub>3</sub>As<sub>2</sub> and transition metal monpnictides</b> O. Pulci <sup>1</sup> , D. Grassano <sup>1</sup> , A. Mosca Conte <sup>2</sup> , F. Bechstedt <sup>3</sup> , <sup>1</sup> Universita di Roma Tor Vergata, Via della Ricerca Scientifica 1, 00133 Rome, Italy, <sup>2</sup> Mediterranean Institute of Fundamental Physics, Via Appia Nuova, Marino, Italy, <sup>3</sup> Friedrich-Schiller-Universitat, Max-Wien-Platz 1, 07743 Jena, Germany . . . . .	18
10:15-10:30	<b>Multi-particle excitations in doped single-walled carbon nanotubes</b> T.V. Eremin <sup>1,2,5</sup> , P.A. Obraztsov <sup>2,3</sup> , V.A. Velikanov <sup>2,4</sup> , T.V. Shubina <sup>2</sup> , E.D. Obraztsova <sup>2</sup> , <sup>1</sup> Faculty of Physics of M.V. Lomonosov Moscow State University, Leninskie Gory Str. 1, 119991 Moscow, Russia, <sup>2</sup> A.M. Prokhorov General Physics Institute, RAS, 38 Vavilov street, 119991, Moscow, Russia, <sup>3</sup> Department of Physics and Mathematics, University of Eastern Finland, Joensuu, Finland, <sup>4</sup> National Research Nuclear University, Moscow Engineering Physics Institute, 31 Kashirskoe Highway, 115409 Moscow, Russia, <sup>5</sup> Ioffe institute, RAS, Politechnicheskaya street, 26, 194021 St Petersburg, Russia . . . . .	19
11:00-11:30	<b>Raman spectroscopy of two-dimensional materials and related heterostructures</b> Ping-Heng Tan <sup>1,2</sup> , <sup>1</sup> State Key Laboratory of Superlattices and Microstructures, Institute of Semiconductors, Chinese Academy of Sciences, Beijing 100083, China, <sup>2</sup> CAS Center of Excellence in Topological Quantum Computation, and College of Materials Science and Opto-Electronic Technology, University of Chinese Academy of Science, Beijing 100049, China. . . . .	20
11:30-12:00	<b>All-carbon mixed-dimensional van der Waals heterostructures: diffusion and atomic scale deformations</b> Kimmo Mustonen <sup>1</sup> , Aqeel Hussain <sup>2</sup> , Rasim Mirzayev <sup>1</sup> , Christoph Hofer <sup>1</sup> , Mohammad Monazam <sup>1</sup> , Toma Susi <sup>1</sup> , Esko I. Kauppinen <sup>2</sup> , Jani Kotakoski <sup>1</sup> and Jannik C. Meyer <sup>1</sup> , <sup>1</sup> Faculty of Physics, University of Vienna, Boltzmanngasse 5, A-1090 Vienna, Austria, <sup>2</sup> Department of Applied Physics, Aalto University School of Science, P.O. Box 15100, FI-00076 Aalto, Finland . . . . .	21
12:00-12:30	<b>Single-carbon-nanotube manipulations and devices based on macroscale flakes</b> Boyuan Shen, Yunxiang Bai, Zhenxing Zhu, Jinyan Zhang, Huanhuan Xie and Fei Wei, <i>Beijing Key Laboratory of Green Chemical Reaction Engineering and Technology and Department of Chemical Engineering, Tsinghua University, Beijing 100084, China</i> . . . . .	22
14:30-15:00	<b>Nanocarbon materials for short-pulse fiber lasers and photonic devices</b> Shinji Yamashita, <i>Research Center for Advanced Science and Technology, The University of Tokyo, 4-6-1, Komaba, Meguro-ku, Tokyo, 153-8904, Japan</i> . . . . .	23
15:00-15:30	<b>Nonlinear optics with low-dimensional materials</b> Zhipei Sun <sup>1,2</sup> , <sup>1</sup> Department of Electronics and Nanoengineering, Aalto University, Tietotie 3, FI-02150, Finland <sup>2</sup> QTF Centre of Excellence, Department of Applied Physics, Aalto University, FI-00076 Aalto, Finland . . . . .	24
15:30-16:00	<b>Tunable nonlinear optical response from 2D materials</b> Shiwei Wu, <i>Fudan University, Shanghai 200433, China</i> . . . . .	25
16:30-17:15	<b>Synthesis and properties of SWCNT@FWBNNT – Single-walled carbon nanotubes co-axially wrapped with mono- and few-layer boron nitride nanotubes –</b> Rong Xiang <sup>1</sup> , Taiki Inoue <sup>1</sup> , Yongjia Zheng <sup>1</sup> , Ming Liu <sup>1</sup> , Jia Guo <sup>1,2</sup> , Yan Li <sup>1,2</sup> , Shohei Chiashi <sup>1</sup> , Shigeo Maruyama <sup>1,3</sup> , <sup>1</sup> Departure of Mechanical Engineering, The University of Tokyo, Tokyo 113-8656, Japan, <sup>2</sup> College of Chemistry and Molecular Engineering, Peking University, Beijing 100871, China, <sup>3</sup> Energy Nano Engineering Lab., National Institute of Advanced Industrial Science and Technology (AIST), Ibaraki 305-8564, Japan . . . . .	26



17:15-17:45	<b>Surface-enhanced Raman detection of individual single-walled carbon nanotubes and single molecules inside</b> Juan Yang, Daqi Zhang, Chenmaya Xia, Yan Li, <i>College of Chemistry and Molecular Engineering, Peking University, Beijing 100871, China</i> . . . . .	27
17:45-18:00	<b>Experimental evidence of electronic Raman scattering in individual double-walled carbon nanotubes</b> D. I. Levshov <sup>1</sup> , M. V. Avramenko <sup>1</sup> , J.-L. Sauvajol <sup>2</sup> , M. Paillet <sup>2</sup> , <sup>1</sup> <i>Department of Nanotechnology, Faculty of Physics, Southern Federal University, Rostov-on-Don, 5 Zorge Str., 344090, Russia</i> , <sup>2</sup> <i>Laboratoire Charles Coulomb, University of Montpellier, Montpellier, France</i> . . . . .	28
<b>Poster session I</b>		<b>29</b>
PI.1	<b>Geometry-controllable nanohair structure effects cellular movement</b> Chaejeong Heo <sup>1,2</sup> , Chanho Jeong <sup>3</sup> , Hyeon Seong Im <sup>3</sup> , and Tae-il Kim <sup>3</sup> , <sup>1</sup> <i>Center for Integrated Nanostructure Physics (CINAP), Institute for Basic Science (IBS), Suwon 16419, Republic of Korea</i> , <sup>2</sup> <i>Sungkyunkwan University (SKKU), Suwon, Korea</i> , <sup>3</sup> <i>School of Chemical Engineering, Sungkyunkwan University (SKKU), Suwon 16419, Republic of Korea</i> . . . . .	31
PI.2	<b>Pristine and platinum-deposited metallic molybdenum ditelluride for hydrogen evolution reaction</b> Jinbong Seok <sup>1,2</sup> , Jun-Ho Lee <sup>3</sup> , Byungdo Ji <sup>1</sup> , Young-Woo Son <sup>3</sup> , Suyeon Cho <sup>4</sup> and Young Hee Lee <sup>1,2</sup> , Heejun Yang <sup>1</sup> , <sup>1</sup> <i>Department of Energy Science, Sungkyunkwan University, Suwon 16419, Korea</i> , <sup>2</sup> <i>IBS Center for Integrated Nanostructure Physics (CINAP), Institute for Basic Science, Sungkyunkwan University, Suwon 16419, Korea</i> , <sup>3</sup> <i>Korea Institute for Advanced Study, Seoul 02455, Korea</i> , <sup>4</sup> <i>Division of Chemical Engineering and Materials Science, Ewha Womans University, Seoul 03760, Korea</i> . . . . .	32
PI.3	<b>Carbon nanotube film flexible terahertz detectors on polymer films with series electrodes for sensitivity enhancement</b> K. Li, D. Suzuki, Y. Ochiai, M. Sun, and Y. Kawano, <i>Labratory for Future Interdisciplinary Research of Science and Technology, Tokyo Institute of Technology, 2-12-1, Ookayama, Meguro-ku, Tokyo 152-8550, Japan</i> . . . . .	33
PI.4	<b>Terahertz absorption and emission tuning in graphene sandwich structures</b> Konstantin Batrakov <sup>1,2</sup> and Polina Kuzhir <sup>1,2</sup> , <sup>1</sup> <i>Institute for Nuclear Problems BSU, Minsk, Belarus</i> , <sup>2</sup> <i>Tomsk State University (TSU), Tomsk, Russia</i> . . . . .	34
PI.5	<b>Gigahertz repetition rate dual-wavelength mode-locking of waveguide lasers with graphene</b> M.V. Ponarina, A.G. Okhrimchuk, M.G. Rybin, A.A. Tarakanovsky, T.V. Dolmatov, V.V. Bukin, I.V. Zhluktova, V.A. Kamynin, P.A. Obratsov, A.M. Prokhorov <i>General Physics Institute, RAS, 119991, Moscow, Russia</i> . . . . .	35
PI.6	<b>Raman spectra of nitrogen- and boron-doped carbon dots</b> A. E. Tomskaya, M. N. Egorova, S. A. Smagulova, <i>North-Eastern Federal University, Yakutsk, Russia</i> . . . . .	36
PI.7	<b>Influence of electrochemical hydrogenation on the surface photocurrent in the Ag/Pd nanocomposite</b> A. S. Saushin, R. G. Zonov, V. M. Styapshin, E. V. Alexandrovich, G. M. Mikheev, <i>Institute of Mechanics, Udmurt Federal Research Center of the UB RAS, Izhevsk, Russia 426067</i> . . . . .	37
PI.8	<b>Bipolar polarization-sensitive surface photocurrent pulses in the Ag/Pd nanocomposite</b> A. S. Saushin <sup>1</sup> , V. M. Styapshin <sup>1</sup> , G. M. Mikheev <sup>1</sup> , Y. P. Svirko <sup>2</sup> , <sup>1</sup> <i>Institute of Mechanics, Udmurt Federal Research Center of the UB RAS, Izhevsk, Russia 426067</i> , <sup>2</sup> <i>Institute of Photonics, University of Eastern Finland, 80101 Joensuu, Finland</i> . . . . .	38
PI.9	<b>Investigation of the optical properties of single-walled carbon nanotubes doped in acid medium</b> V. A. Velikanov <sup>1,2</sup> , T. V. Eremin <sup>2</sup> , E. D. Obratsova <sup>2</sup> , <sup>1</sup> <i>NRNU MEPhI, Moscow</i> , <sup>2</sup> <i>A.M. Prokhorov General Physics Institute, RAS, 119991, Moscow, Russia</i> . . . . .	39
PI.10	<b>Investigation of multilayer MoS<sub>2</sub> film grown by CVD method on transferred CVD graphene</b> P. V. Vinokurov, E. I. Zakharkina, A. A. Semenova, S. A. Smagulova, <i>North-Eastern Federal University, 677000, Belinskogo str., Yakutsk, Republic of Sakha (Yakutia), Russia</i> . . . . .	40

PI.11	<b>Saturable absorption in detonation nanodiamond films</b> R.Yu. Krivenkov <sup>1</sup> , K.G. Mikheev <sup>1</sup> , T.N. Mogileva <sup>1</sup> , N. Nunn <sup>2</sup> , O. A. Shenderova <sup>2</sup> , G. M. Mikheev <sup>1</sup> , <sup>1</sup> <i>Institute of Mechanics UB RAS, 34, str. T. Baramzinoy, Izhevsk, 426067, Russia,</i> <sup>2</sup> <i>Adamas Nanotechnologies, Inc., 8100 Brownleigh Dr, Suite 120, Raleigh, NC 27617, USA</i> . . . . .	41
PI.12	<b>Tuning electrical and optical properties of SWCNT films</b> A. A. Tonkikh <sup>1</sup> , V. I. Tsebro <sup>2,3</sup> , I. I. Kondrashov <sup>1</sup> , V. A. Eremina <sup>1</sup> , E. A. Obraztsova <sup>1,4</sup> , A. S. Orekhov <sup>5,6</sup> , E. I. Kauppinen <sup>7</sup> , A. L. Chuviln <sup>8,9</sup> , E. D. Obraztsova <sup>1</sup> , <sup>1</sup> <i>A.M. Prokhorov General Physics Institute, RAS, 38 Vavilov Street, 119991 Moscow, Russia,</i> <sup>2</sup> <i>P.N. Lebedev Physical Institute, RAS, 53 Leninsky Prospect, 119991 Moscow, Russia,</i> <sup>3</sup> <i>Kapitza Institute for Physical Problems, RAS, 2 Kosygina Street, 119334 Moscow, Russia,</i> <sup>4</sup> <i>Shemyakin and Ovchinnikov Institute of Bioorganic Chemistry, RAS, 16/10 Miklukho-Maklaya Street, 117871 Moscow, Russia,</i> <sup>5</sup> <i>National Research Center "Kurchatov Institute", 123182 Moscow, Russia,</i> <sup>6</sup> <i>Electron Microscopy for Materials Science (EMAT), University of Antwerp, 2020 Antwerpen, Belgium,</i> <sup>7</sup> <i>Department of Applied Physics, Aalto University, School of Science, P.O. Box 15100, FI-00076 Espoo, Finland,</i> <sup>8</sup> <i>CIC nanoGUNE Consolider, Tolosa Hiribidea 76, 20018 Donostia-San Sebastian, Spain,</i> <sup>9</sup> <i>IKERBASQUE Basque Foundation for Science, Maria Diaz de Haro 3, E-48013 Bilbao, Spain</i> . . . . .	42
PI.13	<b>Thermal effects of Er<sup>3+</sup> / Yb<sup>3+</sup> doped NaYF<sub>4</sub> phosphor induced by 980 nm laser diode irradiation</b> Hong Wang, Xiumei Yin, Mingming Xing, Yao Fu, Ying Tian, and Xixian Luo, <i>Physics Department, Dalian Maritime University, Dalian, Liaoning 116026, P. R. China</i> . . . . .	43
<b>Thursday, August 9</b>		<b>45</b>
9:00-9:45	<b>Diamond based quantum sensing and imaging</b> Fedor Jelezko, <i>Institute of Quantum optics, Ulm University</i> . . . . .	47
9:45-10:15	<b>Diamond nanoneedles under high electric field and laser illumination: electrical, optical and thermal properties studied by ion and photon emission</b> A. Vella <sup>1</sup> , L. Venturi <sup>1</sup> , M. Borz <sup>1</sup> , I. Blum <sup>1</sup> , J. Houard <sup>1</sup> , L. Arnoldi <sup>1</sup> , L. Rigutti <sup>1</sup> , A.N. Obraztsov <sup>2,3</sup> , <sup>1</sup> <i>GPM - UMR 6634 CNRS-INSU-Université de Rouen, Normandie Université, France,</i> <sup>2</sup> <i>M. V. Lomonosov Moscow State University, Department of Physics, Moscow, Russia,</i> <sup>3</sup> <i>University of Eastern Finland, Department of Physics and Mathematics, Joensuu 80101, Finland</i> . . . . .	48
10:15-10:30	<b>GeV, SiV and NV color centers in single crystal diamond needles</b> S.A. Malykhin <sup>1,2,3</sup> , R.R. Ismagilov <sup>2</sup> , A.S. Orekhov <sup>4</sup> , E.A. Obraztsova <sup>5</sup> , A.N. Obraztsov <sup>1,2</sup> , <sup>1</sup> <i>Department of Physics and Mathematics, University of Eastern Finland, Joensuu, Finland,</i> <sup>2</sup> <i>Department of Physics, Lomonosov Moscow State University, Moscow, Russia,</i> <sup>3</sup> <i>Lebedev Physical Institute, Russian Academy of Sciences, Moscow, Russia,</i> <sup>4</sup> <i>Russian Research Centre Kurchatov Institute, Moscow, Russia,</i> <sup>5</sup> <i>Shemyakin and Ovchinnikov Institute of Bioorganic Chemistry, Russian Academy of Sciences, Moscow, Russia</i> . . . . .	49
11:00-11:30	<b>Meter-scale single-wall carbon nanotube films for the use in flexible and transparent integrated circuits</b> Dong-Ming Sun, Bing-Wei Wang, Chang Liu, Hui-Ming Cheng, <sup>1</sup> <i>Shenyang National Laboratory for Materials Science, Institute of Metal Research, Chinese Academy of Sciences, 72 Wenhua Road, Shenyang, 110016, P. R. China,</i> <sup>2</sup> <i>School of Material Science and Engineering, University of Science and Technology of China, 96 Jinzhai Road, Hefei, 230026, P. R. China,</i>	50
11:30-12:00	<b>Carbon nanotube-based analog circuits for wearable sensor applications: Device modeling, circuit design and fabrication</b> Yutaka Ohno, <i>Institute of Materials and Systems for Sustainability, Nagoya University, Furocho, Chikusa-ku, Nagoya 464-8603, Japan</i> . . . . .	51
12:00-12:15	<b>Transport properties of semiconducting and metallic single-walled carbon nanotubes thin films</b> V.A. Eremina <sup>1,2</sup> , T. Matsui <sup>3</sup> , H. Fukuyama <sup>3,4</sup> , E.D. Obraztsova <sup>1,2</sup> , <sup>1</sup> <i>Physics Department of M.V. Lomonosov Moscow State University, 1 Leninskie gori, Moscow, Russia,</i> <sup>2</sup> <i>A.M. Prokhorov General Physics Institute, RAS, 38 Vavilov street, 119991 Moscow, Russia,</i> <sup>3</sup> <i>Department of Physics, The University of Tokyo, 7-3-1 Hongo, Bunkyo-ku, Tokyo 113-0033, Japan,</i> <sup>4</sup> <i>Cryogenic Research Center, The University of Tokyo, 2-1-16 Yayoi, Bunkyo-ku, Tokyo 113-0032, Japan</i>	52

12:15-12:30	<b>Revealing floating-catalyst carbon nanotube quality by ultraclean individual CNT transistor array</b> Nan Wei <sup>1</sup> , Patrik Laiho <sup>1</sup> , Saeed Ahmad <sup>1</sup> , Aqeel Hussain <sup>1</sup> , Qiang Zhang <sup>1</sup> , Taher Khan <sup>1</sup> , Yongping Liao <sup>1</sup> , Ying Tian <sup>1,3</sup> , Er-Xiong Ding <sup>1</sup> , Yutaka Ohno <sup>2</sup> , Esko I. Kauppinen <sup>1</sup> , <sup>1</sup> <i>Department of Applied Physics, Aalto University School of Science, Puumiehenkuja 2, 00076 Aalto, Finland,</i> <sup>2</sup> <i>Institute of Materials and Systems for Sustainability, Nagoya University, Furo-cho, Chikusa-ku, Nagoya 464-8603, Japan,</i> <sup>3</sup> <i>Department of Physics, Dalian Maritime University, Dalian, Liaoning 116026, China</i> . . . . .	53
14:30-15:00	<b>Air-suspended carbon nanotubes for nanoscale quantum photonics</b> Yuichiro K. Kato <sup>1,2</sup> , <sup>1</sup> <i>Nanoscale Quantum Photonics Laboratory, RIKEN, Saitama 351-0198, Japan,</i> <sup>2</sup> <i>Quantum Optoelectronics Research Team, RIKEN Center for Advanced Photonics, Saitama 351-0198, Japan</i> . . . . .	54
15:00-15:30	<b>Ultrafast field emission from carbon nanotubes</b> Chi Li <sup>1</sup> , Xu Zhou <sup>2</sup> , Feng Zhai <sup>3</sup> , Zhenjun Li <sup>1</sup> , Fengrui Yao <sup>2</sup> , Ruixi Qiao <sup>2</sup> , Ke Chen <sup>1</sup> , Dapeng Yu <sup>2</sup> , Zhipei Sun <sup>4</sup> , Kaihui Liu <sup>2</sup> , Qing Dai <sup>1</sup> , <sup>1</sup> <i>Nanophotonics Research Division, CAS Center for Excellence in Nanoscience, National Center for Nanoscience and Technology, Beijing 100190, China,</i> <sup>2</sup> <i>School of Physics, Academy for Advanced Interdisciplinary Studies, Collaborative Innovation Center of Quantum Matter, Peking University, Beijing 100871, China,</i> <sup>3</sup> <i>Department of Physics, Zhejiang Normal University, Jinhua 321004, China,</i> <sup>4</sup> <i>Department of Electronics and Nanoengineering, Aalto University, Tietotie 3, FI-02150 Espoo, Finland</i> . . . . .	55
15:30-16:00	<b>Use of carbon nanotubes in organic and perovskite solar cells</b> Yutaka Matsuo <sup>1,2</sup> , Il Jeon <sup>1</sup> , Esko I. Kauppinen <sup>3</sup> , Shigeo Maruyama <sup>1,4</sup> , <sup>1</sup> <i>University of Tokyo, Japan,</i> <sup>2</sup> <i>University of Science and Technology of China, Hefei, China,</i> <sup>3</sup> <i>School of Science, Aalto University, Espoo, Finland,</i> <sup>4</sup> <i>AIST, Japan</i> . . . . .	56
16:30-17:00	<b>Tailoring electronic structure of SWCNTs for transparent and conductive film applications</b> Alexey P. Tsapenko <sup>1</sup> , Daria S. Kopylova <sup>1</sup> , Fedor S. Fedorov <sup>1</sup> , Alena A. Alekseeva <sup>1</sup> , Evgenia P. Gilshteyn <sup>1</sup> , Pramod M. Rajanna <sup>1</sup> , Vsevolod Iakovlev <sup>1</sup> and Albert G. Nasibulin <sup>1,2</sup> , <sup>1</sup> <i>Skolkovo Institute of Science and Technology, Nobel str. 3, Moscow, 143026, Russia,</i> <sup>2</sup> <i>Aalto University, Department of Applied Physics, 00076, Aalto, Finland</i> . . . . .	57
17:00-17:30	<b>Graphene functionalized and optically forged by femtosecond laser</b> Andreas Johansson <sup>1,2</sup> , Pasi Myllyperkiö <sup>1</sup> , Pekka Koskinen <sup>2</sup> , Jukka Aumanen <sup>1</sup> , Juha Koivistoinen <sup>1</sup> , Hung- Chieh Tsai <sup>3</sup> , Chia-Hao Chen <sup>4</sup> , Lo-Yueh Chang <sup>4</sup> , Vesa-Matti Hiltunen <sup>2</sup> , Jyrki J. Manninen <sup>2</sup> , Kamila Mentel <sup>1</sup> , Wei Yen Woon <sup>3</sup> , Mika Pettersson <sup>1</sup> , <sup>1,2</sup> <i>Nanoscience Center, Department of Chemistry<sup>1</sup>, and Physics<sup>2</sup>, P.O. Box 35, FI-40014, University of Jyväskylä, Finland,</i> <sup>3</sup> <i>Department of Physics, National Central University, Jungli, 32054, Taiwan, Republic of China,</i> <sup>4</sup> <i>National Synchrotron Radiation Research Center, Hsinchu, 30076, Taiwan, Republic of China</i> . . . . .	58
17:30-18:00	<b>High aspect ratio laser cutting of CFRP using nanosecond UV laser pulses</b> Junji Yumoto, <i>Inst. for Photon Sci. and Tech., The Univ. of Tokyo, 7-3-1, Hongo Bunkyo-ku, Tokyo 113-0033 Japan</i> . . . . .	59
<b>Poster session II</b>		<b>61</b>
P11.1	<b>Floating catalyst CVD synthesis of single walled carbon nanotubes using ethylene as carbon precursor for transparent electrode</b> Aqeel Hussain, Yongping Liao, Qiang Zhang, Er-Xiong Ding, Patrik Laiho, Saeed Ahmad, Hua Jiang, Esko I. Kauppinen, <i>Department of Applied Physics, Aalto University School of Science, P.O. Box 15100, FI-00076 Aalto, Finland</i> . . . . .	63
P11.2	<b>Influence of the carbon nanoparticles structure on their lithium storage capacity</b> L.L. Lapteva <sup>1,2</sup> , Yu.V. Fedoseeva <sup>1,2</sup> , E.V. Shlyakhova <sup>1,2</sup> , L.G. Bulusheva <sup>1,2</sup> , A.V. Okotrub <sup>1,2</sup> , <sup>1</sup> <i>Nikolaev Institute of Inorganic Chemistry SB RAS, 3 Acad. Lavrentiev Avenue, 630090 Novosibirsk, Russia,</i> <sup>2</sup> <i>Novosibirsk State University, 2 Pirogova Street, 630090 Novosibirsk, Russia</i> . . . . .	64
P11.3	<b>Electrochemical properties of carbon nanostructures modified by oxygen containing groups</b> E.O. Fedorovskaya <sup>1,2</sup> , A. G. Kurennya <sup>1,2</sup> , I. P. Asanov <sup>1,2</sup> , L. G. Bulusheva <sup>1,2</sup> , A. V. Okotrub <sup>1,2</sup> ,	

	<sup>1</sup> Novosibirsk State University, 2 Pirogova Street, 630090 Novosibirsk, Russia, <sup>2</sup> Nikolaev Institute of Inorganic Chemistry SB RAS, 3 Acad. Lavrentiev Avenue, 630090 Novosibirsk, Russia	65
PII.4	<b>Carbon nanotube buckypaper, reduced graphene oxide and polypyrrole nanocomposites for supercapacitor applications</b> A. A. Iurchekova <sup>1,2</sup> , K. M. Popov <sup>2</sup> , E.O. Fedorovskaya <sup>1,2</sup> , L. G. Bulusheva <sup>1,2</sup> , A. V. Okotrub <sup>1,2</sup> , <sup>1</sup> Novosibirsk State University, 2 Pirogova Street, 630090 Novosibirsk, Russia, <sup>2</sup> Nikolaev Institute of Inorganic Chemistry SB RAS, 3 Acad. Lavrentiev Avenue, 630090 Novosibirsk, Russia	66
PII.5	<b>Purification of single-wall carbon nanotubes by magnetic separation</b> O.A. Gurova <sup>1</sup> , V.E. Arkhipov <sup>1</sup> , E.N. Vostretsova <sup>2</sup> , V.O. Koroteev <sup>1</sup> , A.V. Okotrub <sup>1</sup> , <sup>1</sup> Nikolaev Institute of Inorganic Chemistry SB RAS, 3 Acad. Lavrentiev Avenue, 630090 Novosibirsk, Russia, <sup>2</sup> Tomsk State University, 36 Lenin ave., Tomsk, 634050, Russia	67
PII.6	<b>FCCVD growth of SWCNTs by spark discharge based metallic and bimetallic catalysts particles</b> Saeed Ahmad, Aqeel Hussain, Yongping Liao, Er-Xiong Ding, Qiang Zhang, Esko I. Kauppinen, Department of Applied Physics, Aalto University School of Science, P.O. Box 15100, FI-00076 Aalto, Finland	68
PII.7	<b>Compact chemical vapor deposition system with embedded scanning probe microscope for <i>in situ</i> study of material growth</b> A. B. Loginov, R. R. Ismagilov, A. N. Obraztsov, Lomonosov Moscow State University, Department of Physics, Moscow 119991, Russia	69
PII.8	<b>Single-crystal diamond pyramids formation by hot filament chemical vapor deposition</b> I. P. Kudarenko <sup>1</sup> , R. R. Ismagilov <sup>1</sup> , S. A. Malykhin <sup>1,2</sup> , A. N. Obraztsov <sup>1,2</sup> , <sup>1</sup> Department of Physics, Lomonosov Moscow State University, Moscow 119991, Russia, <sup>2</sup> Department of Physics and Mathematics, University of Eastern Finland, Joensuu 80101, Finland	70
PII.9	<b>Continuous direct production of carbon nanotube films and fibers by floating-catalyst CVD</b> Qiang Zhang <sup>1</sup> , Weiya Zhou <sup>2</sup> , Sishen Xie <sup>2</sup> , Esko I. Kauppinen <sup>1</sup> , <sup>1</sup> Department of Applied Physics, Aalto University School of Science, P.O. Box 15100, FI-00076, Aalto, Finland, <sup>2</sup> Beijing National Laboratory for Condensed Matter Physics, Institute of Physics, Chinese Academy of Sciences, Beijing, 100190, P.R. China	71
PII.10	<b>Temperature dependence of aqueous two-phase extraction of single-walled carbon nanotubes</b> D.A. Musatov <sup>1</sup> , V.A. Eremina <sup>2</sup> , E.D. Obraztsova <sup>2</sup> , <sup>1</sup> Department of Problems of Physics and Energetics, Moscow Institute of Physics and Technology (State University), 7 Institutskiy per., Dolgoprudny, Moscow Region, Russia, <sup>2</sup> A.M. Prokhorov General Physics Institute, RAS, 38 Vavilov street, 119991 Moscow, Russia	72
PII.11	<b>Morphology and transport properties of B, N and BN-doped carbon materials synthesized using arc discharge procedure</b> O.V. Sedelnikova <sup>1,2</sup> , Yu. V. Fedoseeva, A.I. Romanenko, D.S. Bychanok <sup>3</sup> , L.G. Bulusheva <sup>1,2</sup> , A.V. Okotrub <sup>1,2</sup> , <sup>1</sup> Nikolaev Institute of Inorganic Chemistry SB RAS, 3 Acad. Lavrentiev Avenue, 630090 Novosibirsk, Russia, <sup>2</sup> Novosibirsk State University, 2 Pirogova Street, 630090 Novosibirsk, Russia, <sup>3</sup> Research Institute for Nuclear Problems, Belarusian State University, 220030 Minsk, Belarus	73
PII.12	<b>Highly conductive and transparent single-walled carbon nanotube film fabricated by floating catalyst chemical vapor deposition using liquid carbon source</b> Er-Xiong Ding, Hua Jiang, Qiang Zhang, Yongping Liao, Aqeel Hussain, Esko I. Kauppinen, Department of Applied Physics, Aalto University School of Science, Puumiehenkuja 2, 00076 Aalto, Espoo, Finland	74
PII.13	<b>Controlled graphene synthesis from solid carbon sources</b> Ivan Kondrashov, Maxim Rybin and Elena Obraztsova, A.M. Prokhorov General Physics Institute, Vavilov str. 38, Moscow, Russia, 119991	75

9:00-9:45	<b>Graphdiyne: A new member of carbon family</b> Jin Zhang, <i>Center for Nanochemistry, College of Chemistry and Molecular Engineering, Peking University, Beijing 100871, China</i> . . . . .	79
09:45-10:15	<b>The chemistry and physics of carbon from first-principles, multiscale simulations, and experiments</b> Simone Taioli, <i>European Centre for Theoretical Studies in Nuclear Physics and Related Areas (ECT), Trento, Italy &amp; Faculty of Mathematics and Physics, Charles University, Prague, Czech Republic</i> . . . . .	80
10:15-10:30	<b>Polybromide formation in carbons</b> O.V. Sedelnikova <sup>1,2</sup> , C.P. Ewels <sup>3</sup> , G.N. Chekhova <sup>1</sup> , D.V. Pinakov <sup>1,2</sup> , E. Flahaut <sup>4,5</sup> , L.G. Bulusheva <sup>1,2</sup> , and A.V. Okotrub <sup>1,2</sup> , <sup>1</sup> Nikolaev Institute of Inorganic Chemistry SB RAS, 3 Acad. Lavrentiev Avenue, 630090 Novosibirsk, Russia, <sup>2</sup> Novosibirsk State University, 2 Pirogova Street, 630090 Novosibirsk, Russia, <sup>3</sup> Institut des Matériaux Jean Rouxel, CNRS-Université de Nantes, UMR6502, Nantes, France, <sup>4</sup> Université de Toulouse; UPS, INP; Institut Carnot Cirimat; 118, route de Narbonne, F-31062 Toulouse cedex 9, France, <sup>5</sup> CNRS, Institut Carnot Cirimat, F-31062 Toulouse, France . . . . .	81
11:00-11:30	<b>Radiative tolerance of graphene: THz components for space applications</b> Alesia Paddubskaya <sup>1</sup> , Polina Kuzhir <sup>1,2</sup> , A. Stepanov <sup>2</sup> , G. Remnev <sup>2</sup> , Tommi Kaplas <sup>3</sup> , Yuri P. Svirko <sup>3</sup> , <sup>1</sup> Institute for Nuclear Problems of Belarusian State University, Minsk Belarus, <sup>2</sup> Tomsk Polytechnic University, Lenin Ave, 30, Tomsk, Tomskaya oblast', Russia, 634050, <sup>3</sup> Institute of Photonics, University of Eastern Finland, Joensuu, Finland . . . . .	82
11:30-12:00	<b>Wafer-scale transfer of CVD graphene for flexible electronics</b> Harri Lipsanen, <i>Department of Electronics and Nanoengineering, Aalto University, Tietotie 3, 02150 Espoo, Finland</i> . . . . .	83
12:00-12:30	<b>Multifunctional polymer film in graphene transfer</b> Tommi Kaplas, Arijit Bera and Pertti Pääkkönen, <i>Institute of Photonics, University of Eastern Finland, Yliopistokatu 7, 80101 Joensuu, Finland</i> . . . . .	84
14:00-14:30	<b>Stacking-dependent interlayer couplings in 2D materials</b> Kaihui Liu, <i>School of Physics, Peking University, Beijing 100871, China</i> . . . . .	85
14:30-15:00	<b>Aberration-corrected TEM/ETEM-based research on single-walled carbon nanotubes</b> Hua Jiang <sup>1</sup> , Ying Tian <sup>1,2</sup> , Yongping Liao <sup>1</sup> , Qiang Zhang <sup>1</sup> , Nan Wei <sup>1</sup> and Esko I. Kauppinen <sup>1</sup> , <sup>1</sup> Department of Physics, Aalto University School of Science, Espoo, Finland, <sup>2</sup> Department of Physics, Dalian Maritime University, Dalian, Liaoning 116026, China . . . . .	86
15:00-15:15	<b>Tailoring the morphology and properties of carbon-based materials by <i>in situ</i> TEM</b> Simona Moldovan <sup>1,2</sup> , Georgian Melinte <sup>1</sup> , Walid Baaziz <sup>1</sup> , Cuong Pham-Huu <sup>3</sup> , Ovidiu Ersen <sup>1</sup> , <sup>1</sup> Institut de Physique et Chimie des Matériaux de Strasbourg, CNRS-Université de Strasbourg, 23 rue du Loess 67000, Strasbourg, France, <sup>2</sup> Groupe de Physique des Matériaux, CNRS-INSA Rouen, avenue de l'Université, Rouen, France, <sup>3</sup> Institut de Chimie et Procédés pour l'Energie, l'Environnement et la Santé (ICPEES), CNRS, ECPM, Université de Strasbourg 25, rue Becquerel, 67087 Strasbourg, France . . . . .	87
15:45-17:00	<b>Carbon nanotube saturable absorber with electrical gating for control over pulse generation regime</b> Yu. Gladush <sup>1</sup> , A. Mkrtchyan <sup>1</sup> , V. Iakovlev <sup>1</sup> , D.S. Kopylova <sup>1</sup> , A. Kheday <sup>2</sup> , M. Melkumov <sup>1</sup> , A. G. Nasibulin <sup>1,3</sup> , <sup>1</sup> Skolkovo Institute of Science and Technology, Nobel str. 3, Moscow, 143026, Russia, <sup>2</sup> Fiber optics research center, Vavilov str. 38, Moscow, Russia, <sup>3</sup> Aalto University, Department of Applied Physics, 00076, Aalto, Finland . . . . .	88
16:30-17:00	<b>Electronic properties and electrochemical applications of UV irradiated fluorinated graphene films</b> A.V. Okotrub, V.I. Sysoev, K.M. Popov, V.E. Arkhipov, D.V. Gorodetskii, L.G. Bulusheva, Nikolaev Institute of Inorganic Chemistry SB RAS, pr. Lavrenteva, 3, Novosibirsk, 630090, Russia . . . . .	89
17:00-17:30	<b>Fluorinated and chlorinated double-walled carbon nanotubes for gas sensing</b> L. G. Bulusheva <sup>1</sup> , V. I. Sysoev <sup>1</sup> , E. V. Lobiak <sup>1</sup> , A. V. Okotrub <sup>1</sup> , E. Flahaut <sup>2</sup> , <sup>1</sup> Nikolaev Institute of Inorganic Chemistry SB RAS, pr. Lavrenteva, 3, Novosibirsk, 630090, Russia, <sup>2</sup> CNRS, Institut Carnot Cirimat, F-31062 Toulouse, France . . . . .	90

17:30-18:00	<b>Carbon nanotubes as promising materials to design a new class of high-performance electrocatalysts</b>	
	Mohammad Tavakkoli, Tanja Kallio, Albert G. Nasibulin, Esko I. Kauppinen, and Kari Laasonen, <i>Aalto University, Espoo, Finland</i> . . . . .	91
	<b>Author index</b>	<b>92</b>



## Tuesday, August 7



©J. Turunen





# 2D Materials for Smart Life

**Kaustav Banerjee**

Department of Electrical and Computer Engineering, University of California, Santa Barbara, CA, USA  
kaustav@ece.ucsb.edu

## 1. Abstract

Two-dimensional (2D) materials such as graphene and various transition metal dichalcogenides (TMDs) possess a wide range of remarkable properties that make them attractive for a number of applications, including sub-10 nm transistors, sensors, interconnect and passives [1]. In this lecture, I will highlight the prospects of 2D materials for building next-generation electronics targeted to support the emerging paradigm of the *Internet of Things*.

## 2. Applications Uniquely Enabled by 2D Materials

In contrast to conventional bulk materials, 2D materials (Fig. 1) are formed by weak interlayer van der Waals bonds. This unique structure enables many extraordinary properties such as extremely small thickness (few Å/layer), uniform band gap over large area, and pristine interfaces without out-of-plane dangling bonds [1], based on which novel applications can be explored. For example, TMDs allow efficient electrostatics, reduction of short channel effects for nanoscale transistors, fewer traps on a semiconductor-dielectric interface, and a high degree of vertical scaling. I will bring forward a few important developments on transistors [2-6], sensors [7], interconnects [8], and passives [9], all uniquely enabled by 2D materials, which have been realized in my lab.

More specifically, I will highlight the world's first "kinetic inductor" [9] that exploits the *kinetic inductance* at room temperature and thereby overcomes a 200 years old limitation of the original device designed by Michael Faraday. I will discuss the first 2D-channel band-to-band tunneling transistor [5] that can switch at 0.1V and potentially lead to significant (> 90%) lowering of power dissipation, as well as a radical interconnect

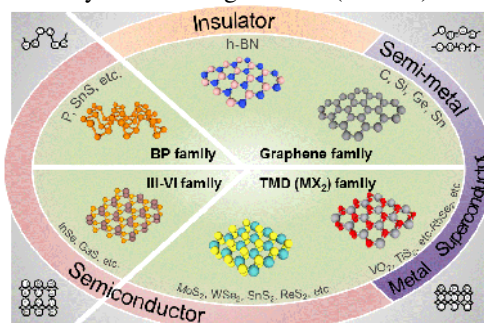


Fig. 1. 2D materials family [1].

technology based on intercalation doped graphene-nanoribbons [8], which overcomes the fundamental limitations of conventional metals and provides an attractive pathway toward an energy-efficient and highly reliable interconnect technology for next-generation integrated circuits. I will also bring forward a new class of ultra-sensitive and low-power sensors being developed in my lab using 2D materials for ubiquitous sensing and connectivity to improve quality of life. Progress on key issues in 2D electronics including large-area synthesis, contacts and interfaces [10], high-k gate dielectrics, and doping will be summarized.

## 3. Acknowledgement

The author gratefully acknowledges the contributions of his lab members and collaborators as well as funding from NSF, SRC, DARPA, DOE, DoD, AFOSR, JST, UC MRPI and Lab Fees Research Programs, and Intel.

## 4. References

- [1] P. Ajayan, P. Kim, and K. Banerjee, "Two - dimensional van der Waals materials," *Physics Today*, vol. 69, no. 9, 38-44, 2016.
- [2] W. Cao, J. Kang, D. Sarkar, W. Liu, and K. Banerjee, "2D semiconductor FETs - Projections and design for sub-10 nm VLSI," *IEEE Trans. Electron Devices*, vol. 62, no. 11, pp. 3459-3469, 2015.
- [3] W. Cao, W. Liu, J. Kang, and K. Banerjee, "An ultra-short channel monolayer MoS<sub>2</sub> FET defined by the curvature of a thin nanowire," *IEEE Electron Device Letters*, vol. 37, no. 11, pp. 1497-1500, 2016.
- [4] J. Kang, W. Cao, A. Pal, S. Pandey, S. Kramer, R. Hill, G. Sandhu, and K. Banerjee, "Computational study of gate-induced drain leakage in 2D-semiconductor field-effect transistors," *IEDM Tech. Dig.*, 2017, pp. 31.2.1-31.2.4.
- [5] D. Sarkar, X. Xie, W. Liu, W. Cao, J. Kang, Y. Gong, S. Kraemer, P. M. Ajayan, and K. Banerjee, "A subthermionic tunnel field-effect transistor with an atomically thin channel," *Nature*, 526, pp. 91-95, 2015.
- [6] W. Cao, J. Jiang, J. Kang, D. Sarkar, W. Liu, and K. Banerjee, "Designing band-to-band tunneling field-effect transistors with 2D semiconductors for next-generation low-power VLSI," *IEDM Tech. Dig.*, 2015, p. 12.3.1-12.3.4.
- [7] D. Sarkar, W. Liu, X. Xie, A. Anselmo, S. Mitragotri, and K. Banerjee, "MoS<sub>2</sub> field-effect transistor for next-generation label-free biosensors," *ACS Nano*, vol. 8, no. 4, 3992-4003, 2014.
- [8] J. Jiang, J. Kang, W. Cao, X. Xie, H. Zhang, J. H. Chu, W. Liu, and K. Banerjee, "Intercalation doped multilayer-graphene nanoribbons for next-generation interconnects," *Nano Letters*, 17(3), pp. 1482-1488, 2017.
- [9] J. Kang, Y. Matsumoto, X. Li, J. Jiang, X. Xie, K. Kawamoto, M. Kenmoku, J. H. Chu, W. Liu, J. Mao, K. Ueno, and K. Banerjee, "On-chip intercalated-graphene inductors for next-generation radio frequency electronics," *Nature Electronics*, 1(1), pp. 46-51, 2018.
- [10] A. Allain, J. Kang, K. Banerjee and A. Kis, "Electrical contacts to two-dimensional semiconductors," *Nature Materials*, 14, pp. 1195-1205, 2015.

## Safety of carbon nanomaterials towards the environment

E. Flahaut<sup>1</sup>, F. Mouchet<sup>2</sup>, C. Line<sup>1,2</sup>, M. Garacci<sup>2</sup>, L. Lagier<sup>2</sup>, L. Evariste<sup>2</sup>, A. Mottier<sup>2</sup>, C. Sarrieu<sup>1</sup>, A-M. Galibert<sup>1</sup>, L. Verneuil<sup>2</sup>, C. Matei Ghimbeu<sup>3</sup>, C. Larue<sup>2</sup>, E. Pinelli<sup>2</sup>, L. Gauthier<sup>2</sup>

<sup>1</sup> CIRIMAT, Université de Toulouse, UMR CNRS-UPS-INP N°5085, Toulouse, France

<sup>2</sup> EcoLab, Université de Toulouse, UMR CNRS-UPS-INP N°5245, Toulouse, France

<sup>3</sup> IS2M, Université de Haute Alsace, UMR CNRS-UHA N°7360, Mulhouse, France

flahaut@chimie.ups-tlse.fr

### Abstract

The estimated increasing production of carbon nanotubes (CNTs) and more recently graphene and related materials (GRMs) is driven by many applications – some of which being already on the market (energy storage, paints and composite materials for example). In parallel, questions are also raising about their safe handling and use (mainly for workers, including researchers), but also about their end of life in the environment. The CIRIMAT is focusing for about 20 years on the CCVD synthesis of double-walled CNTs (DWNTs) [1] because they represent unique objects at the interface between single-wall CNTs (SWNTs) and larger multi-walled CNTs (MWNTs). The protection offered by the outer tube allows to modify the interface with the environment (solvent, matrix, etc.) while minimizing interferences with the inner one, and keeping a morphology close to that of SWNTs. We have also developed a synthesis of few-layer graphene (FLG) by sonication-assisted exfoliation of graphite [2]. Together with EcoLab, we have investigated the potential environmental impact of different carbon nanomaterials on the environment using different models (amphibians [3-5], algae [6, 7], but also plants more recently). We will discuss some issues about the influence of sample processing and exposure protocols as well as of the metrics for the comparison of the results [8-10]. In particular, comparing the growth inhibition using the dose expressed in  $\text{mg.L}^{-1}$ ,  $\text{N}^\circ$  of particles. $\text{L}^{-1}$  or  $\text{m}^2.\text{L}^{-1}$ , we have shown that the surface concentration is the most suitable metric. It allows to unify the data for very different carbon nanomaterials (from 0D to 2D) and thus to become predictive.

For risk assessment of food safety, it is important to determine if carbon nanomaterials are transferred to the edible parts of plants [11]. However, detection of carbon particles in carbon matrices represents a technological bottleneck. We tested different analytical methods, rarely used in biology, to detect CNTs in plant samples such as Raman spectroscopy, bi-photonic microscopy, transmission electronic microscopy, isotopic labelling using  $^{13}\text{C}$ , etc. We established that CNTs can enter into plants by the roots, and be transported via the sap to the leaves.

Finally, we are also reducing graphene oxide in order to prepare a range of nanocarbons with similar morphology but a different surface chemistry, and we have shown that this approach can be used to make safer the use of carbon nanomaterials such as graphene oxide for example, by cancelling its genotoxicity.

### Acknowledgement.

The research has also received funding from the European Union Seventh Framework Program under grant agreement N°604391 Graphene flagship. We also acknowledge the PRES University of Toulouse and Region Occitanie for financial support through the grant N°2016-16.

### References

- [1] E. Flahaut, R. Bacsá, A. Peigney, Ch. Laurent, *Gram-Scale CCVD Synthesis of Double-Walled Carbon Nanotubes*, Chem Commun., **12**, 1442-1443 (2003).
- [2] Y. Celik, E. Flahaut, E. Suvaci, *A Comparative Study on Few-layer Graphene Production by Exfoliation of Different Starting Materials in a Low Boiling Point Solvent*, FlatChem, **1**, 74–88 (2017).
- [3] F. Mouchet, P. Landois, P. Puech, E. Pinelli, E. Flahaut, L. Gauthier, *CNT ecotoxicity in amphibians: assessment of multi-walled carbon nanotubes and comparison with double-walled carbon nanotubes*, Nanomedicine, **5**, 963-974 (2010).
- [4] F. Bourdiol, F. Mouchet, A. Perrault, I. Fourquaux, L. Datas, C. Gancet, J-C. Boutonnet, E. Pinelli, L. Gauthier, E. Flahaut, *Biocompatible polymer-assisted dispersion of multi walled carbon nanotubes in water, application to the investigation of their ecotoxicity using Xenopus laevis amphibian larvae*, Carbon, **54**, 175-191 (2013).
- [5] F. Mouchet, C. Gancet, E. Flahaut, E. Pinelli, J-C. Boutonnet, L. Gauthier, *International standardized procedures for in vivo evaluation of multi-walled carbon nanotube toxicity in water*, Toxicol. Environ. Chem., **98**, 829-847 (2016).
- [6] L. Verneuil, J. Silvestre, I. Randrianjatovo, C-E. Romain-Marcato, E. Girbal-Neuhausser, F. Mouchet, E. Flahaut, L. Gauthier, E. Pinelli, *Double walled carbon nanotubes promote the overproduction of extracellular protein-like polymers in Nitzschia palea: an adhesive response for an adaptive issue*, Carbon, **88**, 113-125 (2015).
- [7] M. Garacci, M. Barret, F. Mouchet, C. Sarrieu, P. Lonchambon, E. Flahaut, L. Gauthier, J. Silvestre, E. Pinelli, *Few Layer Graphene sticking by biofilm of freshwater diatom Nitzschia palea as a mitigation to its ecotoxicity*, Carbon, **113**, 139-150 (2017).
- [8] A. Mottier, F. Mouchet, C. Laplanche, S. Cadarsi, L. Lagier, J-C. Arnault, ..., E. Pinelli, L. Gauthier, E. Flahaut, *Surface area of carbon nanoparticle: a dose-metric for a more realistic ecotoxicological assessment*, Nano Letters, **16**, 3514-3518 (2016).
- [9] A. Mottier, F. Mouchet, E. Pinelli, L. Gauthier, E. Flahaut, *Environmental impact of engineered carbon nanoparticles: from releases to effects on the aquatic biota*, Current Opinion in Biotechnology, **46**, 1-6 (2016).
- [10] L. Lagier, F. Mouchet, C. Laplanche, A. Mottier, S. Cadarsi, L. Evariste, P. Lonchambon, E. Pinelli, E. Flahaut, L. Gauthier, *Surface area of carbon-based nanoparticles prevails on dispersion for growth inhibition in amphibians*, Carbon, **119**, 72-81 (2017).
- [11] C. Liné, C. Larue, E. Flahaut, *CNTs: impacts and behaviour in the terrestrial ecosystem - A review*, Carbon, **123**, 767-785 (2017).

# Dynamical tuning of graphene plasmonic resonances by ultraviolet illuminations

**Yunyun Dai, Yuyu Xia, Tao Jiang, Ang Chen, Yiwen Zhang, Yujie Bai, Fang Guan, Shiwei Wu, Xiaohan Liu\*, Lei Shi\* and Jian Zi\***

Department of Physics, Key Laboratory of Micro- and Nano-Photonic Structures (Ministry of Education),  
and State Key Laboratory of Surface Physics, Fudan University, Shanghai 200433, China

*Corresponding author e-mail: lshi@fudan.edu.cn*

Structured graphene such as graphene ribbons and disks can support interesting plasmonic resonances in the mid- and far-infrared ranges, showing many unique properties like deep subwavelength confinement, high enhancement of optical near-fields, and tunability. Among those properties, the unique features of plasmonic resonances in graphene structures is the enabled tunability through external means. Up to now, electrical gating has been extensively adopted to tune graphene plasmonic resonances. Nevertheless, the method of electrical gating has some disadvantages. To realize a dynamical tuning, graphene structures should have electrical connections. As a result, electrodes, ion-gels, or conducting substrates have to be introduced to attain an electrical connection. The method has been successfully applied to graphene sheets and ribbons. However, it is especially difficult and challenging for isolated graphene structures such as graphene disks. Moreover, intrinsic absorptions from either conducting substrates or ion-gels are inevitable, which may degrade considerably graphene plasmonic resonances. Thus, to find a way to tune plasmonic resonances in all kinds of graphene structures without the introduction of electrical connections is of great significance.

In this paper, we develop a simple and efficient method to tune graphene plasmonic resonances by UV illuminations. We show that UV illuminations can induce a dynamical tuning of plasmonic resonances in all kinds of graphene structures without introducing electrodes, ion-gel, or conducting layers required in electrical gating, which is of great significance especially for isolated graphene structures. Factors that influence this tuning process including the operating wavelength, power density, and illumination time of UV light sources are discussed. Our optical tuning method could shed new light on graphene-based tunable devices.

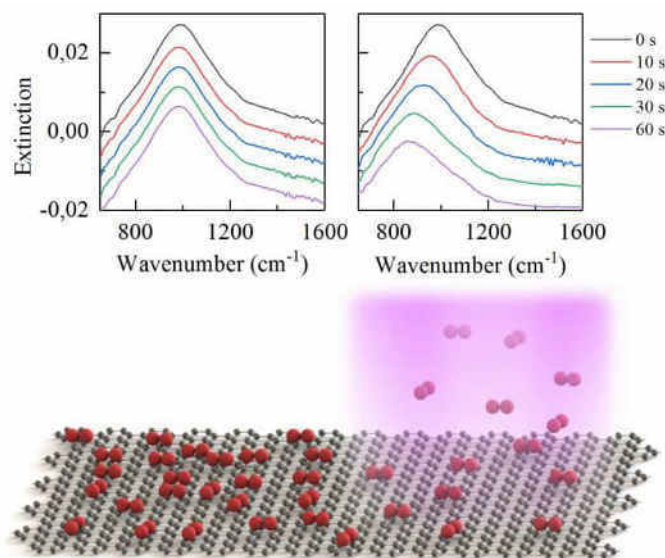


Figure: Optical tuning of plasmonic resonances in structured graphene with (upper left) and without (upper right) UV illuminations. Lower: the schematic view of the optical tuning mechanism.

[1] Yunyun Dai, et al. Advanced Optical Materials 6, 1701081, 2018.

## Towards optical modulators based on graphene surface plasmons

**T Wood\*, M Kemiche, J Lhuillier, P Demongodin, S Callard, B Vilquin, P Rojo-Romeo, C Monat**

*University of Lyon, Institut des Nanotechnologies de Lyon, Ecole Centrale de Lyon / INSA de Lyon*

*\*tomwood321@hotmail.com*

Graphene is a two-dimensional material displaying unique optoelectronic properties; namely a high in-plane conductivity and a dielectric constant that can be strongly tuned through relatively small modifications to its charge carrier concentration. This places graphene at the interface between optical and electrical devices, and numerous applications have been demonstrated in the literature [1,2] including fast photodetectors, high-transparency electrodes, and polarisers. The ERC GRAPHICS project at Ecole Centrale de Lyon seeks to develop graphene for on-chip optical information processing systems [3]. Among the components being developed, including mode-locked lasers and wavelength converters, this presentation will focus on low power consumption electro-optic modulators.

Over the past five years, graphene's surface plasmon polariton (SPP) – a surface mode corresponding to a strong coupling between photons and charge waves on the graphene lattice – has been the subject of intense interest [4,5]. Such modes appear only at photon energies for which graphene is optically transparent, requiring doping levels that scale with the square of the energy in question. The high wavevectors associated with SPPs translate to confinement of light in sub-wavelength components, whilst presenting challenges for meeting the phase matching conditions necessary to couple to them. In this work, two issues will be addressed in order to unlock graphene's SPPs at optical communications wavelengths: how to electrically dope graphene sufficiently and in a modulatable fashion for data encoding, and how to efficiently couple light from free-space or standard waveguides into SPP modes. Simulations of optimised coupler structures will be presented, along with an overview of device realisation.

This work has been financed by the European Research Council under the project GRAPHICS.

- [1] "Graphene integrated photodetectors and opto-electronic devices— a review", X Wang, X Gan, Chin. Phys. B, Vol. 26, No. 3, 034203, 2017.
- [2] "Graphene Photonics, Plasmonics, and Broadband Optoelectronic Devices", Q Bao, K P Loh, ACS Nano, Vol.6, No.5, 3677-3694, 2012.
- [3] "Le graphène : à nos crayons pour redessiner le paysage de l'optoélectronique", T Wood, M Kemiche, J Lhuillier, S Callard, C Monat, Photoniques 87, p31, 2017.
- [4] "Infrared Nanophotonics Based on Graphene Plasmonics", Q Guo et al, ACS Photonics, ASAP article: doi: 10.1021/acsp Photonics.7b00547, 2017.
- [5] "Graphene Plasmonics: Challenges and Opportunities", F J Garcia de Abajo, ACS Photonics 1, 135-152, 2014.

# Surface-enhanced infrared spectroscopy with graphene plasmon

Xiaoxia Yang, Hai Hu, Xiangdong Guo, Qing Dai

*Division of Nanophotonics, National Center for Nanoscience and Technology, Beijing, China*

[daiq@nanoctr.cn](mailto:daiq@nanoctr.cn), [yangxx@nanoctr.cn](mailto:yangxx@nanoctr.cn)

Far-field mid-infrared spectroscopy has an increasingly important role for numerous applications (for example, chemical detection, food safety and biosensing) through directly probing vibrational characteristics of a broad range of molecular species and compounds. However, molecular fingerprinting at the nanoscale level still remains a significant challenge, due to weak light-matter interaction between micron-wavelengthed infrared light and nano-sized molecules.

Surface-enhanced infrared absorption (SEIRA) has been shown to significantly increase the detection sensitivity in the IR up to several orders of magnitude via enhanced light-matter interactions assisted by surface-plasmon polaritons [1]. Graphene plasmon is a promising candidate for SEIRA due to its ultrahigh field confinement and electrical tunability.

We have demonstrated molecular fingerprinting at the nanoscale level using our specially designed graphene plasmonic structure on  $\text{CaF}_2$  nanofilm, as shown in Fig. 1a. This structure not only avoids the plasmon-phonon hybridization, but also provides in situ electrically-tunable graphene plasmon covering the entire molecular fingerprint region, which was previously unattainable [2]. The vibrational signatures of  $\sim 8$  nm thick PEO film are enhanced more than 20-fold (Fig. 1b). In addition, undisturbed and highly confined graphene plasmon offers simultaneous detection of in-plane and out-of-plane vibrational modes with ultrahigh detection sensitivity down to the sub-monolayer level, significantly pushing the current detection limit of far-field mid-infrared spectroscopies.

Furthermore, by designing graphene plasmonic structures to introduce Fano resonance or metallic integrating structures, the sensitivity of SEIRA can be further improved [3,4]. Our results provide a platform for the fingerprint detection of nano-scale molecules.

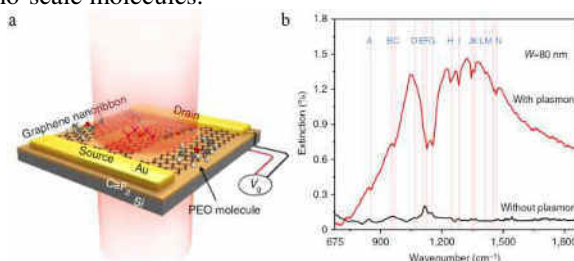


Fig.1 (a) Schematic of the graphene plasmon-based sensor. (b) A comparison of the sensing results for an 8-nm-thick PEO film with and without graphene plasmon.

## References

- [1] X. X. Yang, Z. P. Sun, T. Low, H. Hu, X. D. Guo, F. J. G. de Abajo, P. Avouris, Q. Dai, *Advanced Materials*, DOI:10.1002/adma.201704896 (2018).
- [2] H. Hu, X. X. Yang, F. Zhai, D. B. Hu, R. N. Liu, K. H. Liu, Z. P. Sun, Q. Dai, *Nature Communications*, **7**, 12334 (2016).
- [3] X. D. Guo, H. Hu, X. Zhu, X. X. Yang, Q. Dai, *Nanoscale*, **9**, 14998 (2017).
- [4] X. D. Guo, H. Hu, B. X. Liao, X. Zhu, X. X. Yang, Q. Dai, *Nanotechnology*, **29**, 184004 (2018).

# Systematical investigation of two orthogonal plasmonic modes of graphene ellipse array

Yuyu Xia, Yunyun Dai, Ang Chen, Yanbin Zhang, Bo Wang, Yiwen Zhang, Fang Guan, Xiaohan Liu, Lei Shi and Jian Zi

*Y. Xia, Dr. Y. Dai, Dr. A. Chen, Y. Zhang, B. Wang, Y. Zhang, Dr. F. Guan, Prof. X. Liu, Prof. L. Shi, Prof. J. Zi  
Department of Physics, Key Laboratory of Micro- and Nano-Photonic Structures (Ministry of Education), and State Key Laboratory of  
Surface Physics, Fudan University, Shanghai 200433, China  
E-mail: lshi@fudan.edu.cn; liuxh@fudan.edu.cn; jzi@fudan.edu.cn*

*Dr. Y. Dai*

*Department of Electronics and Nanoengineering, School of Electric Engineering, Aalto University, FI-00076 Aalto, Finland*

Graphene nanostructures can support localized plasmonic resonances from terahertz to infrared ranges, showing many unique characteristics such as subwavelength confinement, strong field localization and tunability [1]. Localized plasmonic resonances have been extensively studied in various structures such as graphene nanoribbons and nanodisks [2], possessing potential applications in photonics and optoelectronics [3].

The graphene ellipses support two orthogonal plasmonic modes along major and minor axis, showing polarization-dependent resonances [4]. This provides another degree of freedom, compared to graphene ribbons and disks, in manipulation of the interaction between matter with light, which deserves further investigation both theoretically and experimentally.

In this paper, we develop a theoretical model to describe the plasmonic resonances of graphene ellipse array on an isotropic substrate (Figure 1(a)). The extinction spectra for two orthogonal modes, namely the high-frequency mode along the minor axis and the low-frequency mode along the major axis, calculated by theoretical model agree well with the experiment results. The polarization dependence of the two orthogonal modes are fully studied as shown in Figure 1(b) and 1(c). By experimentally controlling the parameters including ellipticity of the structure, fermi energy of graphene and the substrate material, the resonance modes can be dynamically tuned.

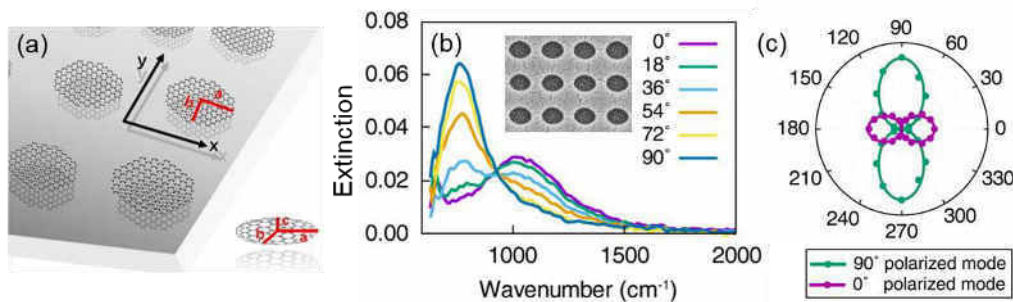


Fig. 1(a) Schematic diagram of the graphene ellipse array on a substrate. (b) The extinction spectra of two orthogonal plasmonic modes of graphene ellipses at different polarization angles. (c) The polarization-dependence of the two plasmonic modes.

In conclusion, we investigate both the theory and experiments of the plasmonic modes supported by graphene ellipse array, which provides valuable insight into the properties of plasmonic resonators. The two polarization-dependent modes show red shift with increasing length of the axis and decreasing fermi level of graphene, respectively. Furthermore, with a polar substrate, the interaction of graphene plasmons with substrate phonons brings hybridization of the two modes in each direction of the ellipse. Therefore, the graphene ellipses have potential applications as detectors, filters and sensors in infrared range with the guidance of the theoretical model and experiment results.

- [1] A. N. Grigorenko, M. Polini and K. S. Novoselov, *Nature Photonics*, **6** (11), 749-758 (2012).
- [2] F. J. García De Abajo, *ACS Photonics*, **1** (3), 135-152 (2014).
- [3] F. Bonaccorso, Z. Sun, T. Hasan and A. C. Ferrari, *Nature Photonics*, **4** (9), 611-622 (2010).
- [4] J. Chen, Y. Zeng, X. Xu, X. Chen, Z. Zhou, P. Shi, Z. Yi, X. Ye, S. Xiao and Y. Yi, *Nanomaterials* **8** (3), 175 (2018).

# Zero-energy vortices in graphene

C. A. Downing<sup>1</sup> and M. E. Portnoi<sup>2,3,4</sup>

<sup>1</sup>*Departamento de Física Teórica de la Materia Condensada, Universidad Autónoma de Madrid, 28049 Madrid, Spain*

<sup>2</sup>*School of Physics, University of Exeter, Stocker Road, Exeter EX4 4QL, United Kingdom*

<sup>3</sup>*ITMO University, St. Petersburg 197101, Russia*

<sup>4</sup>*Corresponding author: m.e.portnoi@exeter.ac.uk*

Contrary to a widespread belief, full electrostatic confinement is possible for Dirac-Weyl fermions with linear dispersion in gapless 2D systems such as graphene, surface states on the surface of topological insulators and gapless HgTe quantum wells. The confinement is possible precisely at the Dirac point where the particles pseudospin is ill-defined, and these bound states must possess non-zero angular momentum (vorticity) [1]. Formation of zero-energy vortices provides an alternative explanation for various STM experiments in graphene.

We also show [2] that a pair of two-dimensional massless Dirac-Weyl fermions can form a bound state independently on the sign of the inter-particle interaction potential, as long as this potential decays at large distances faster than Kepler's inverse distance law which is always the case in back-gated graphene. The coupling occurs only at the Dirac point, when the charge carriers lose their chirality. These two-particle states must have a non-zero internal angular momentum, meaning that they only exist as stationary vortices. This leads to the emergence of a new type of energetically-favorable quasiparticles: double-charged zero-energy vortices. Their bosonic nature allows condensation and gives rise to Majorana physics without invoking a superconductor. Arguably, the reservoir of bosonic vortices can play a similar role to that of a superconductor in proximity to a Weyl semimetal by enforcing electron-hole symmetry. Indeed, adding an electron to the considered system is equivalent to adding a hole and another zero-energy vortex which makes this system a promising candidate in the on-going search of Majorana modes in solids. The presence of dark-matter-like immobile vortices explains a range of poorly understood experiments in gated graphene structures at low doping. The formation of bielectron vortices depends on the dimensionless strength  $\alpha^*$  of electron-electron interaction – the fine structure constant divided by the dielectric permittivity and multiplied by the ratio of the speed of light to the Fermi velocity. For suspended graphene the value of  $\alpha^*$  is very close to the threshold required for electro-electron binding. Local strains (ripples in the case of graphene) help reinforcing binding, which is energetically favorable as it allows reducing the Fermi energy of the system. In other 2D Weyl systems, which have smaller Fermi velocities, the formation of double-charged vortices is even more favorable. The predicted peak in the density of states at the apex of the Dirac cone can also serve as a source of carriers with energies corresponding to the strong non-linear electromagnetic response making low-doped graphene and other 2D Weyl semimetals better suited for relevant applications.

## Acknowledgement

This work is supported by the EU H2020 RISE project CoExAN (Grant No. H2020-644076) and by ITMO Visitors Programme.

## References

- [1] C.A. Downing, D.A. Stone, and M.E. Portnoi "Zero-energy states in graphene quantum dots and rings", *Phys. Rev. B* **84**, 155437 (2011).
- [2] C. A. Downing and M. E. Portnoi "Bielectron vortices in two-dimensional Dirac semimetals" *Nature Communications* **8**, 897 (2017).



# Topological edge photocurrents in graphene in the quantum Hall effect regime

S.A. Tarasenko<sup>1</sup>, M.V. Durnev<sup>1</sup>, H. Plank<sup>2</sup>, and S.D. Ganichev<sup>2</sup>

<sup>1</sup>*Ioffe Institute, 194021 St. Petersburg, Russia*

<sup>2</sup>*University of Regensburg, Terahertz Center, 93040 Regensburg, Germany*  
tarasenko@coherent.ioffe.ru

## 1. Introduction

The study of a photoresponse of conducting channels emerging at the edges of materials with non-trivial topology is central to the optoelectronics of topological insulators [1]. Such one-dimensional chiral channels naturally occur in two-dimensional electron systems subjected to a strong perpendicular magnetic field in the regime of the quantum Hall effect. Graphene with the Dirac-like electron spectrum is a unique system for the study of topological effects because the large cyclotron gap (between the zero and the first orbit Landau levels) of about 30 meV is achieved already in the magnetic field of 1 T, which enables the observation of the Hall conductivity quantization at room temperature [2], and is promising for electronic applications [3].

In this talk, we report the observation, theoretical and experimental study of the photogalvanic effect in chiral edge channels in graphene in the quantum Hall effect regime. We show that the excitation of a graphene sample by microwave or terahertz radiation gives rise to an electric current circulating along the sample edges.

## 2. Microscopic picture

Electron states in graphene are 4-fold degenerate because of the spin and valley degrees of freedom. The valley mixing at a graphene edge shifts the valley degeneracy and forms, in a strong perpendicular magnetic field, the electron-like and hole-like chiral edge channels which are responsible for the Hall conductivity quantization [4]. The excitation of the edge carriers by a high-frequency electric field destroys the thermal equilibrium in the channel. For the photon energy smaller than the bulk cyclotron gap, the absorption is dominated by the indirect optical (Drude-like) transitions involving momentum scattering. Because of the edge-channel dispersion, such transitions are possible and lead to a dissipative contribution to the edge current measurable in experiments. While the current direction is controlled by the magnetic field polarity, its magnitude depends on the radiation polarization since the edge-channel absorbance is polarization sensitivity.

## 3. Experimental details

Experiments were done on Hall-bar samples made of stacks of exfoliated graphene covered with hexagonal boron nitride at 4.2 K. Transport data reveal that the first plateau of the quantum Hall effect is achieved at 0.5 T. Exciting an unbiased sample by terahertz radiation we detect electric currents which flow in the opposite directions at the opposite edges of the sample. At magnetic field values corresponding to the first quantum Hall plateau, the edge currents become uni-directional, being the same for *n*-type and *p*-type structures, while the current amplitude depends on the radiation polarization, which supports the microscopic picture above.

The theoretical work was supported by the Government of the Russian Federation (contract #14.W03.31.0011 at Ioffe Institute).

[1] K.-M. Dantscher, D.A. Kozlov, M.T. Scherr, S. Gebert, J. Bärenfänger, M.V. Durnev, S.A. Tarasenko, V.V. Bel'kov, N.N. Mikhailov, S.A. Dvoretzky, Z. D. Kvon, J. Ziegler, D. Weiss, and S.D. Ganichev, *Phys. Rev. B* **95**, 201103(R) (2017).

[2] K.S. Novoselov, Z. Jiang, Y. Zhang, S.V. Morozov, H.L. Stormer, U. Zeitler, J.C. Maan, G.S. Boebinger, P. Kim, and A.K. Geim, *Science* **315**, 1379 (2007).

[3] Yu.B. Vasilyev, G.Yu. Vasileva, S. Novikov, S.A. Tarasenko, S.N. Danilov, and S.D. Ganichev, *Appl. Phys. Lett.* **112**, 041111 (2018).

[4] D.A. Abanin, P.A. Lee, and L.S. Levitov, *Solid State Commun.* **143**, 77 (2007).

## SHG studies on surface states of 3D topological insulators and TMDCs

**Wei-Tao Liu**

*Department of Physics, Fudan University, Shanghai, China*  
[wliu@fudan.edu.cn](mailto:wliu@fudan.edu.cn)

The scope of nonlinear optics has expanded rapidly in recent decades, and found applications and new phenomena in emerging materials of low dimensionalities. During the past few years, we have been exploring the utility of nonlinear optics in characterizing two-dimensional systems, such as surface states of 3D topological materials (TIs) and transition metal dichalcogenides (TMDCs). We investigated the nature of SHG response from TI surface states, showing that it is both sensitive to the out-of-plane polar ordering at the interface, as well as the deviation from the parabolic band dispersion at the Fermi level. We also used the optical second harmonic generation to resolve the atomic structures of artificial bilayers and grain boundaries of TMDC materials, which helped to reveal the interplay between spin, layer, and valley pseudospins in related systems. [1-2]

### References

- [1] T. Jiang, H. Liu, D. Huang, S. Zhang, Y. Li, X. Gong\*, Y. R. Shen, Wei-Tao Liu\*, and S. Wu\*, *Nature Nanotech.* **9**, 825 (2014).
- [2] Hui Shi, Yu Zhang, Mengyu Yao, Fuhao Ji, Dong Qian, Shan Qiao, Y. R. Shen, and Wei-Tao Liu, *PRB*, **94**, 205307 (2016).

# Femtosecond dynamics of exciton and structure in 2H-MoTe<sub>2</sub>

Ji-Hee Kim and Young Hee Lee

Center for Integrated Nanostructure Physics, Institute for Basic Science (IBS), Sungkyunkwan University, Suwon 16419, South Korea  
[kimj@skku.edu](mailto:kimj@skku.edu), [leeyoung@skku.edu](mailto:leeyoung@skku.edu)

Van der Waals (vdW) layered materials have great potential for optoelectronic devices, such as photodetectors, photovoltaics with efficient power conversion, and high-speed memory/switching devices [1-3]. Reduced dimensionality in the vdW layered materials provides strong Coulomb interaction with a large exciton binding energy of about 0.3~1 eV in a monolayer although these values are scaled down to less than 0.1 eV by charge screening in thin film. Here, we will discuss the photoexcited excitons and structure dynamics of 2H-MoTe<sub>2</sub> by using femtosecond pump-probe spectroscopy. When photoexcited charge carrier density in the vdW layered material is sufficiently low, exciton-exciton scattering prevails over exciton-phonon scattering which makes efficient carrier multiplication phenomena more competitive with other relaxation pathways due to the strong Coulomb coupling (Fig. 1a) [4]. When the carrier density is over 10<sup>14</sup> cm<sup>-2</sup> per monolayer, the structural deformation from semiconducting to metallic phases occurs (Fig. 1b). This phase transition is fully reversible within a picosecond via light control.

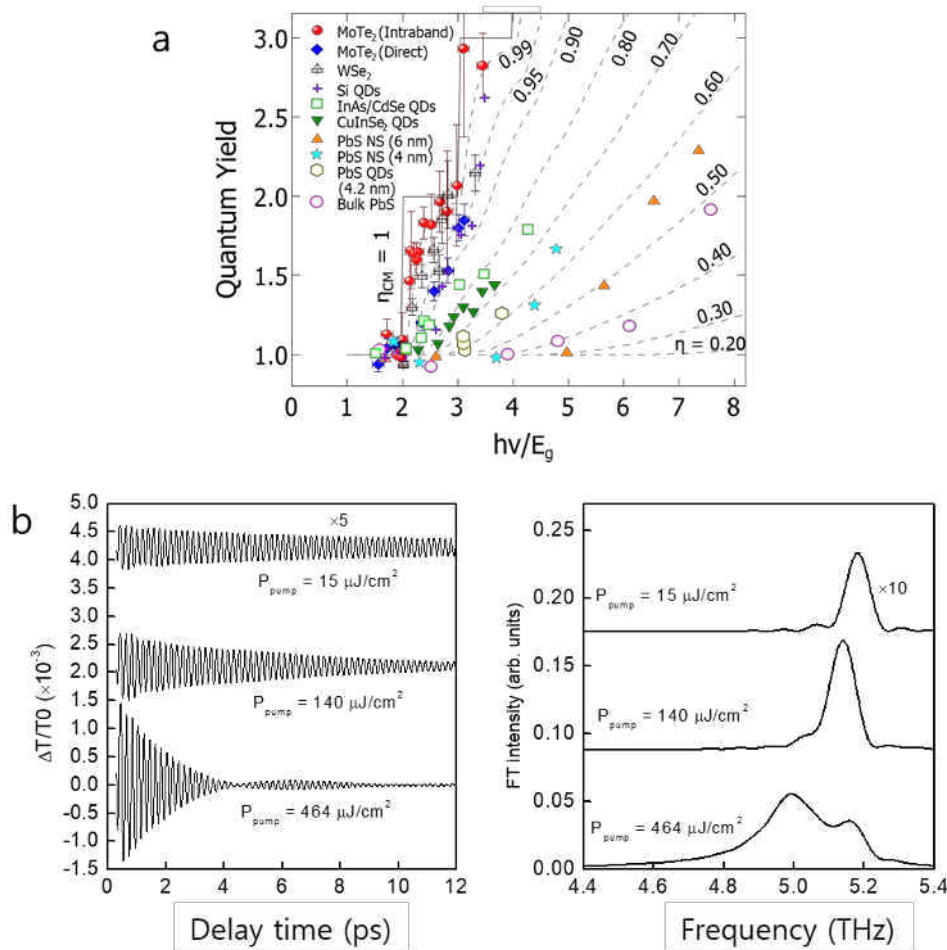


Fig. 1. (a) Carrier multiplication conversion efficiency in various nanostructure including 2H-MoTe<sub>2</sub>. (b) Coherent phonon oscillations and Fourier transformation spectra with different pump fluence.

- [1] Dung-Sheng Tsai, Keng-Ku Liu, Der-Hsien Lien, Meng-Lin Tsai, Chen-Fang Kang, Chin-An Lin, Lain-Jong Li, and Jr-Hau He, ACS Nano 7, 3905 (2013).
- [2] He Tian, Bingchen Deng, Matthew L. Chin, Xiaodong Yan, Hao Jiang, Shu-Jen Han, Vivian Sun, Qiangfei Xia, Madan Dubey, Fengnian Xia, and Han Wang, ACS Nano 10, 10428 (2016).
- [3] Meng-Lin Tsai, Sheng-Han Su, Jan-Kai Chang, Dung-Sheng Tsai, Chang-Hsiao Chen, Chih-I Wu, Lain-Jong Li, Lih-Juann Chen, and Jr-Hau He, ACS Nano 8, 8317 (2014).
- [4] Ji-Hee Kim, Matthew R. Bergren, Jin Cheol Park, Subash Adhikari, Michael Lorke, Thomas Fraunheim, Duk-Hyun Choe, Beom Kim, Hyunyoung Choi, Tom Gregorkiewicz, and Young Hee Lee, arXiv:1801.01675.

# Nonlinear optics and transport of excitons in two-dimensional crystals

**M.M. Glazov**

*Ioffe Institute, 194021, St.-Petersburg, Russia  
glazov@coherent.ioffe.ru*

Two-dimensional transition metal dichalcogenides form a family of direct-band semiconductors with strong excitonic effects. Due to relatively large effective masses of the charge carriers and rather weak screening of the Coulomb interaction Wannier-Mott excitons with the binding energies on the order of several hundreds of millielectronvolts dominate the optical properties of these exemplary two-dimensional materials. Excitons form a series of  $1s$ ,  $2s$ ,  $2p$ , etc., hydrogen-like states. The exciton wavefunctions and binding energies deviate from the two-dimensional hydrogenic series mainly due to specific screening of the Coulomb interaction in two-dimensional systems.

Here we present the results of theoretical and experimental investigations of several nonlinear optical and transport effects on excitons in  $\text{MX}_2$  monolayers, where  $M$  is the transition metal and  $X$  is the chalcogen ( $M=\text{Mo}, \text{W}$  and  $X=\text{S}, \text{Se}$  as a rule).

First, we address two-photon absorption by excitons. We show that both  $s$ - and  $p$ -excitons are active in two-photon processes. This is because  $\text{MX}_2$  monolayers lack an inversion center. The symmetry of the monolayers allows for the mixing of the  $s$ - and  $p$ -excitons. Moreover, it allows linear in the wavevector terms in the interband transition matrix element. Both effects contribute to the two-photon activity of  $s$ -excitons. By contrast, the two-photon absorption on  $p$ -excitons does not require any symmetry reduction [1].

Due to simultaneous single and two-photon activity of excitons, the second harmonic generation becomes possible. In this nonlinear process a given state is excited by the two photons and emits coherently a single photon of a double frequency. We demonstrate the second harmonic emission it is strongly enhanced if the fundamental frequency is twice smaller than the exciton resonance frequency. The mechanisms of the second harmonic are established [1].

Furthermore, we study the exciton-mediated upconversion, i.e., the two-photon absorption where the single photon energy is close to the exciton energy. Due to efficient Auger process one of the photocreated excitons recombines nonradiatively transferring its energy to another one. It gives rise to the upconversion photoluminescence [2].

Finally, we study excitonic transport in two-dimensional  $\text{MX}_2$  semiconductors. Depending on the exciton density three regimes of exciton transport can be identified. First, in the linear regime exciton-exciton interactions are unimportant and the excitons simply diffuse in the monolayer plane. Second, with an increase in the exciton density the Auger recombination comes into play making exciton distribution in the real space more flat and giving rise to an increase of the apparent diffusion coefficient. Third, for even higher densities the memory effects become important and a halo-like distribution of excitons in the real space is formed with a dip at the excitation spot [3].

[1] M. M. Glazov, L. E. Golub, G. Wang, X. Marie, T. Amand, and B. Urbaszek, Phys. Rev. B **95**, 035311 (2017).

[2] M. Manca, M. M. Glazov, C. Robert, F. Cadiz, T. Taniguchi, K. Watanabe, E. Courtade, T. Amand, P. Renucci, X. Marie, G. Wang, B. Urbaszek, Nature Communications **8**, 14927 (2017).

[3] A. Chernikov, M.M. Glazov, et al., Nonlinear exciton propagation and halo effects in atomically thin semiconductors, in press.

## Tuning of optical gap in layered gallium selenide

N.R. Arutyunyan<sup>1</sup>, E.A. Obratsova<sup>2</sup>, D.V. Rybkovsky<sup>3,1</sup>, E.D. Obratsova<sup>1</sup>

<sup>1</sup> A.M. Prokhorov General Physics Institute RAS, Vavilova st. 38, Moscow 119991, Russia

<sup>2</sup> M.M. Shemyakin and Yu.A. Ovchinnikov Institute of Bioorganic Chemistry RAS, Miklukho Maklaya st. 16/10, Moscow 117997, Russia

<sup>3</sup> Skolkovo Institute of Science and Technology (Skoltech), Nobelya Ulitsa 3, Moscow 121205, Russia

Corresponding author: natalia.arutyunyan@gmail.com

Due to the unusual sombrero-like shape of the top of the valence band [1], few-layered gallium selenide (GaSe) is of great interest for the applications in optoelectronics, as photodetectors or non-linear optical elements. Depending on the thickness of the layer, the shape of the valence band and the value of bandgap changes [1-4]. For the bulk material valence band has a maximum at  $\Gamma$  point. If the crystal has only few layers, the parabolic-like shape of the top of the valence band transforms into sombrero-like, when there is a local minimum at  $\Gamma$  point, surrounded by ring-shape maximum. The optical bandgap for the bulk material is about 2 eV. When the thickness of the crystal becomes smaller, the optical bandgap should increase up to 3.2 eV for single tetralayer [5].

Here, the Raman and photoluminescence spectra of few-layered GaSe crystals, produced on the Si:SiO<sub>2</sub> wafers by micro-mechanical exfoliation (Fig.1), are presented. The shift of the luminescence band (Fig.2) as well as the evolution of the Raman bands is shown. The degradation of the GaSe flakes due to the oxidation and appearance of the amorphous Se under the laser beam is discussed.

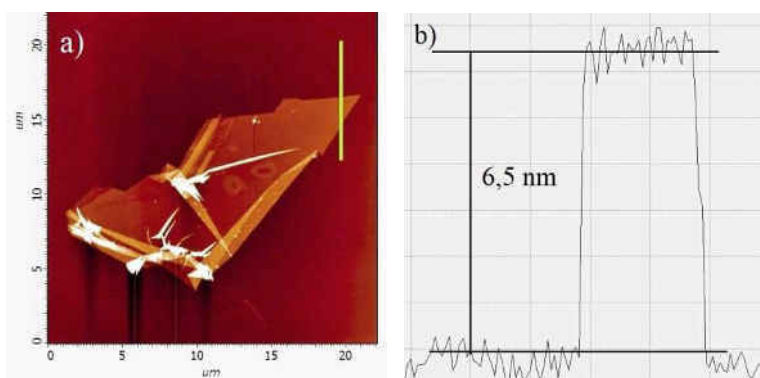


Fig.1. a) Few-layered flake of GaSe on Si:SiO<sub>2</sub> b) The profile of the height of the flake, which corresponds to 7 tetralayers.

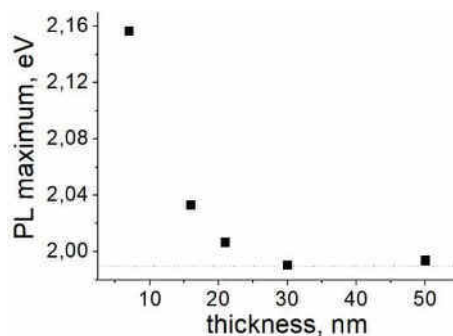


Fig.2. Positions of photoluminescence bands for flakes of various thickness (from 6 nm to bulk material).

[1] D.V. Rybkovskiy, A. V. Osadchy, and E. D. Obratsova, PRB **90**, 235302 (2014).

[2] D. V. Rybkovskiy, N. R. Arutyunyan, A. S. Orekhov, I. A. Gromchenko, I. V. Vorobiev, A. V. Osadchy, E. Yu. Salaev, T. K. Baykara, K. R. Allahverdiev, and E. D. Obratsova, PRB **84**, 085314 (2011).

[3] D. Andres-Penares, A. Cros, J.P. Martínez-Pastor and J. F. Sánchez-Royo, Nanotechnology **28** 175701 (2017).

[4] Z. Ben Aziza, D. Pierucci, H. Henck, M. G. Silly, C. David, M. Yoon, F. Sirotti, K. Xiao, M. Eddrief, J.-C. Girard, and A. Ouerghi, PRB **96**, 035407 (2017).

[5] Gabriel Antonius, Diana Y. Qiu, and Steven G. Louie, Nano Letters **18**, 1925 (2018).

## Wednesday, August 8



©Yu. Svirko



## Photocurrents in Weyl semimetals of gyrotropic classes

**E.L. Ivchenko**

*Ioffe Institute of RAS, 26 Politekhnicheskaya, 194021 Saint-Petersburg, Russia*  
[ivchenko@coherent.ioffe.ru](mailto:ivchenko@coherent.ioffe.ru)

In the past decade, the discoveries of topological insulators and Weyl semimetals (WSMs) have taken center stage in condensed matter science. After neutrinos were found to possess a small mass, the electrons near accidental band touching points, or Weyl nodes, in the Brillouin zone of WSMs remain the only particles with a massless linear energy dispersion and a definite chirality. Unlike the original elementary Weyl fermions, in solids the dispersion cones can be tilted or even overtilted which is realized, respectively, in type I and type II WSMs. The topological properties of WSMs manifest themselves in the chiral anomaly in the presence of parallel electric and magnetic fields, topological surface states (Fermi arcs) and topological charges (monopoles) in the reciprocal  $\mathbf{k}$ -space.

The discovery of WSMs has been followed by both theoretical and experimental studies of their transport and optical properties, linear and nonlinear. In particular, it has been shown that the interaction of circularly-polarized light with chiral fermions is governed by the Berry curvature of the Weyl node. This allows a new look at the Circular PhotoGalvanic Effect (CPGE), an appearance of a helicity-dependent electric photocurrent upon shining circularly-polarized light on the sample [1]. This effect is allowed by the symmetry of gyrotropic (or optically active) media, and many WSMs belong to the family of gyrotropic crystals. It has been demonstrated that, in each Weyl valley, the CPGE reveals universal features independent of details of the material. However, in the Weyl node of opposite chirality the CPGE current has the opposite polarity. As a result, the net current induced within two Weyl nodes of opposite chirality becomes nonvanishing only in tilted WSMs where it, however, loses its universality and depends on the tilt parameter.

In Refs. [2,3] we have developed a theory of the circular photogalvanic effect in Weyl semimetals with the point groups containing improper symmetry operations, mirror-reflection planes and rotoinversion axes, and proposed minimal models which allow for the CPGE. In semimetals of the  $C_{2v}$  symmetry with the linear energy dispersion, the net CPGE photocurrent becomes nonzero taking into account a spin-independent tilt term in the electron effective Hamiltonian. However, this is insufficient for the crystal class  $C_{4v}$ , like the TaAs Weyl semimetal. In this case one needs to add to the Hamiltonian not only the tilt but also spin-dependent terms of the second or third order in the electron quasi-momentum referred to the Weyl node.

We have complementarily investigated the magneto-gyrotropic photogalvanic effect, i.e. the generation of a photocurrent under unpolarized excitation in a magnetic field. In quantized magnetic fields, the photocurrent is caused by optical transitions between the one-dimensional magnetic subbands. A value of the photocurrent is particularly high if one of the photocarriers, an electron or a hole, is excited to the chiral subband with the energy below the cyclotron energy.

[1] E. L. Ivchenko, *Optical Spectroscopy of Semiconductor Nanostructures* (Alpha Science Int., Harrow, UK, 2005)

[2] L. E. Golub, E. L. Ivchenko and B. Z. Spivak, JETP Lett. **105**, 782 (2017).

[3] L. E. Golub and E. L. Ivchenko, arXiv:1803.02850.



## Validity of Dirac and Weyl fermion picture for $\text{Cd}_3\text{As}_2$ and transition metal monpnictides

O. Pulci<sup>1</sup>, D. Grassano<sup>1</sup>, A. Mosca Conte<sup>2</sup>, F. Bechstedt<sup>3</sup>

<sup>1</sup>Universita' di Roma Tor Vergata, Via della Ricerca Scientifica 1, 00133 Rome, Italy

<sup>2</sup>Mediterranean Institute of Fundamental Physics, Via Appia Nuova, Marino, Italy

<sup>3</sup>Friedrich-Schiller-Universität, Max-Wien-Platz 1, 07743 Jena, Germany

Corresponding author: olivia.pulci@roma2.infn.it

Topological semimetals have opened a new fascinating field for solid-state physicists. Despite strong spin-orbit interaction (SOI), significant band overlap gives rise to linear bands and Dirac cones in these three-dimensional (3D) bulk solids. Gapless electronic excitations, Dirac or Weyl fermions, which are protected by topology and symmetry, appear. While Dirac semimetals, e.g.  $\text{Cd}_3\text{As}_2$ , possess both time-reversal and inversion symmetry, one of these symmetries is broken in Weyl semimetals such as TaAs, TaP, NbAs, and NbP (see Fig. 1). The overlap of Ta5d- and Nb4d-derived conduction and valence bands leads to electron and/or hole pockets near the Fermi level at the 24 Weyl nodes. The semimetals are investigated by means of ab initio methods for atomic geometries and electronic structures but also optical properties. They are interpreted as 3D analogues of graphene. However, in contrast to two-dimensional graphene the Dirac physics does not yield to a constant IR absorbance ruled by the Sommerfeld finestructure constant [1]. Instead, in 3D a linear frequency increase is predicted for the optical conductivity. Indeed, the bct structure of the  $\text{Cd}_3\text{As}_2$ , as a Dirac semimetal, exhibits this behavior. However, the Dirac fermions appear only for small excitation energies, whereas Kane electrons are found for larger energies [2]. Weyl fermions are discussed for topological Weyl semimetals, especially bct TaAs, with 12 pairs of W1 or W2 Weyl nodes, comparing with ARPES results and measured optical spectra [3]. Linear bands lead to an optical conductivity varying linearly with frequency, thereby indicating the Weyl character for small photon energies. This behavior is, however, modified by band occupation, anisotropy, light polarization, and trivial carriers and even destroyed for larger energies.

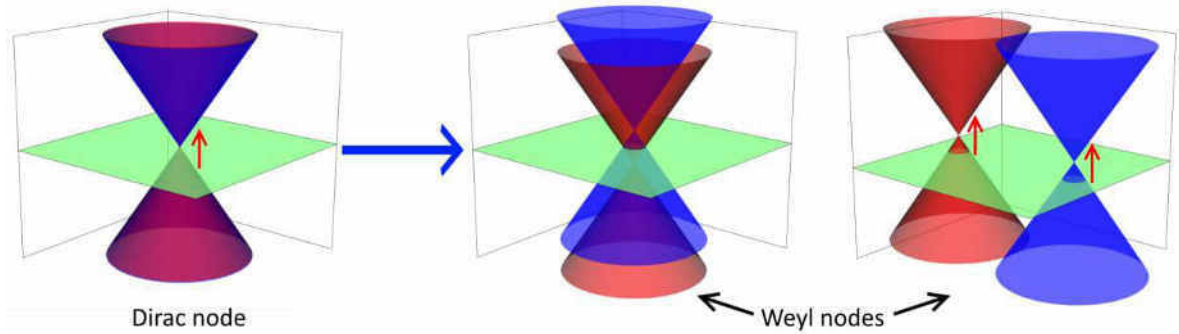


Fig. 1 Splitting of a Dirac node into Weyl nodes violating time-reversal or inversion.

### References

- [1] L. Matthes, O. Pulci, F. Bechstedt, Phys. Rev. B **78**, 035438 (2013).
- [2] A. Mosca Conte, O. Pulci, F. Bechstedt, Scientific Reports **7**, 45500 (2017).
- [3] D. Grassano, O. Pulci, F. B., Scientific Reports **8**, 3534 (2018).

# Multi-Particle Excitations in Doped Single-Walled Carbon Nanotubes

**T.V. Eremin<sup>1,2,5</sup>, P.A. Obraztsov<sup>2,3</sup>, V.A. Velikanov<sup>2,4</sup>, T.V. Shubina<sup>5</sup>, E.D. Obraztsova<sup>2</sup>**

<sup>1</sup> Faculty of Physics of M.V. Lomonosov Moscow State University, Leninskie Gory Str. 1, 119991 Moscow, Russia

<sup>2</sup> A.M. Prokhorov General Physics Institute, RAS, 38 Vavilov street, 119991, Moscow, Russia

<sup>3</sup> Department of Physics and Mathematics, University of Eastern Finland, Joensuu, Finland

<sup>4</sup> National Research Nuclear University, Moscow Engineering Physics Institute, 31 Kashirskoe Highway, 115409 Moscow, Russia

<sup>5</sup> Ioffe institute, RAS, Politechnicheskaya street, 26, 194021 St Petersburg, Russia

[timaeremin@yandex.ru](mailto:timaeremin@yandex.ru)

Doping of single-walled carbon nanotubes leads to spectacular changes of their optical and electronic properties. Commonly used doping technique via filling of nanotubes with dopants deal with films or powder of nanotubes making photoluminescence studying complicated due to fast irradiative relaxation of electronic excitations in bundles. However, doping can also be performed via adding of dopants to the solution of individual nanotubes.

We report a comprehensive study of changes of optical properties of single-walled carbon nanotubes caused by doping in acid medium. In this work, hydrochloric acid was added to an aqueous solution of nanotubes wrapped with sodium cholate. Besides the suppression of RBM modes in a Raman scattering spectrum and the suppression of the first optical transition in an optical absorption spectrum, we observed the emergence of a new band in a photoluminescence spectrum at approximately 200 meV below the main photoluminescence band (Fig. 1a). This new band was assigned to trions, quasiparticles consisting of two holes and one electron [1]

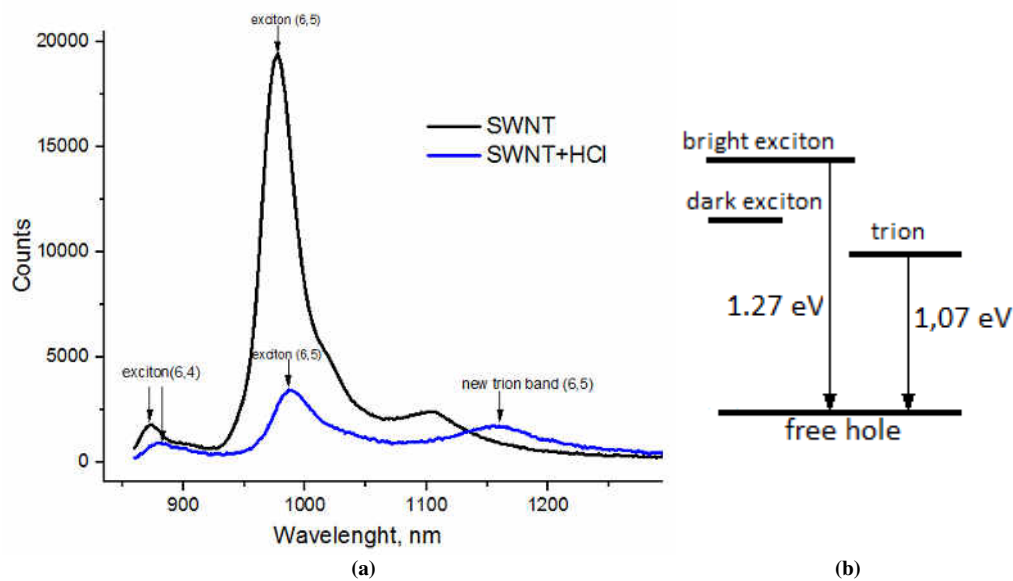


**Fig.1** (a) Photoluminescence spectrum of initial SWNT suspension (black line) and SWNT suspension with added HCl (blue line).

Excitation wavelength is 570 nm (b) Energy level diagram.

**Acknowledgements.** This work was supported by RFBR project 17-302-50008. This work was partially supported by Russian Science Foundation grant #17-72-10303 and Academy of Finland Grant #318596. T.V.S. appreciates the partial support by the Government of the Russian Federation (contract # 14.W03.31.0011 at the Ioffe Institute of RAS).

[1] Matsunaga, Ryusuke, Kazunari Matsuda, and Yoshihiko Kanemitsu. "Observation of charged excitons in hole-doped carbon nanotubes using photoluminescence and absorption spectroscopy." *Physical review letters* 106.3 (2011): 037404.

# Raman spectroscopy of two-dimensional materials and related heterostructures

Ping-Heng Tan<sup>1,2</sup>

<sup>1</sup>State Key Laboratory of Superlattices and Microstructures, Institute of Semiconductors, Chinese Academy of Sciences, Beijing 100083, China

<sup>2</sup>CAS Center of Excellence in Topological Quantum Computation, and College of Materials Science and Opto-Electronic Technology, University of Chinese Academy of Science, Beijing 100049, China.

Corresponding author e-mail: phtan@semi.ac.cn

Two-dimensional materials (2DMs), such as graphene and transition metal dichalcogenides (TMDs), have been under intensive investigation. The rapid progress of research on graphene and TMDs is now stimulating the exploration of different types of 2DMs. The atoms within each layer in 2DMs are joined together by covalent bonds, while van der Waals interactions keep the layers together to form multilayer 2DMs, which makes the physical and chemical properties of 2DMs strongly dependent on their thickness (or layer numbers). These various 2DMs could be re-stacked/assembled horizontally or vertically in a chosen sequence to form van der Waals heterostructures (vdWHs), which can offer huge opportunities for designing the functionalities of such heterostructures. Two or more 2DMs with similar properties can be alloyed into a new type of 2DMs, namely, 2D alloy, which can offer tunable band gaps for promising applications in nanoelectronics and optoelectronics. Except the isotropic 2DMs such as graphene and 2H TMDs, anisotropic 2DMs such as black phosphorus (BP), SnSe, rhenium disulfide and rhenium diselenide (ReSe<sub>2</sub>) have one more degree of freedom to deliver various physical properties.

Raman spectroscopy is becoming increasingly important in the area of 2DMs. Raman spectroscopy can reveal information on the crystal structure, electronic structure, lattice vibrations and flake thickness of 2DMs, and can be used to probe the strain, stability, charger transfer, stoichiometry, and stacking orders of 2DMs. In particular, the unique interlayer vibrations have been widely used to develop a substrate-free layer-number identification of 2DMs, and to probe the strength of interlayer coupling in 2DMs and the interface coupling in artificial vdWHs. Here, we will review the recent advances on Raman spectroscopy in the characterization of different kinds of 2DMs and the corresponding 2D alloy and vdWHs. We will show that Raman spectroscopy is an ideal tool to probe the fundamental physics and potential applications of these various 2DMs, particularly when they are reduced down to monolayers or multilayers.

## Acknowledgement.

We acknowledge support from the National Key Research and Development Program of China (Grant No. 2016YFA0301204), the National Natural Science Foundation of China (Grant No. 11474277 and 11434010), the Key Research Program of the Chinese Academy of Sciences (Grant No. XDPB06-02, XDPB08-2), and Beijing Municipal Science and Technology Commission.

# All-carbon mixed-dimensional van der Waals heterostructures: diffusion and atomic scale deformations

Kimmo Mustonen<sup>1</sup>, Aqeel Hussain<sup>2</sup>, Rasim Mirzayev<sup>1</sup>, Christoph Hofer<sup>1</sup>, Mohammad Monazam<sup>1</sup>, Toma Susi<sup>1</sup>, Esko I. Kauppinen<sup>2</sup>, Jani Kotakoski<sup>1</sup> and Jannik C. Meyer<sup>1</sup>

<sup>1</sup> Faculty of Physics, University of Vienna, Boltzmanngasse 5, A-1090 Vienna, Austria<sup>SEP</sup>

<sup>2</sup> Department of Applied Physics, Aalto University School of Science, P.O. Box 15100, FI-00076 Aalto, Finland

kimmo.mustonen@univie.ac.at

Carbon nanomaterials—including fullerenes, nanotubes and graphene—have been among the most studied structures in materials science during the past decades. Building on enormous advances in graphene research, interest has recently shifted towards the creation of so-called van der Waals heterostructures (vdWHs) [1-3]. Such materials typically combine graphene or other two- or lower dimensional molecules into vertical stacks [2-3]. The leading idea of the concept is to preserve the covalent bonding structure of the constituent molecules interacting mainly through van der Waals forces (vdW), all the while allowing strong electronic and light-matter interactions in between and within the constituent layers [4-6].

My talk will cover our recent work in fabrication and characterization of mixed-dimensional all carbon vdWHs, including buckyball sandwiches incorporating monolayers of C<sub>60</sub> molecule in between two graphene sheets and single-walled carbon nanotubes (SWCNTs) likewise suspended on graphene [7,8]. In the former our room temperature scanning transmission electron microscope experiments reveal, among other things, truncated intermolecular spacing, the diffusion and rotation of individual C<sub>60</sub> molecules at room temperature and finally the seizing of such motion upon merging in the electron irradiation. By acquiring several atomically resolved projections of SWCNTs on graphene the 3D shape of the interface is reconstructed through energy minimization [9], showing morphological aberrations emerging from the interlayer vdW forces. We further show that these topographic features are strain correlated but show no sensitivity to SWCNT helicity or electronic structure. Finally, we show that in an atomically clean heterostructure the competition between strain and vdW forces result in aligned carbon-carbon interfaces in some cases spanning up to several hundreds of nanometers.

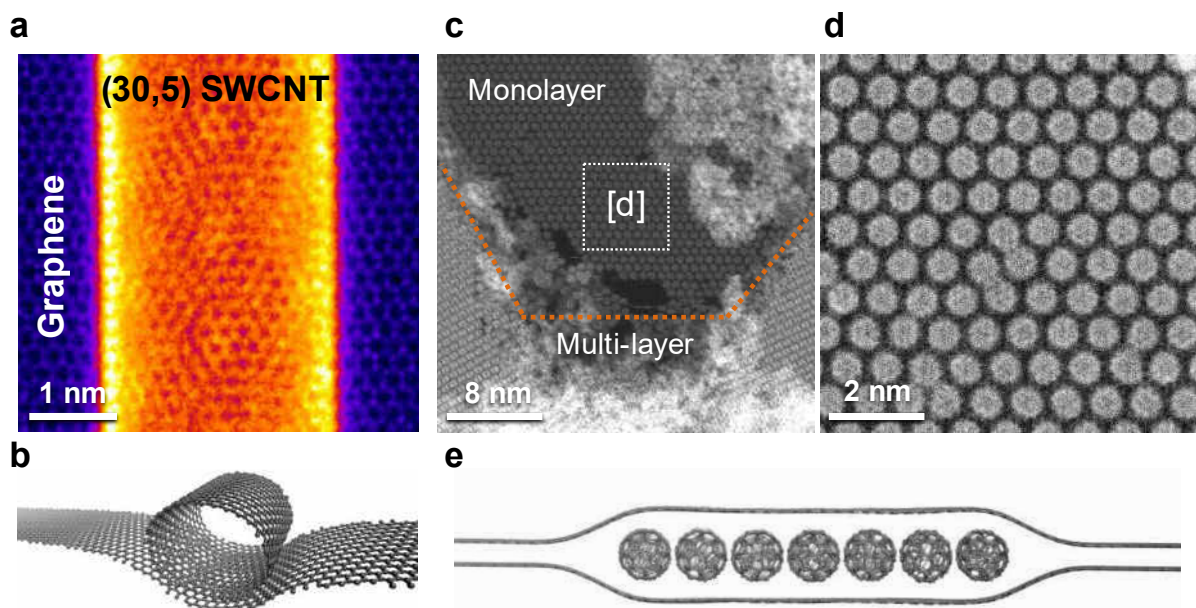


Fig. 1 **a**) A (30,5) SWCNT suspended on graphene and **b**) the recovered 3D structure of the molecular pair. **c**) An overview of a buckyball sandwich showing both mono- and multi-layer regions and **d**) an atomically resolved magnification of the monolayer and finally in **e**) a simulated sandwich structure.

[1] Geim, A. K. & Grigorieva, I. V. Van der waals heterostructures. *Nature* **499**, 419–425 (2013).

[2] Jariwala, D. *et al.* Mixed-dimensional van der waals heterostructures. *Nature materials* (2016).<sup>SEP</sup>

[3] Liu, Y. *et al.* Van der waals heterostructures and devices. *Nature review materials* **1**, 16042 (2016).<sup>SEP</sup>

[4] Britnell, L. *et al.* Strong light-matter interactions in heterostructures of atomically thin films. *Science* **340**, 1311–1314 (2013).

[5] Zheng, Q. *et al.* Phonon-assisted ultrafast charge transfer at van der waals heterostructure interface. *Nano letters* **17**, 6435–6442 (2017).

[6] Gjerding, M. N. *et al.* Layered van der waals crystals with hyperbolic light dispersion. *Nature communications* **8**, 320 (2017).

[7] Mirzayev, R. *et al.* Buckyball sandwiches. *Science Advances* **3**, e1700176 (2017).

[8] Mustonen, K. *et al.* atomic-scale deformations at the interface of a mixed-dimensional van der Waals heterostructure ,Submitted.

[9] Hofer, C. *et al.* Revealing the 3D structure of graphene defects, Submitted.

# Single-Carbon-Nanotube Manipulations and Devices Based on Macroscale Flakes

Boyuan Shen, Yunxiang Bai, Zhenxing Zhu, Jinyan Zhang, Huanhuan Xie and Fei Wei\*

*Beijing Key Laboratory of Green Chemical Reaction Engineering and Technology, Department of Chemical Engineering, Tsinghua University, Beijing 100084, China  
E-mail: wf-dce@tsinghua.edu.cn*

Because of the outstanding mechanical and electrical properties of carbon nanotubes (CNTs), a CNT-based torsion pendulum is demonstrated to show great potential in nano-electromechanical systems. It is also expected to achieve various manipulations for further characterization and increase device sensitivity using ultralong CNTs and macroscale moving parts. However, the reported top-down method limits the CNT performance and device size by introducing inevitable contamination and destruction, which greatly hinders the development of single-molecule devices. Here, a bottom-up method is introduced to fabricate heterostructures of anthracene flakes (AFs) and suspended CNTs, providing a nondamaging CNT mechanical measurement before further applications, especially for the twisting behavior, and providing a controllable and clean transfer method to fabricate CNT-based electrical devices under ambient conditions. Based on the unique geometry of CNT/AF heterostructures, various complex manipulations of single-CNT devices are conducted to investigate CNT mechanical properties and prompt novel applications of similar structures in nanotechnology. The AF-decorated CNTs show high Young's modulus ( $\approx 1$  TPa) and tensile strength ( $\approx 100$  GPa), and can be considered as the finest and strongest torsional springs. CNT-based torsion balance enables to measure fN-level forces and the torsional spring constant is two orders of magnitude lower than previously reported values.

We fabricate centimeters long CNT bundles (CNTBs) composing of ultralong defect-free CNTs with tensile strength over 80 GPa and specific tensile strength over 50 GPa/(g/cm<sup>3</sup>). We find that the tensile strength of CNTBs is controlled by the Daniels effect due to the nonuniformity of the initial strains in the bundle components. A synchronous tightening and relaxing strategy is proposed to release the nonuniform initial strains of the CNTB components. For CNTBs consisting of a large number of components with parallel alignment, defect-free structures, continuous lengths and uniform initial strains, the tensile strength is as high as 80 GPa, which is far higher than that of any other strong fibers ever fabricated.

- [1] R. Zhang, Q. Wen, W. Qian, D. S. Su, Q. Zhang, F. Wei, *Adv. Mater.* 2011, 23, 3387.
- [2] Z. Zhu, N. Wei, H. Xie, R. Zhang, Y. Bai, Q. Wang, C. Zhang, S. Wang, L. Peng, L. Dai, F. Wei, *Sci. Adv.* 2016, 2, e1601572.
- [3] R. Zhang, Z. Ning, Y. Zhang, Q. Zheng, Q. Chen, H. Xie, Q. Zhang, W. Qian, F. Wei, *Nat. Nanotechnol.* 2013, 8, 912.
- [4] R. Zhang, Z. Ning, Z. Xu, Y. Zhang, H. Xie, F. Ding, Q. Chen, Q. Zhang, W. Qian, Y. Cui, F. Wei, *Nano Lett.* 2016, 16, 1367.
- [5] R. Zhang, Y. Zhang, Q. Zhang, H. Xie, H. Wang, J. Nie, Q. Wen, F. Wei, *Nat. Commun.* 2013, 4, 1727.
- [6] Boyuan Shen, Zhenxing Zhu, Jinyan Zhang, Huanhuan Xie, Yunxiang Bai and Fei Wei, *Adv. Mater.* 2017, 1705844

# Nanocarbon materials for short-pulse fiber lasers and photonic devices

**Shinji Yamashita**

*Research Center for Advanced Science and Technology, The University of Tokyo, 4-6-1, Komaba, Meguro-ku, Tokyo, 153-8904, Japan  
syama@ee.t.u-tokyo.ac.jp*

We review the optical properties of carbon nanotubes (CNTs) and graphene, and describe how those properties have been used for the implementation of various nonlinear fiber optic applications. Early studies on the optical properties of CNTs revealed that these materials exhibit high third order susceptibility and a broadband saturable absorption with a sub-picosecond response time. Recent discovery of similar nonlinear optical properties in graphene attracts much attention in this field. Such ultrafast, highly nonlinear optical response means that they can be employed for noise suppression and for the mode-locking of fiber lasers, and their high third order nonlinearity holds great promise for the implementation of various other nonlinear fiber optic devices such as wavelength converters based on four wave mixing. In addition, absorption in graphene is known to be controllable by the adjustment of its Fermi level, which can lead to the electrically controllable optical modulators.

In this talk, we will discuss the various methods that have been considered thus far for the integration of CNTs and graphene in optical systems and highlight the advantages and limitations of using the saturable absorption of CNTs and graphene for the passive mode-locking of fiber lasers, and the current status of CNT and graphene saturable absorbers in the state of art fiber laser technologies. We also introduce our works on nonlinear photonic devices and optical modulators using CNT and graphene.

## References

- [1] S. Yamashita, "A tutorial on nonlinear photonic applications of carbon nanotube and graphene (Invited Tutorial)," *Journal of Lightwave Technology*, vol.30, no.4, pp.427-447, Feb. 2012.
- [2] A. Martinez, B. Xu and S. Yamashita, "Nanotube based nonlinear fiber devices for fiber lasers (Invited)," *Journal of Selected Topics in Quantum Electronics*, vol.20, no.5, pp.89-98, Sept. 2014.
- [3] S. Yamashita, A. Martinez, and B. Xu, "Short pulse fiber lasers mode-locked by carbon nanotube and graphene (Invited)," *Optical Fiber Technology*, vol.20, no.6, pp.702-713, Dec. 2014.
- [3] S. Yamashita, Y. Saito, and J. H. Choi (ed.), *Carbon nanotubes and graphene for photonic applications*, Woodhead Publishing, 2013.

## Nonlinear optics with low-dimensional materials

Zhipei Sun

*Department of Electronics and Nanoengineering, Aalto University, Tietotie 3, FI-02150, Finland  
QTF Centre of Excellence, Department of Applied Physics, Aalto University, FI-00076 Aalto, Finland  
Corresponding author Zhipei.sun@aalto.fi*

In this talk, I will discuss our recent results on nonlinear optics with one-dimensional (e.g., carbon nanotubes [1]) and two-dimensional layered (e.g., graphene [2-3], transition metal dichalcogenides [3-5], and black phosphorus [6-7]) materials. These results show advantages of utilizing low-dimensional nanomaterials for various photonic and optoelectronic applications, such as high-purity quantum emitters [1], wavelength converters [2-5], and ultrafast lasers [2,6,7]. Further, I will present our recent advances employing hybrid structures, such as two-dimensional heterostructures [2], plasmonic structures [8-10], and silicon/fibre waveguides integrated structures [8-10].

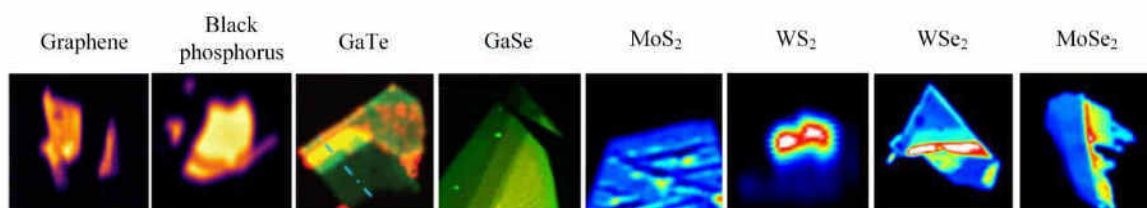


Figure 1. Nonlinear optical images of different two-dimensional layered materials [10]

### References

- [1] K. F. Lee *et al.*, Adv. Mater. **29**, 1605978 (2017); C. Li *et al.*, Adv. Mater. **29**, 1701580 (2017).
- [2] Z. Sun *et al.*, Nat. Photon. **10**, 227(2016); A. Martinez *et al.*, Nat. Photon. **7**, 842(2013).
- [3] F. Bonaccorso *et al.*, Nat. Photon. **4**, 611(2010); F. Bonaccorso, Z. Sun, Opt. Mater. Exp. **4**, 63(2014).
- [4] A. Säynätjoki *et al.*, Nat. Commun. **8**, 893(2017).
- [5] L. Karvonen *et al.*, Nat. Comm. **8**, 15714(2017).
- [6] D. Li, *et al.*, Sci. Rep. **5**, 15899 (2015); D. Li, *et al.*, Appl. Mater. Tod. **4**, 17(2016)
- [7] A. Autere *et al.*, J. Phys. Chem. Lett. **8**, 1343(2017); G. Hu, *et al.*, Nat. Commun. **8**, 278 (2017); H. Yang, *et al.*, ACS Photonics, **4**, 3023 (2017).
- [8] H. Hu *et al.*, Nat. Comm. **7**, 12334 (2016); X. Yang *et al.*, Adv. Mater. **28**, 2931(2016); D. Hu *et al.*, Nat. Comm. **8**, 1471 (2017); X. Yang *et al.*, Adv. Mater. DOI: 10.1002/adma.201704896 (2018).
- [9] H. Jussia *et al.*, Optica **3**, 151 (2016); H. Jussia *et al.*, ACS Omega **2**, 2630 (2017).
- [10] A. Autere *et al.*, Adv. Mater. DOI: 10.1002/adma.201705963 (2018); D. Li *et al.*, 2D Mater. **4**, 025095 (2017).

## Tunable nonlinear optical response from 2D materials

**Shiwei Wu**

*Fudan University, Shanghai 200433, China  
e-mail: swwu@fudan.edu.cn*

Atomically thin two dimensional materials such as graphene and transition metal dichalcogenide monolayers have recently spurred a great of interests due to their unique mechanic, electronic, optical and magnetic properties. And often these properties could be greatly tuned by external stimuli such as electric, magnetic and force field. Individual member in this class of 2D materials is characteristic in term of structural symmetry. Moreover, the structural symmetry could also be tuned, depending on how monolayers are stacked on one another. These variations in symmetry have given rise to even richer properties among different 2D materials and their homo-/hetero-structures. Therefore, they provide a new playground for nonlinear optics because of its sensitivity to structural symmetry. Vice versa, nonlinear optics becomes a powerful technique to study 2D materials. In this talk, I will present some of our recent results on nonlinear optical microscopy and spectroscopy of 2D materials [1-4].

- [1] T. Jiang, H.R. Liu, D. Huang, S. Zhang, Y.G. Li, X.G. Gong\*, Y.R. Shen, W.T. Liu\*, S.W. Wu\*, Nature Nanotechnology 9, 825-829 (2014).
- [2] J.X. Cheng, T. Jiang, Q.Q. Ji, Y. Zhang, Z.M. Li, Y.W. Shan, Y.F. Zhang, X.G. Gong, W.T. Liu, S.W. Wu\*, Advanced Materials 27, 4069-4074 (2015).
- [3] Xu Zhou, Jingxin Cheng, Yubing Zhou, Ting Cao, Hao Hong, Zhimin Liao, Shiwei Wu\*, Hailin Peng\*, Kaihui Liu\*, Dapeng Yu, Journal of the American Chemical Society 137, 7994-7997 (2015).
- [4] Tao Jiang, Di Huang, Jinluo Cheng, Xiaodong Fan, Zhihong Zhang, Yuwei Shan, Yangfan Yi, Yunyun Dai, Lei Shi, Kaihui Liu, Changgan Zeng, Jian Zi, J.E. Sipe, Yuen-Ron Shen, Wei-Tao Liu, Shiwei Wu, arXiv: 1710.04758.



## Synthesis and properties of SWCNT@FWBNNT -- Single-walled carbon nanotubes co-axially wrapped with mono- and few-layer boron nitride nanotubes --

Rong Xiang<sup>1</sup>, Taiki Inoue<sup>1</sup>, Yongjia Zheng<sup>1</sup>, Ming Liu<sup>1</sup>, Jia Guo<sup>1,2</sup>, Yan Li<sup>1,2</sup>, Shohei Chiashi<sup>1</sup>, Shigeo Maruyama<sup>1,3</sup>

<sup>1</sup> *Department of Mechanical Engineering, The University of Tokyo, Tokyo 113-8656, Japan*

<sup>2</sup> *College of Chemistry and Molecular Engineering, Peking University, Beijing 100871, China*

<sup>3</sup> *Energy Nano Engineering Lab., National Institute of Advanced Industrial Science and Technology (AIST), Ibaraki 305-8564, Japan*

We propose a conceptually new structure, in which mono- or few BN layers seamlessly wrap around a single-walled carbon nanotube (SWNT), and result in an atomically smooth coaxial tube consisting two different materials, as shown in Fig. 1. The structure is synthesized by chemical vapor deposition (CVD). As the reaction occurs on outer surface of the existing SWNTs, we name this process conformal CVD. Various SWNTs, e.g. vertically aligned array, horizontally aligned arrays, suspended SWNTs, random network and films, are employed as the starting material, and successful coating are achieved on all of them. Our characterizations confirm that the outside BN coating started locally on the wall of a SWNT and then merge into a BN nanotube on the curved surface of the SWNT which served as a template. The number of walls can be tuned from 1 to few by controlling the CVD condition. The structure of inside SWNTs are almost not effected by the conformal CVD, as evidenced by Raman and many other characterizations. The crystallization and cleanness of the starting SWNT template are believed to be critical for the successful fabrication of outside walls. This structure is expected to have a broad interest and impact in many fields, which include but not limited in investigating the intrinsic optical properties of environment-isolated SWNTs, fabricating BN-protected or gated SWNT devices, and building more sophisticated 1D material systems.

### Acknowledgement.

Part of this work was supported by JSPS KAKENHI Grant Numbers JP25107002 and JP15H05760.

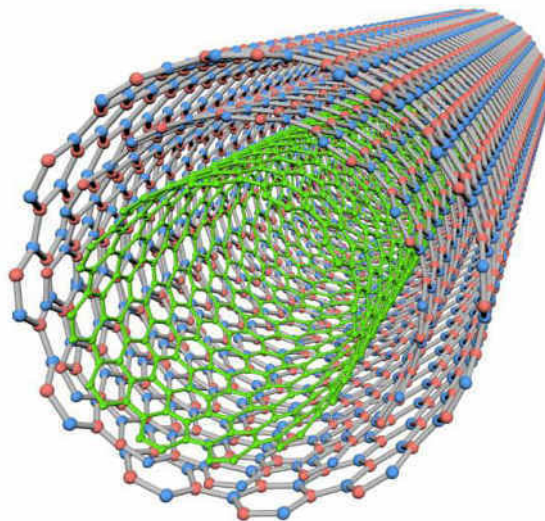


Fig.1 Schematic structure of an SWCNT wrapped with a bilayer BN nanotube.

## Surface-enhanced Raman detection of individual single-walled carbon nanotubes and single molecules inside

Juan Yang, Daqi Zhang, Chenmaya Xia, Yan Li\*

*College of Chemistry and Molecular Engineering, Peking University, Beijing 100871, China.  
yanli@pku.edu.cn*

The resonant Raman spectroscopy can only detect on-resonance single-walled carbon nanotubes (SWNTs) within the laser resonance window. In principle, surface-enhanced Raman scattering (SERS) spectroscopy can expand the resonance window. However, detection of off-resonance SWNTs by SERS remains challenging due to the difficulties in locating the SWNTs exactly at the hot spots with enormous SERS enhancements. Here, we report a facile ultrasonic spray pyrolysis method to in-situ form closely spaced polyhedral gold nanocrystals (AuNCs) on SWNTs. The fact that the edges of the AuNCs attach to the SWNTs ensures the location of SWNTs at the hot spots. Consequently, we achieve enormous enhancements that enable the detection of many off-resonance SWNTs. The enormous enhancements also allow the detection of several new Raman bands of the SWNTs that have not been reported previously.

The study of single-molecule (SM) behaviour can provide fundamental physical and chemical information otherwise obscured by the ensemble averaging due to the existence of vast molecules and accessible microstates. Large efforts have been made to immobilize the single molecules in order to in-situ study the SM behaviour. Here, we used SWNTs to encapsulate and immobilize single molecules. The interior of the nanotube can serve as a nanoscale confined space with definite and uniform environments to facilitate the SM study. We utilize SERS to achieve the ultrasensitivity that can detect the SM signals and to provide the chemical specificity that can distinguish different molecular moieties via the vibrational fingerprints. We show that a single molecule located inside the SWNT and at the SERS hot spot can not only be unambiguously detected, but also provide non-blinking and stable SERS signals with little spectral wandering, whereas signal fluctuations including temporal blinking, intensity variation, and spectral wandering are widely considered as the characteristic behaviour of single molecules in the SERS community. This approach opens new possibilities toward SM chemistry and physics in nanoscale confined space.

## Experimental evidence of electronic Raman scattering in individual double-walled carbon nanotubes

**D. I. Levshov<sup>1</sup>, M. V. Avramenko<sup>1</sup>, J.-L. Sauvajol<sup>2</sup>, M. Paillet<sup>2</sup>**

*1- Department of Nanotechnology, Faculty of Physics, Southern Federal University, Rostov-on-Don, 5 Zorge Str., 344090, Russia*

*2- Laboratoire Charles Coulomb, University of Montpellier, Montpellier, France  
avramenko.marina@gmail.com*

Electronic Raman scattering (ERS) previously observed in metallic [1] and semiconducting [2] individual single-walled carbon nanotubes (CNTs) and their small bundles [3, 4] has been registered in individual double-walled CNTs for the first time allowing one to obtain additional information on peculiarities of their electronic structure. All individual double-walled CNTs were carefully examined by a combination [5] of such experimental methods as electron diffraction, high resolution transmission electron microscopy, Rayleigh and Raman scattering spectroscopies at different excitation wavelengths. In a number of structure-identified double-walled CNTs good ERS signal has been obtained and analyzed.

This work was supported by the RFBR grant No. 18-32-00397 mol\_a.

[1] H. Farhat, S. Berciaud, M. Kalbac et al., *Phys. Rev. Lett.*, **107**, 157401 (2011).

[2] X. Chen, B. Zhu, A. Zhang et al., *Sci. Rep.*, **4**, 5969 (2014).

[3] D. Zhang, J. Yang, E. H. Hasdeo et al., *Phys. Rev. B*, **93**, 245428 (2016).

[4] D. Zhang, J. Yang, M. Li et al., *ACS Nano*, **10**, 10789 (2016).

[5] D. I. Levshov, H. N. Tran, M. Paillet et al., *Carbon*, **114**, 141 (2017).

## Poster session I



©G. Lepehin



# Geometry-controllable nanohair structure effects cellular movement

Chaejeong Heo<sup>a,b</sup>, Chanho Jeong<sup>c</sup>, Hyeon Seong Im<sup>c</sup>, and Tae-il Kim<sup>c</sup>

*a. Center for Integrated Nanostructure Physics (CINAP), Institute for Basic Science (IBS), Suwon 16419, Republic of Korea.*

*b. Sungkyunkwan University (SKKU), Suwon, Korea.*

*c. School of Chemical Engineering, Sungkyunkwan University (SKKU), Suwon 16419, Republic of Korea.*

Corresponding author, Chaejeong Heo, [neuroheo@gmail.com](mailto:neuroheo@gmail.com)

Vertical pillars in cicada wing have a biocidal feature of rupturing the membrane of bacterial cells [1], while angled pillars of cactus spine can guide a water droplet flow toward the stem [2]. These phenomena have evolved from their respective unique directional structures. Here, we endeavor to develop geometry-controllable nanohairs that mimic the cicada's wing-like vertical hairs and the cactus spine-like stooped hairs, and to quantitatively characterize the cell migration behavior on the hairy structures. It was found that the neuronal cells are highly sensitive to the variation of surfaces: flat, vertical, and stooped 100 nm diameter and 900 nm height hairs. The cells on the vertical hairs showed significantly decreased proliferation. It was also found that the behavior of cells cultured on stooped nanohairs is strongly influenced by the direction of the stooped pattern of hairs when we quantitatively measured the migration of cells on flat, vertical, and stooped structures. However, the cells on the flat structures showed random movement and the cells on the vertical nanohairs restricted the nanohair movement. Cells on the stooped structure showed higher forward migration preference compared to that of the other structures. Furthermore, we found that these cellular behaviors on the different patterns of nanohairs were affected by intracellular actin filament change. Consistent with these results, the vertical and stooped structures can facilitate the control of cell viability and guide directional migration for many biomedical applications such as organogenesis and wound healing processes.

## Figures

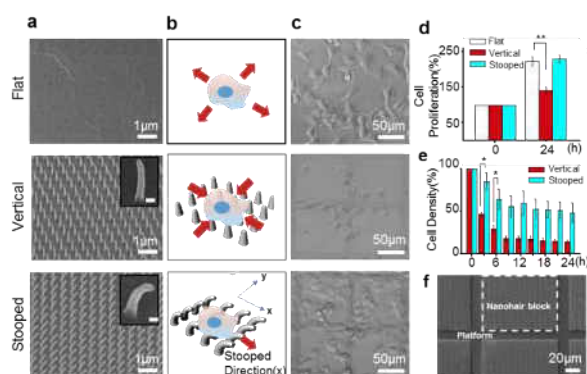


Fig. 1. a) SEM images of nanohair patterned substrates for flat, vertical, and stooped hairs made of PUA polymer. b) Illustration of the expected cell behavior on different types of nanostructures. c) SHSY5Y cells image on the three different substrates after 24 hours. d) Proliferation of cells on each substrate after 24 hours. Flat and stooped nanohair substrates show similar proliferation rate, while the vertical nanohair substrate has a significantly lower rate. Two-tailed Student's t-test: \*\*,  $p < 0.01$ . e) Graph shows migrating cells' density from the nanohair block (white dashed box in f) to the platform. Two-tailed Student's t-test: \*,  $p < 0.05$ . f) Position of nanohair block and platform area.

**Acknowledgement** This work is supported by the IBS-R015-D1 and the Pioneer Research Center Program (NRF-2014M3C1A3001208) through the National Research Foundation of Korea funded by the Ministry of Science, ICT and Future Planning

## References

- [1] E. P. Ivanova, J. Hasan, H. K. Webb, V. K. Truong, G. S. Watson, J. A. Watson, V. A. Baulin, S. Pogodin, J. Y. Wang, M. J. Tobin, C. Lobbe, R. J. Crawford, *Small*, **8**, 2489 (2012).
- [2] J. Ju, H. Bai, Y. M. Zheng, T. Y. Zhao, R. C. Fang, L. Jiang, *Nat. Commun.*, **3**, 1247 (2012).

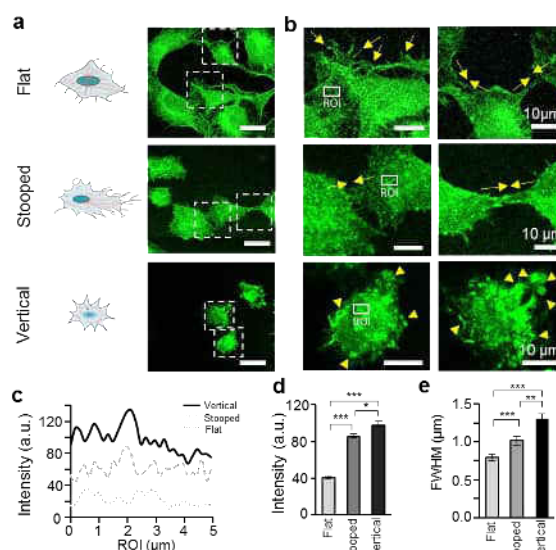


Fig. 2. a) Schematic cell shape and actin filament (F-actin) fluorescence images show the intracellular actin filamentous structure of the neuronal cells on flat, vertical, and stooped nanohairs. b) Magnified images of boxes in (a) and yellow arrows indicate the protruding direction of the F-actin in filopodia and yellow arrow-heads represent the small aggregated form of F-actin which is clearly observed in the vertical nanohair group. c) Fluorescence intensity profile of intracellular region of cells grown on each substrate and d) average intensity profile of each group. e) FWHM of the intensity profile shows a gradual increase of the sharpness of the nanohair structure ( $n = 20$  in each group).



# Pristine and Platinum-deposited metallic Molybdenum ditelluride for Hydrogen Evolution Reaction

Jinbong Seok, Jun-Ho Lee, Byungdo Ji, Young-Woo Son, Suyeon Cho and Young Hee Lee, Heejun Yang

Jinbong Seok, Byungdo Ji, Prof. Young Hee Lee, Prof. Heejun Yang

Department of Energy Science, Sungkyunkwan University, Suwon 16419, Korea.

Jinbong Seok, Prof. Young Hee Lee

IBS Center for Integrated Nanostructure Physics (CINAP), Institute for Basic Science, Sungkyunkwan University, Suwon 16419, Korea.

Dr. Jun-Ho Lee, Prof. Young-Woo Son

Korea Institute for Advanced Study, Seoul 02455, Korea.

Prof. Suyeon Cho

Division of Chemical Engineering and Materials Science, Ewha Womans University, Seoul 03760, Korea.

*h.yang@skku.edu, s.cho@ewha.ac.kr*

## 1. Abstract

Electrochemical catalysts based on transition metal dichalcogenides (TMDs) have been intensively studied in hydrosulfurization, hydrogenation, and the hydrogen evolution reaction (HER) [1-3]. Moreover, TMDs have polymorphism, which has stimulated extensive studies on tuning of surface electronic structures for active HER. The polymorphism in TMDs provides an opportunity for new hybrid catalysts with TMDs and other catalytic metals via surface engineering that can create novel facets of the catalytic metals for active HER. Here, we report a hybrid catalyst with monoclinic MoTe<sub>2</sub> and platinum (Pt) for the HER. Pt atoms were decorated on the surface of monoclinic MoTe<sub>2</sub> that has an atomically-distorted lattice structure, which produces a distinct Pt-Te alloy layer. The Pt/MoTe<sub>2</sub> hybrid catalyst exhibits an active HER with a Tafel slope of 22 mV per decade and an exchange current density of 1.0 mA/cm<sup>2</sup>, which are the best values among those reported for TMD-based catalysts. The decoration of catalytic metals on atomically-distorted metallic TMDs realizes rich catalytic active sites on large basal planes for efficient hydrogen production.

## 2. Figures and tables

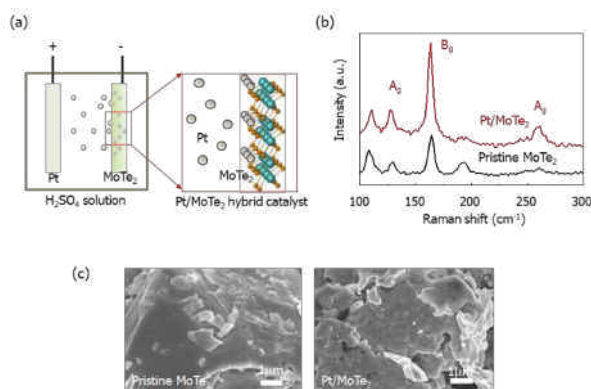


Figure 1: Preparation of Pt/MoTe<sub>2</sub> hybrid catalyst a) Schematic picture b) Raman spectra c) Scanning electron microscope (SEM) images

## 3. References

- [1] R.R. Chianelli, M.H. Siadati, M.P. De la Rosa, et al, Cat. Rev. - Sci. Eng., 48 (2006) 1
- [2] Y. Qu, H. Pan, C.T. Kwok, Sci Rep., 6 (2016) 34186
- [3] M. Chhowalla, H.S. Shin, G. Eda, L.-J. Li, K.P. Loh, H. Zhang, Nat. Chem., 5 (2013) 236

# Carbon Nanotube Film Flexible Terahertz Detectors on Polymer Films with Series Electrodes for Sensitivity Enhancement

K. Li<sup>1</sup>, D. Suzuki<sup>1</sup>, Y. Ochiai<sup>1</sup>, M. Sun<sup>1</sup>, and Y. Kawano<sup>1</sup>

<sup>1</sup>Laboratory for Future Interdisciplinary Research of Science and Technology, Tokyo Institute of Technology,  
2-12-1, Ookayama, Meguro-ku, Tokyo 152-8550, Japan  
lee.k.al@m.titech.ac.jp

## 1. Introduction

Terahertz (THz) imaging has been attracting much attention for its strong possibility of powerful applications such as non-destructive in-line inspection and non-contact bio-sensing [1]. Nevertheless, conventional unbendable THz detectors have been unavailable to scan three dimensional objects whose surfaces are curved. To solve this problem, we have developed flexible THz imagers which consist of macroscopically bendable carbon nanotube (CNT) films [2-3] for multi-view THz imaging. However, the electrode shape of the CNT film THz detector remains unclear, and there is still room for improvement.

In this work, we clarified key parameters of the electrode structure that are directly linked to the sensitivity of THz detection, and also developed a fabrication method and device structure of CNT film THz detectors with better performances. We achieved the sensitivity enhancement by a factor of about 60, compared to the earlier type of CNT film THz detector.

## 2. Results

The mechanism of THz detection with our CNT film THz detectors is based on the photothermoelectric effect, and the THz response  $\Delta V$  can be calculated as follows:

$$\Delta V = \left| S_{CNT} - \frac{t_{Electrode} \sigma_{Electrode} S_{Electrode} + t_{CNT} \sigma_{CNT} S_{CNT}}{t_{Electrode} \sigma_{Electrode} + t_{CNT} \sigma_{CNT}} \right| \Delta T \quad (1)$$

where  $S_{CNT}$  and  $S_{Electrode}$  are the Seebeck coefficient of the CNT film and electrode,  $\Delta T$  is the temperature gradient generated by the THz irradiation,  $t_{CNT}$  and  $t_{Electrode}$  are the thickness,  $\sigma_{CNT}$  and  $\sigma_{Electrode}$  are the electrical conductivity, respectively. Based on the Equation (1), THz response is suppressed when the CNT film is much thicker than the electrode, resulting in low sensitivity of THz detection. Our previous CNT film THz detectors suffer from this technical difficulty regardless of type of electrode materials.

Here, we propose a refined device structure as shown in Figure 1 (a). We deposited the series electrode next to a hole on the polymer film, and then formed CNT film on the hole. The THz response detected with the present device structure can be described as:

$$\Delta V = |S_{CNT} - S_{Electrode}| \Delta T \quad (2)$$

Since we used p-type CNT film in this work, we used Bi ( $S_{Bi} = -77 \mu V/K$ ) as the series electrode, whose surface was covered with Au thin layer to protect Bi from the surface oxidation. Figure 1 (b) compares THz responses between the conventional and present structures. This result clearly shows that the THz response was dramatically enhanced through the present method, where the sensitivity of THz detection was enhanced by a factor of 58.5 compared to the conventional device design.

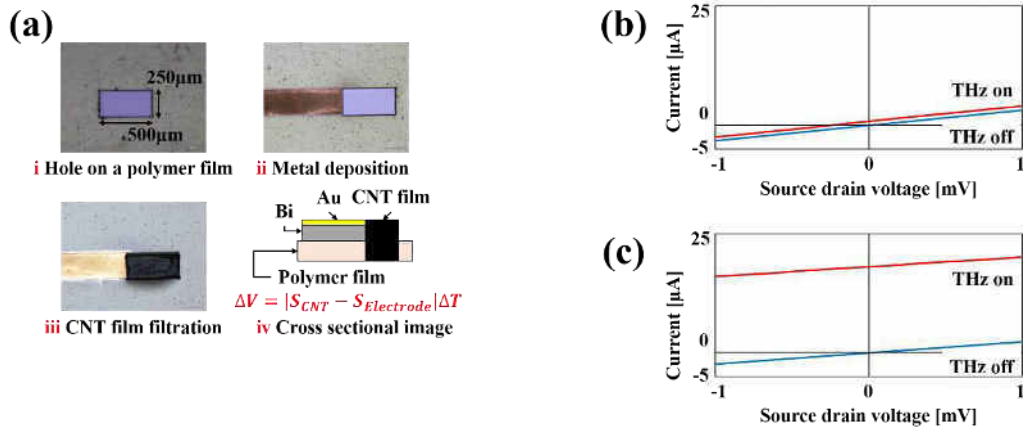


Fig.1 (a) Optical images of fabrication processes and schematic image of the present device structure. (b) Current-voltage characteristic of the conventional device under 29-THz irradiation. (c) Current-voltage characteristic of the present device under 29-THz irradiation.

## References

- [1] M. Tonouchi, *Nature Photonics*, 1, pp. 97-105 (2007)
- [2] D. Suzuki, S. Oda, and Y. Kawano, *Nature Photonics*, 10, pp. 809-814 (2016)
- [3] D. Suzuki, Y. Ochiai, and Y. Kawano, *ACS Omega*, 3, pp. 3540-3547 (2018)



# Terahertz absorption and emission tuning in graphene sandwich structures

**Batrakov K., Kuzhir P.**

*Institute for Nuclear Problems BSU,  
Tomsk State University (TSU)  
kgbatrakov@gmail.com*

Relatively simple graphene physical parameters regulation opens wide possibilities for different applications. Flexible and discrete tuning of electromagnetic wave-graphene interaction (EM transmission, absorption and emission) is important type of such applications that can be used for developing of detectors/sensors and EM sources, particularly in terahertz range. Our work presents EM interaction with sandwich structure [1]. Electromagnetic parameters tuning in that case can be provided by electrostatic doping of one or several sandwich layers (flexible tuning) or by varying the number of layers (discrete tuning). These tuning methods give possibility to change as strength, so the frequency range of interaction. Some examples of tuning are presented on Fig. 1. Fig 1a demonstrates dependence of graphene absorption on chemical potential ( $\mu$ ) for sandwich, Fig 1b shows dependence of Cherenkov emission resonance frequency on  $\mu$  for sandwich and Fig. 1c gives dependence of cyclotron resonant frequency on  $\mu$  for one graphene layer. It was shown that effective chemical potential for symmetric plasmon-polariton mode in graphene sandwich [1, 2] is a sum of chemical potentials of its layers. Therefore, combination of layers number and doping level of single levels gives possibility to realize conditions corresponding to Fig.1.

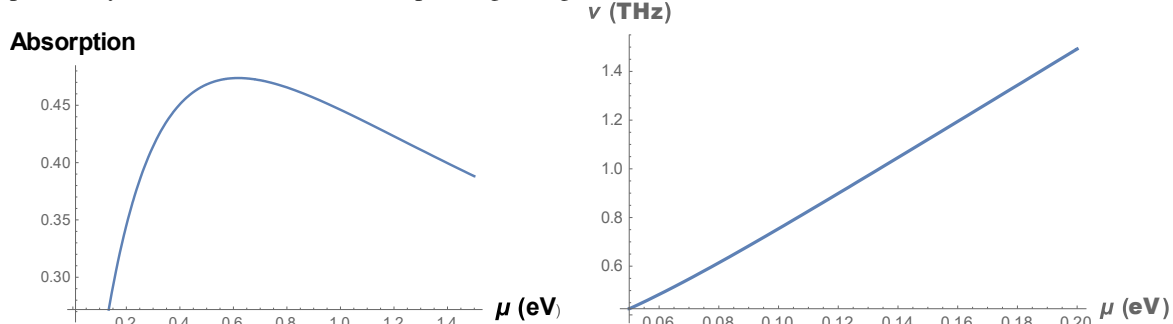


Fig 1a. Dependence of graphene absorption on chemical potential, frequency is 1 THz.

Fig 1b. Dependence of Cherenkov resonant frequency on chemical potential, energy of electron beam is 60 KeV.

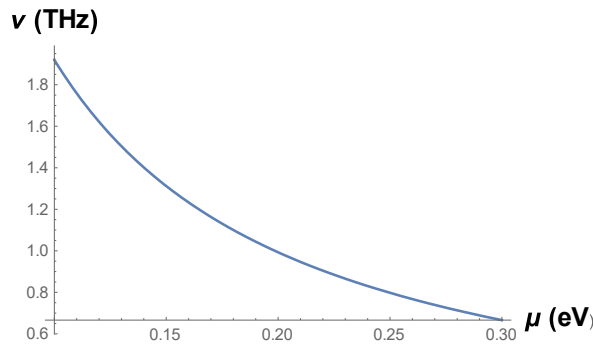


Fig. 1c Dependence of cyclotron frequency on chemical potential. Magnetic field strength is 1 T.

## Acknowledgement.

This work was supported by a grant EU Horizon 2020 Project No. H2020-644076 CoExAN.

## References

- [1] K Batrakov, P Kuzhir, S Maksimenko, et al, Scientific Reports, **4**, 7191 (2014)
- [2] K Batrakov, S Maksimenko, Physical Review B, **95** 205408 (2017)

# Gigahertz repetition rate dual-wavelength mode-locking of waveguide lasers with graphene

M.V. Ponarina, A.G. Okhrimchuk, M.G. Rybin, A.A. Tarakanovsky, T.V. Dolmatov,  
V.V. Bukin, I.V. Zhukhtova, V.A. Kamynin, P.A. Obraztsov  
Prokhorov General Physics Institute of RAS, Moscow, Russia  
[ponarinamariya@gmail.com](mailto:ponarinamariya@gmail.com)

Over the last few years much attention is paid to the development of high repetition rate (over 1 GHz) ultrafast lasers. These lasers are important for applications in telecommunications, frequency metrology and in fundamental physics. There are different approaches to achieve generation of ultrashort pulses with GHz repetition rates such as passive and active mode-locking of bulk or fiber solid-state lasers, semiconductor waveguide lasers and VCSELs. However, one of the simplest and compact design of mode-locked lasers with GHz repetition rate is based on a short plane parallel mirrors cavity, completely or almost completely filled with gain medium, containing saturable absorber, which provides passive mode-locking[1], [2]. An important condition for achievement of a stable mode-locking regime is operation in a fundamental transversal mode (TEM<sub>00</sub>).

Here we report an approach to build-up compact ultrafast lasers with gigahertz repetition rate based on the use of single-layer graphene saturable absorber mirror (GSAM) as the output coupler in waveguide solid-state laser. The stability of self-starting mode-locking can be efficiently controlled by applying the appropriate waveguide geometry[3], while the output lasing parameters and the repetition rate of ultrashort pulses can be precisely controlled by adjustment the gap between the active medium and the GSAM. In particular, due to very efficient coupling of pump light in the waveguide cavity and wavelength insensitive properties of graphene we demonstrate the possibility to achieve synchronous mode-locking at two or more central wavelengths using the same GSAM. We also demonstrate the applicability of the developed laser as a tunable master-oscillator for fiber-based amplified laser systems and achieved 530 mW output power using Yb-doped fiber amplifier.

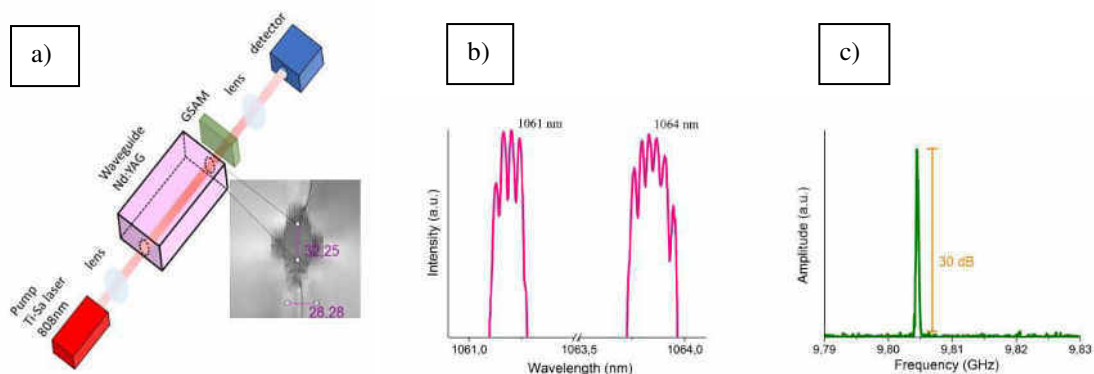


Fig.1. (a) The scheme of the waveguide Nd:YAG laser and obtained optical (b) and RF spectra (c)

Acknowledgement: The work was supported by the RSF grant # 17-72-10303

- [1] A. G. Okhrimchuk and P. A. Obraztsov, "11-GHz waveguide Nd: YAG laser CW mode-locked with single-layer graphene," *Sci. Rep.*, vol. 5, 2015.
- [2] P. A. Obraztsov, A. G. Okhrimchuk, M. G. Rybin, E. D. Obraztsova, and S. V. Garnov, "Multi-gigahertz repetition rate ultrafast waveguide lasers mode-locked with graphene saturable absorbers," *Laser Phys.*, vol. 26, no. 8, 2016.
- [3] A. Okhrimchuk, V. Mezentssev, A. Shestakov, and I. Bennion, "Low loss depressed cladding waveguide inscribed in YAG: Nd single crystal by femtosecond laser pulses," *Opt. Express*, vol. 20, no. 4, pp. 3832–3843, 2012.

## Raman spectra of nitrogen- and boron-doped carbon dots

**Tomskaya A.E., Egorova M.N., Smagulova S.A.**

*North-Eastern Federal University, Yakutsk, Russia  
ae.tomskaya@s-vfu.ru*

The term “carbon dot” implies a nano-sized carbon particle. The common methods of synthesizing CDs, such as hydrothermal and solvothermal methods, contribute to the formation of a crystalline carbon nucleus. The crystalline carbon core larger than 10 nm obtained by such methods does not correspond to a single-layer graphene flake and, in particular, can be a multilayer graphene flake. In this work, we call a carbon dot a certain nanometer-sized particle that has a thickness of 1–4 graphene layers and has functional groups on the surface and at the edges [1].

Synthesis of CDs is simple and does not require the use of expensive equipment, and the raw materials are affordable and cheap. The hydrothermal synthesis method is based on the high solubility of a large amount of organic matter in water at high temperature and pressure, and the possibility of subsequent crystallization of the dissolved material from the liquid phase. The control of vapor pressure, temperature and reaction time provides ample opportunities for the synthesis of high-quality CDs [2].

We report a simple synthesis of two types CDs using the hydrothermal treatment method. The goal of investigation of Raman spectroscopy of obtained CDs is to provide insight into the influence of the organic precursor (citric acid and ascorbic acid) on the properties of structure of the CDs. Besides, during synthesis CDs were doped by nitrogen and boron because N- and B-doped CDs can be used for many optoelectronic devices [3]. The N dopant can inject electrons [4] and B dopant can inject holes into carbon-based materials, thus changing the electronic and transport properties. The resulting CDs have a crystalline structure with functional groups on the surface and exhibit bright photoluminescence in the violet–green region of the spectrum. These synthesized CDs consist mostly of 1–4 layers having a uniform size of about ~10 nm, and the nitrogen and boron atoms were successfully introduced into the lattice of CDs.

Fig. 1 shows the Raman spectra of CDs and graphene oxide (suspension of graphene oxide was synthesized using the modified Hammers method, rather than the hydrothermal method). The identity of the spectra indicates that the CDs are small-sized flakes of graphene oxide. We identified that the ratio of  $I_D/I_G$  peaks changes while the synthesis characteristics change as the processing time and the initial composition of precursors.

The obtained results are useful for understanding the formation of the structure of CDs for further application in various applications of optoelectronics.

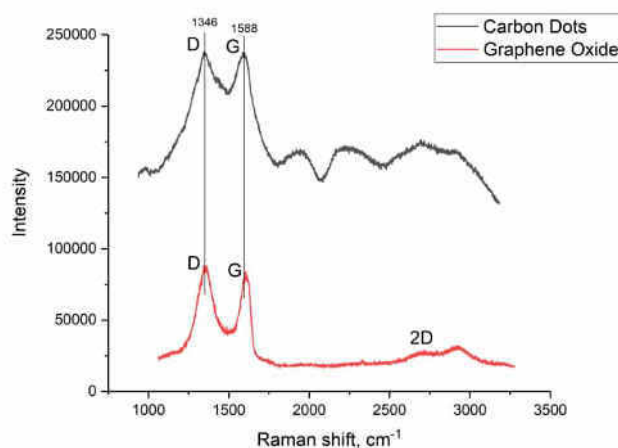


Fig. 1. Raman spectra of nitrogen-doped carbon dots (black line) and graphene oxide (red line).

- [1] A.E. Tomskaya, M.N. Egorova, A.N. Kapitonov, D.V. Nikolaev, V.I. Popov, A.L. Fedorov and S.A. Smagulova, *Physica Status Solidi* (b), **255**, 1700222 (2018).
- [2] A. A. Eliseev, A. V. Lukashin, *Functional Nanomaterials*, (Fizmatlit, Moscow, 2010).
- [3] Y. R. Park, H. Y. Jeong and Y. S. Seo, *Scientific Reports*, **7**, 1 (2017).
- [4] Z. Ma, H. Ming and H. Huang, *New Journal of Chemistry*, **36**, 861 (2012).

# Influence of electrochemical hydrogenation on the surface photocurrent in the Ag/Pd nanocomposite

A. S. Saushin, R. G. Zonov, V. M. Styapshin, E. V. Alexandrovich, G. M. Mikheev

*Institute of Mechanics, Udmurt Federal Research Center of the UB RAS, Izhevsk, Russia 426067*

*alex@udman.ru*

## 1. Introduction

Light-induced surface currents have attracted a considerable attention recently [1]. In our studies [2, 3] we have shown that Ag/Pd nanocomposite films are able to generate photon drag effect surface current. This allows one to employ this material, which is widely used in electronics, for visualizing polarization of powerful laser beams and/or spatial orientation of the Ag/Pd film with respect to the incident laser beam of an arbitrary wavelength. However in the Ag/Pd nanocomposite the photocurrent pulse duration is substantially longer than the duration of exciting laser pulses. That can be due to the presence of Schottky barriers, which are formed by PdO and Ag-Pd solid solution, in the film [4]. It is possible to remove these barriers with the electrochemical hydrogenation.

The aim of this work is the study of electrochemical hydrogenation influence on the temporal profile of the surface photocurrent pulses in the Ag/Pd nanocomposite.

## 2. Experimental and results

Ag/Pd nanocomposite films were produced in accordance with thick film technology based on burning of a special paste on a ceramic substrate. The size of the film obtained was 12.5×11 mm, while its thickness was about ~10 μm. To measure the photocurrent the film was provided with two parallel film electrodes which were arranged along the opposite sides of the film between the dielectric substrate and the Ag/Pd film.

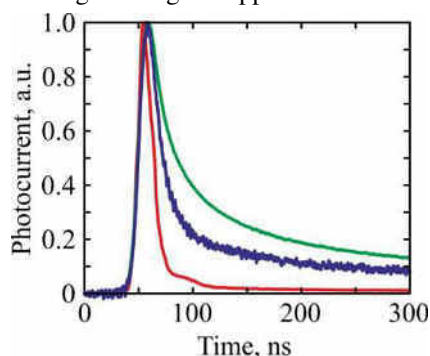


Fig. 1. Oscillograms of the photocurrent pulses before (green line) and after (blue line) electrochemical hydrogenation. Red line shows temporal profile of the excitation laser pulse.

Electrochemical hydrogenation was carried out in weak solution of sulfuric acid in distilled water. The film was placed as cathode into the electrochemical cell with stainless steel anode. Then the Ag/Pd film (cathode) was hydrogenated at a current density of 0.7 mA/cm<sup>2</sup>. After some time interval the film was taken out of electrolyte, washed in distilled water and dried. Further, the shapes of photocurrent pulses were recorded. The photocurrent was excited by *p*- and *s*-polarized 532 nm laser radiation. Then the processes of hydrogenating and measuring were repeated. The phase composition of Ag/Pd films was studied with a D2 PHASER X-ray diffractometer using CuK<sub>α</sub> radiation.

The oscillograms of photocurrent pulses before electrochemical hydrogenation and after 870 s are presented in Figure 1. The temporal profile of the laser pulses is presented as well. One can see that before the treatment the photocurrent pulse duration (~35 ns) significantly exceeds the corresponding parameter of the laser pulses (~15 ns).

Experiments showed that the electrochemical hydrogenation results in shortening of the current pulse time parameters. The photocurrent pulse duration after 870 s hydrogenation is about 21 ns. It is worth noting that the falling edge shape does not match the one before the treatment. Moreover, the electrochemical hydrogenation results in more than 3 times reduction of the photocurrent pulse amplitude. X-ray diffraction measurements showed reduction of the PdO content in the Ag/Pd film with hydrogenation time increase. These pulse changes due to electrochemical hydrogenation can be connected with disappearance of the enhancement effect, which is possible in Schottky barriers formed by PdO and Ag-Pd solid solution.

## 3. Conclusion

Thus in this work we have shown that the electrochemical hydrogenation of Ag/Pd nanocomposite leads to shortening of nanosecond laser excited photocurrent pulse and changing of its temporal profile.

## 3. Acknowledgement

This study was supported by the RFBR (Grant No. 18-32-00224).

## 4. References

- [1] M. Akbari and T. Ishihara, *Opt. Express*, **25**(3), 2143 (2017).
- [2] G. M. Mikheev, A. S. Saushin, R. G. Zonov and V. M. Styapshin, *Tech. Phys. Lett.*, **40**(5), 424 (2014).
- [3] G. M. Mikheev, A. S. Saushin and V. V. Vanyukov, *Quantum Electron*, **45**(7), 635 (2015).
- [4] G. M. Mikheev, A. S. Saushin, V. V. Vanyukov, K. G. Mikheev and Y. P. Svirko, *Phys. Solid State*, **58**(11), 2345 (2016).

# Bipolar polarization-sensitive surface photocurrent pulses in the Ag/Pd nanocomposite

A. S. Saushin<sup>1</sup>, V. M. Styapshin<sup>1</sup>, G. M. Mikheev<sup>1</sup>, Yu. P. Svirko<sup>2</sup>

<sup>1</sup>*Institute of Mechanics, Udmurt Federal Research Center of the UB RAS, Izhevsk, Russia 426067*

<sup>2</sup>*Institute of Photonics, University of Eastern Finland, 80101 Joensuu, Finland*

*alex@udman.ru*

## 1. Introduction

It is known that photon drag effect [1] (PDE) and surface photogalvanic effect [2] (SPGE) currents have a unique polarization and incidence angle dependencies. PDE and SPGE can be observed in centrosymmetric media. PDE photocurrent originates from the transfer of the photon momentum to a free charge carrier, while SPGE photocurrent is due to diffuse scattering of the photoexcited carriers in the subsurface layer. However, despite the different underlying physical mechanisms, these photocurrents have almost indistinguishable dependencies on the polarization and the angle of laser beam incidence.

In this work, we observed bipolar photocurrent pulses that results from a competition between PDE and SPGE in the film consisting of metal (Ag-Pd) and semiconductor (PdO) nanocrystallites.

## 2. Experimental and results

The Ag/Pd samples [3] were fabricated by using the thick-film technology, which is conventionally used to produce hybrid integrated circuits and other electronic devices. The fabricated films have a size of 20×20 mm<sup>2</sup> and thickness of 20 μm. To measure the photocurrent the sample was provided with two parallel film electrodes, which were arranged along the opposite sides of the film between the dielectric substrate and the Ag/Pd film.

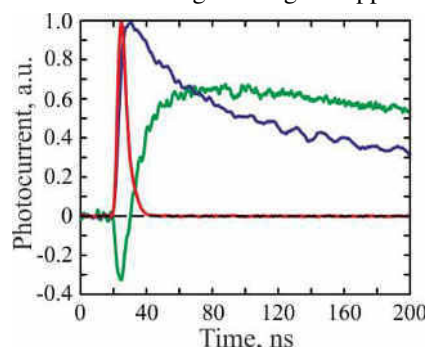


Fig. 1. Oscillograms of the photocurrent pulses induced by *s*-polarized (blue line) and the *p*-polarized (green line) laser beam. Red line shows temporal profile of the excitation laser pulse at 2000 nm.

We measured photocurrent in the Ag/Pd nanocomposite in the spectral range of 1064 – 4000 nm by using a *Q*-switched single-mode Nd<sup>3+</sup>:YAG laser (repetition rate 1Hz, pulse duration at half-height 19 ns) and optical parametric generator (pulse duration at half-height varied from 6 to 8 ns). The temporal profile of the laser pulses was revealed by the high-speed photodetectors and broadband oscilloscope. The photocurrent was excited by the laser beam passed through a half-wave plate. Rotating the half-wave plate, we controlled the polarization azimuth of the incident beam.

By performing measurements in the whole wavelength range of 1064 – 4000 nm we found that the *s*-polarized excitation beam produces unipolar photocurrent pulse, which shape is virtually independent of the wavelength (see Fig. 1). In contrast, the temporal profile of the photocurrent produced by the *p*-polarized laser beam essentially depends on the pump wavelength. Specifically, if the excitation wavelength is shorter than 1670 nm, the photocurrent is a unipolar pulse, which lasts longer than that produced by the *s*-polarized beam. However, at the excitation wavelength of 1670 nm, a negative pulse emerges at the leading edge of the positive longitudinal photocurrent. One can observe from Fig. 1 that at a wavelength of 2000 nm, the longitudinal photocurrent is transformed into a distinct bipolar pulse with a sharp negative front and a long positive tail. This is because of the simultaneous generation of the PDE and SPGE photocurrents, which have opposite polarities and different durations as well as different rise and fall times. A large number of photocurrent generation features are presented in the report.

## 3. Conclusion

Thus we demonstrate that the measurement of photoexcited currents in Ag/Pd nanocomposite allows us to visualize the interplay of the SPGE and PDE. This experimental finding provides a potential to visualize the excitation wavelength without using a spectrum analyzer, i.e. by non-optical means.

## 3. Acknowledgement

This study was supported by the RFBR (Grant No. 18-32-00224), the Academy of Finland (Grant No. 309672).

## 4. References

- [1] A. F. Gibson, M. F. Kimmitt and A. C. Walker, *Applied Physics Letters*, **17**(2), 75 (1970).
- [2] V. L. Alperovich, V. I. Belinicher, V. N. Novikov and A. S. Terekhov, *Sov. Phys. JETP*, **53**(6), 1201 (1981).
- [3] G. M. Mikheev, A. S. Saushin, O. Yu. Goncharov, G. A. Dorofeev, F. Z. Gil'mutdinov and R. G. Zonov, *Phys. Solid State.*, **56**(11), 2286. (2014).

# Investigation of the optical properties of single-walled carbon nanotubes doped in acid medium

**V. A. Velikanov<sup>1,2</sup>, T. V. Eremin<sup>2</sup>, E. D. Obratsova<sup>2</sup>**

<sup>1</sup>NRNU MEPhI, Moscow

<sup>2</sup> A.M. Prokhorov **General Physics Institute, RAS, 38 Vavilov street, 119991 Moscow, Russia**  
[velikanov-v@bk.ru](mailto:velikanov-v@bk.ru)

Single-walled carbon nanotubes have unique optical and electronic properties [1]. One of the most prominent features of carbon nanotubes is the strong correlation between carriers due to the quantum limitation that occurs in one-dimensional (1D) structures. The repulsive electron-electron and attractive electron-hole interactions play an important role in the electronic and optical properties and lead to the appearance of excitons with a significant binding energy [2]. The exciton is a quasiparticle, which is a bound state of an electron and a hole.

When doping nanotubes, trions may arise [3]. Trion is a quasiparticle, which is a triplet of electrons and holes bound by Coulomb forces.

In this paper, we study the change in the spectra of photoluminescence, Raman scattering and optical absorption when the nanotubes are doped with HCl acid. As a result, it is necessary to maintain a certain time interval between doping and measurement, and an increase in the trion peak with an increase in the doping level was observed. These results are shown in Fig. 1.

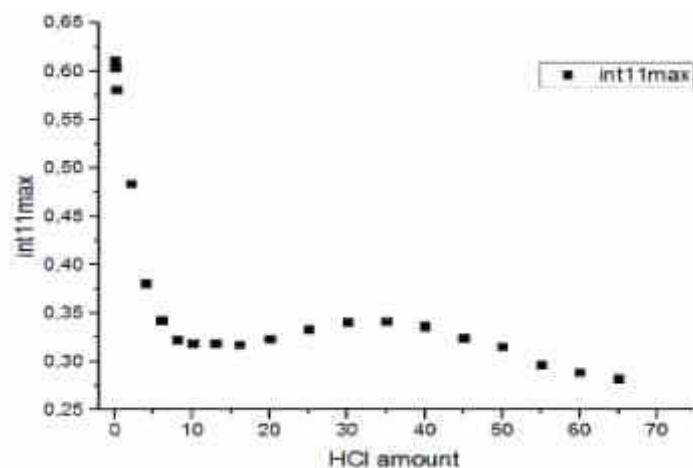


Fig. 1. Dependence of the maximum of the first exciton transition on the amount of added acid HCl (mL).

This work was supported by RFBR project 17-302-50008

[1] Saito, R.; Dresselhaus, G.; Dresselhaus, M. S. *Physical Properties of Carbon Nanotubes*; Imperial College Press: London, 1998.

[2] T. Ando, J. Phys. Excitons in carbon nanotubes Soc. Jpn. 66, 1066 (1997).

[3] Shinichiro Mouri, Yuhei Miyauchi, Munekiyo Iwamura and Kazunari Matsuda, Temperature dependence of photoluminescence spectra in hole-doped single-walled carbon nanotubes: Implications of trion localization, Japan, 2013.



## Investigation of multilayer MoS<sub>2</sub> film grown by CVD method on transferred CVD graphene

**P. V. Vinokurov, E. I. Zakharkina, A. A. Semenova, S. A. Smagulova**

*North-Eastern Federal University, 677000, Belinskogo str., Yakutsk, Republic of Sakha (Yakutia), Russia  
pv.vinokurov@s-vfu.ru*

Two-dimensional semiconductors such as MoS<sub>2</sub>, WS<sub>2</sub> are new family of materials with wide potential for applications in nano- and optoelectronics. Transition metal dichalcogenides (MoS<sub>2</sub>, WS<sub>2</sub>, WSe<sub>2</sub>, MoSe<sub>2</sub>) are a group of layered materials that can be separated into monolayers. The development and study of vertical Van der Waals heterostructures based on MoS<sub>2</sub>, WS<sub>2</sub>, and graphene is a promising task [1].

In this work we synthesize MoS<sub>2</sub> by CVD method on transferred CVD graphene. First of all, CVD graphene was transferred on SiO<sub>2</sub>/Si substrates by PMMA assisted method. After that, sample with CVD graphene and ordinary SiO<sub>2</sub>/Si substrate were placed in furnace (Nabertherm RS 80/750/11). The MoS<sub>2</sub> films were synthesized by annealing at 700C for 15 minutes in Ar flow.

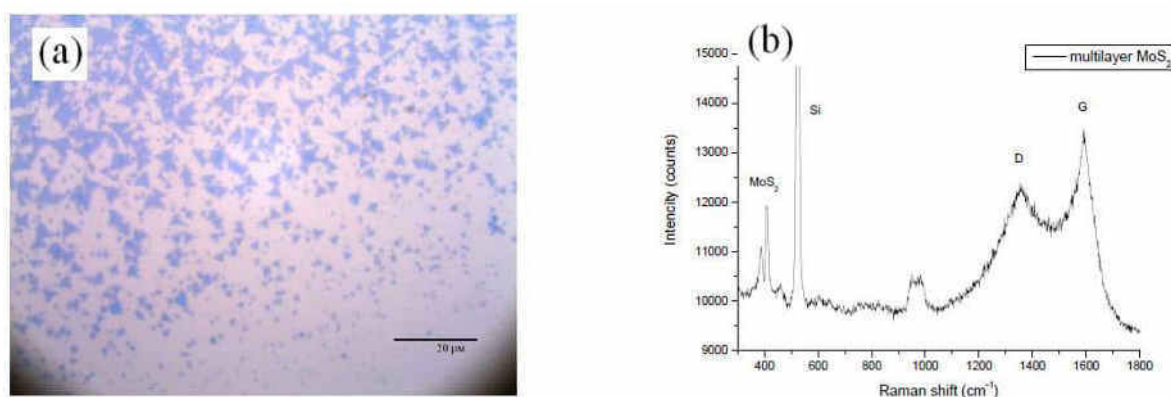


Fig.1. (a) Optical image of MoS<sub>2</sub> on SiO<sub>2</sub>/Si substrate; (b) Raman spectra of multilayer MoS<sub>2</sub> film grown on transferred CVD graphene.

In this work we present investigation of light effect on multilayer film of MoS<sub>2</sub>. There are two types of samples – with multilayer CVD graphene film on the surface of substrate and without. The first type of samples shows change in resistance under the influence of light, and there are no changes of the resistance in the second ones. Raman spectra of samples with CVD graphene showed weak carbon peaks even on area without graphene film, which can be connected with the transfer features. In samples with CVD graphene on it, we clearly saw the light influence on conductivity of MoS<sub>2</sub> films. Developing of clean MoS<sub>2</sub>/graphene interface will be key for fabrication of optoelectronic devices.

### Acknowledgement

The reported study was funded by RFBR according to the research project № 18-32-00730

### References

- [1] Q. Liu, B. Cook, M. Gong, Y. Gon, D. Ewing, M. Casper, A. Stramel, J. Wu, ACS Applied Materials & Interfaces **9**, 023189 (2017)

## Saturable absorption in detonation nanodiamond films

R. Yu. Krivenkov<sup>1</sup>, K. G. Mikheev<sup>1</sup>, T. N. Mogileva<sup>1</sup>, N. Nunn<sup>2</sup>, O. A. Shenderova<sup>2</sup>, G. M. Mikheev<sup>1</sup>

<sup>1</sup>*Institute of Mechanics, Udmurt Federal Research Center of the UB RAS, Izhevsk, Russia 426067*

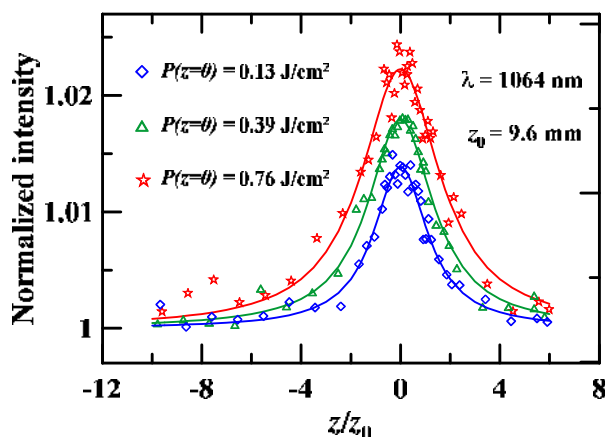
<sup>2</sup>*Adamas Nanotechnologies, Inc., 8100 Brownleigh Dr, Suite 120, Raleigh, NC 27617, USA*

roman@udman.ru

The saturable absorption (SA) is a nonlinear phenomenon, which is characterized by a short-term increase of the optical medium transmittance at high incident light pulse intensity. In the last decade, SA has been intensively studied in single-walled carbon nanotubes (CNTs) and graphene due to the possibility of using these carbon nanomaterials to produce picosecond and femtosecond laser pulses [1–3]. Detonation nanodiamonds (DNDs) are another form of carbon nanomaterials, which are currently being considered as a promising material for various optical applications. Previously, we reported on the SA of DNDs in aqueous suspensions with an average aggregate sizes of ~5, 35, 50, and 110 nm upon excitation by femtosecond and nanosecond laser pulses [4, 5]. Here we report on observation of SA in DND films sedimented on a glass substrate.

DND suspensions with an average aggregate size of 30 nm were prepared according to the technology presented in our previous work [4]. The suspensions exhibited negative zeta potentials ( $\zeta = -45$  mV) at neutral pH. DND films were obtained by the method of slow evaporation of a suspension filled into an optical cuvette. Thus, an optically homogeneous two-layer film was obtained covering the inner surface of the cuvette. The calculated surface density of DND was  $11.9 \mu\text{g}/\text{mm}^2$ . The linear transmittance  $T_0$  of a two-layer film at 1064 nm was 66%. The X-ray diffraction pattern of DNDs was acquired using 0.1541 nm  $\text{CuK}_\alpha$  radiation on a D2 PHASER (Bruker) diffractometer. We observed the diamond reflections from the  $\{111\}$ ,  $\{220\}$ ,  $\{311\}$  planes at  $2\theta = 43.9, 75.3, 91.5^\circ$  respectively.

Experiments were carried out using an open aperture  $z$ -scan technique. Single-frequency radiation of the fundamental of the 1 Hz single-mode  $\text{YAG:Nd}^{3+}$ -laser served as the laser pump [6]. The duration  $\tau_p$  of the laser pulses at  $\lambda = 1064$  nm was 21.2 ns. Laser light was focused by a lens with a focal length of 150 mm, with the



diameter  $2w_0$  of the laser beam waist at 1064 nm being equal to  $114 \mu\text{m}$ , and the Rayleigh length  $z_0 = \pi w_0^2/\lambda$  being of 10 mm. The point  $z = 0$  corresponds to the waist of the focused beam. The nonlinear transmittance  $T$  of the DND film was measured as a function of the film position  $z$  along the axis of the focused laser beam.

Figure 1 shows the normalized transmittance  $T_n(z/z_0)$  of the DND film at 1064 nm for different incident fluences, where  $T_n(z/z_0) = T(z/z_0)/T_0$ . The obtained dependences  $T_n(z/z_0)$  are symmetric relative to the point  $z/z_0 = 0$  and that demonstrates SA in DND films at 1064 nm. The experimental dependences presented in Figure 1 can be approximated using the expression  $\alpha = \alpha_{\text{ns}} + \alpha_0/[1 + I(z)/I_{\text{sat}}]$ , where  $\alpha$  is the

absorption coefficient, characterizing SA;  $I(z)$  is the incident beam intensity;  $\alpha_{\text{ns}}$  is the linear absorption coefficient, which is not related to the SA;  $\alpha_0$  is the absorption coefficient, characterizing the SA at intensity  $I(z)$  tending to zero;  $I_{\text{sat}}$  is the saturation intensity (coefficient determining the ability of a medium to exhibit self-bleaching). The fitted values of  $\alpha_0$  and  $I_{\text{sat}}$  were  $0.19 \text{ cm}^{-1}$  and  $7.3 \text{ MW}/\text{cm}^2$ , respectively.

### Acknowledgement

This work was financially supported by RFBR (project No. 16-42-180147).

### References

- [1] Y. Sakakibara, S. Tatsuura, H. Kataura, M. Tokumoto and Y. Achiba, *Jpn. J. Appl. Phys.*, **42**, 494 (2003).
- [2] A. Martinez and Z. Sun, *Nat. Photonics*, **7**, 842 (2013).
- [3] S. Yamashita, A. Martinez, and B. Xu, *Opt. Fiber Technol.*, **20**, 702 (2014).
- [4] G. M. Mikheev, R. Y. Krivenkov, T. N. Mogileva, K. G. Mikheev, N. Nunn and O. A. Shenderova, *J. Phys. Chem. C*, **121**, 8630 (2017).
- [5] V. Vanyukov, G. Mikheev, T. Mogileva, A. Puzyr, V. Bondar, D. Lyashenko and A. Chuvilin, *J. Nanophot.*, **11**, 032506 (2017).
- [6] G. M. Mikheev, R. Y. Krivenkov, K. G. Mikheev, A. V. Okotrub and T. N. Mogileva, *Quant. Electron.*, **46**, 719 (2016).



## Tuning electrical and optical properties of SWCNT films

A.A. Tonkikh <sup>1,\*</sup>, V.I. Tsebro <sup>2,3</sup>, I. I. Kondrashov <sup>1</sup>, V.A. Eremina <sup>1</sup>, E.A. Obratsova <sup>1,4</sup>, A.S. Orekhov <sup>5,6</sup>, E.I. Kauppinen <sup>7</sup>, A.L. Chuviln <sup>8,9</sup>, E.D. Obratsova <sup>1</sup>

<sup>1</sup> A.M. Prokhorov General Physics Institute, RAS, 38 Vavilov Street, 119991 Moscow, (Russia)

<sup>2</sup> P.N. Lebedev Physical Institute, RAS, 53 Leninsky Prospect, 119991 Moscow, (Russia)

<sup>3</sup> Kapitza Institute for Physical Problems, RAS, 2 Kosygina Street, 119334 Moscow, (Russia)

<sup>4</sup> Shemyakin and Ovchinnikov Institute of Bioorganic Chemistry, RAS, 16/10 Miklukho-Maklaya Street, 117871 Moscow, (Russia)

<sup>5</sup> National Research Center "Kurchatov Institute", 123182 Moscow, (Russia)

<sup>6</sup> Electron Microscopy for Materials Science (EMAT), University of Antwerp, 2020 Antwerpen, (Belgium)

<sup>7</sup> Depart. of Applied Physics, Aalto University, School of Science, P.O. Box 15100, FI-00076 Espoo, (Finland)

<sup>8</sup> CIC nanoGUNE Consolider, Tolosa Hiribidea 76, 20018 Donostia-San Sebastian, (Spain)

<sup>9</sup> IKERBASQUE Basque Foundation for Science, Maria Diaz de Haro 3, E-48013 Bilbao, (Spain)

\*Corresponding author. E-mail: [aatonkikh@gmail.com](mailto:aatonkikh@gmail.com).

Single-wall carbon nanotubes (SWCNTs) exhibit a unique set of electro physical and optical properties such as: a high mobility of charge carriers, a ballistic transport along the nanotube axis, linear and non-linear optical effects, and et al. Unfortunately, these properties are inherent only to the individual SWCNTs. The merge of individual SWCNTs into the films usual cause the loss of all the advantages inherent in individual SWCNTs. So, for the making of conductive electrode, FED devises, photodetectors, transistors and thermoelectric devises these issues have to be overcome.

In the work we exhibited the investigation devoted to tuning and improvement properties of SWCNT films via the filling of interior channels with acceptor or donor molecules. The effects of control doping on SWCNTs merged into the conductive networks were investigated by optical spectroscopes (Raman and optical absorptions) and electrophysical methods (setups of 4-probe sheet resistance and thermopower measurements). The filling and measurements were carried out on films composed of nanotubes of narrow and wide diameter distribution, including extracted semiconductor and metal ones.

### Acknowledgement

The work was supported by RFBR project 16-02-00949, grant № 311533 of Academy of Finland, Russian Federation President Program for young scientist MK-3140.2018.2.

# Thermal effects of $\text{Er}^{3+}$ / $\text{Yb}^{3+}$ doped $\text{NaYF}_4$ phosphor induced by 980 nm laser diode irradiation

Hong Wang, Xiumei Yin, Mingming Xing\*, Yao Fu, Ying Tian, and Xixian Luo\*

Physics Department, Dalian Maritime University, Dalian, Liaoning 116026, P. R. China

Corresponding author e-mail: xingming1112@126.com (M. Xing), luoxixian@126.com (X. Luo).

## 1. Introduction

Upconversion luminescence (UCL) is an anti-stokes luminescence that plays an important role in biological fluorescence labels, silicon solar cells, 3D displays, and anti-counterfeit fields<sup>[1-4]</sup>. Most academic studies focused on their luminescence properties but disregard the photothermal conversion process. In fact, UCL process is accompanied by the generation of thermal effects. The light-heat conversion has a competitive relationship with the light-light conversion when the same amount of absorption energy can be absorbed. In this work, the thermal effects of Er / Yb doped  $\text{NaYF}_4$  phosphor induced by 980 nm laser diode irradiation were intuitively and contrastively investigated using an infrared thermal imaging technology with real-time online monitoring. The  $\text{Yb}^{3+}$  /  $\text{Er}^{3+}$  codoped materials have strong thermal effects and high temperature elevation under 980 nm irradiation. However, the severe thermal effects of materials with higher  $\text{Er}^{3+}$  ion doping concentration is remarkably attributed to the cross relaxation between the  $\text{Er}^{3+}$  ions under 980 nm irradiation. The temperature rising rate and elevation  $\Delta T$  value of samples depend on the ion doping concentration and power density of the laser diode excitation. The internal temperature of the samples exhibits deep temperature gradient under 980 nm laser diode irradiation. By comparing the two kinds of thermometry methods, the temperature value calculated by fluorescence intensity ratio is almost similar to that obtained through infrared thermal imaging technology under higher excitation power pumping.

## 2. Results and discussion

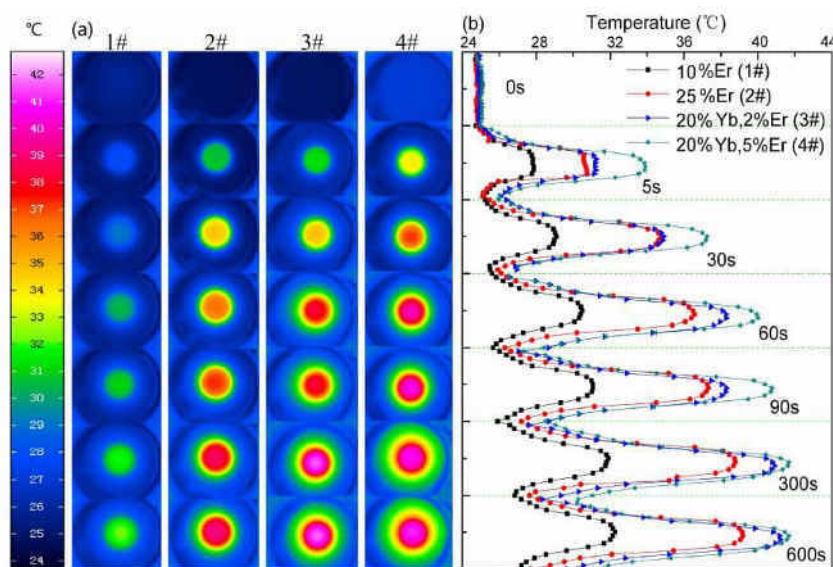


Fig. 1 Temperature images at different irradiation times (a) and the corresponding temperature curves (b), temperature elevation  $\Delta T$  of  $\text{NaYF}_4$ : xEr (x = 10, 25 mol%) and  $\text{NaYF}_4$ : 20%Yb, yEr (y = 2, 5 mol%) samples (c) under irradiation of 980 nm LD.

## 3. Acknowledgement.

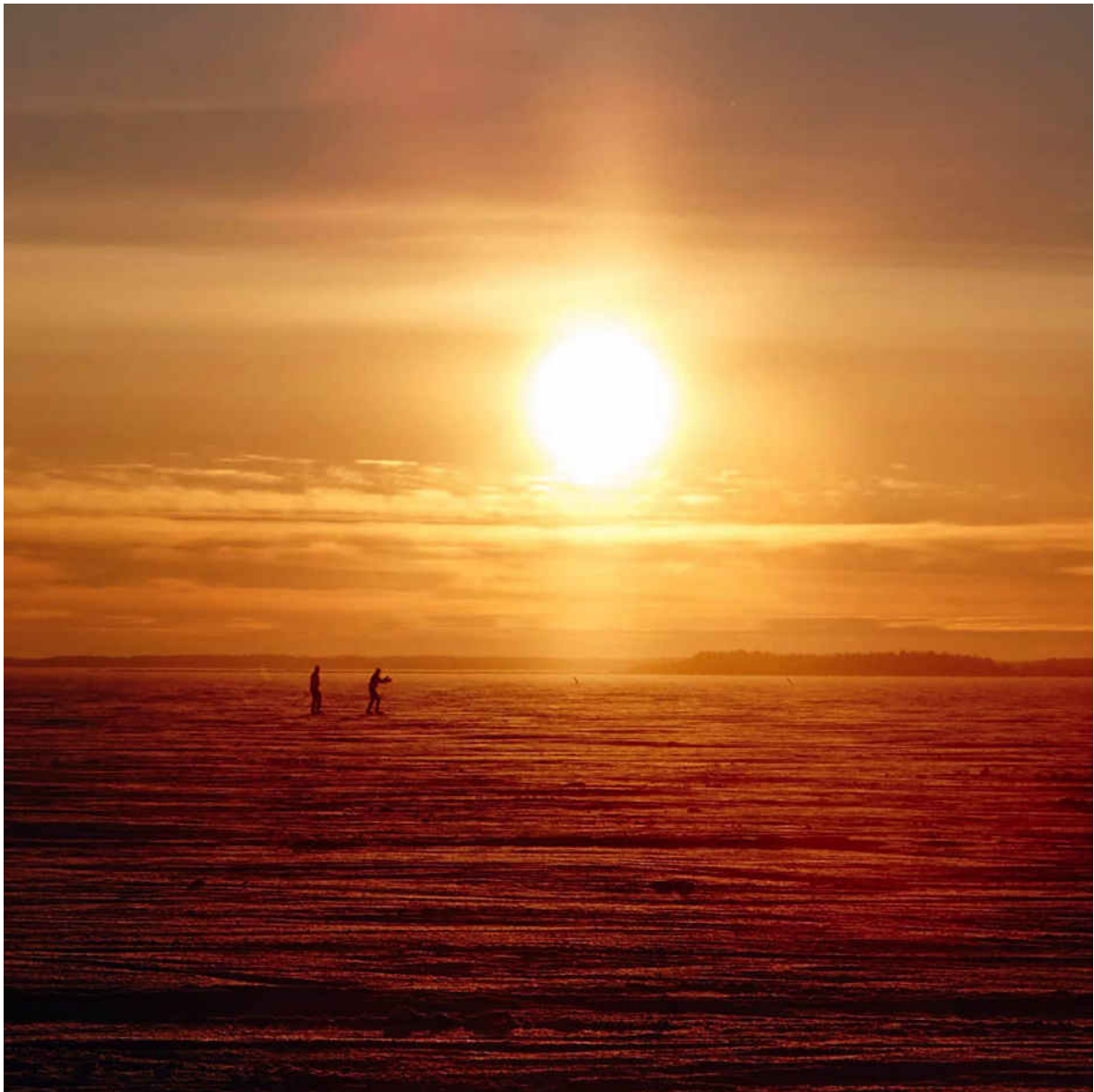
The authors would like to thank the National Natural Science Foundation of China (No. 11504039 and 51502031), Liaoning Provincial Natural Science Foundation of China (No. 2015020206), and Research Program of Application Foundation (Main subject) of Ministry of Transport of PR China (No. 2015329225090), and Fundamental Research Funds for the Central Universities (Grant Nos. 3132017061, 3132017066, and 3132016349) for their financial support.

## 4. References

- [1] B. Zhou, B. Y. Shi, D. Y. Jin, X. G. Liu, *Nature Nanotech.*, 2015, 10, 924 – 936.
- [2] N. M. Idris, M. K. Gnanasamandhan, J. Zhang, P. C. Ho, R. Mahendran, Y. Zhang, *Nat. Med.* 2012, 18, 1580 – 585.
- [3] G. S. Yi, Y. F. Peng, Z. Q. Gao, *Chem. Mater.* 2011, 23, 2729 – 2734.
- [4] Y. H. Zhang, L. X. Zhang, R. R. Deng, J. Tian, Y. Zong, D. Y. Jin, X. G. Liu, *J. Am. Chem. Soc.* 2014, 136, 4893 – 4896.



## Thursday, August 9



©G. Lepehin



## Diamond based quantum sensing and imaging

**Fedor Jelezko**

*Institute of Quantum optics, Ulm University*

Colour centers in diamond are promising candidates for nanoscale quantum sensing and quantum enhanced imaging. In this talk, we will highlight new techniques enabling high spectral resolution in nanoscale NMR (Schmitt et al. 2017). We will also show experiments aiming to develop hyperpolarization enhanced NMR and MRI based on polarization transfer from optically pumped electron spins in diamond to nuclear spins (Scheuer et al. 2016; Scheuer et al. 2017).

### References

- Scheuer, J., I. Schwartz, Q. Chen, D. Schulze-Sunninghausen, P. Carl, P. Hofer, A. Retzker, H. Sumiya, J. Isoya, B. Luy, M. B. Plenio, B. Naydenov, and F. Jelezko. 2016. 'Optically induced dynamic nuclear spin polarisation in diamond', *New Journal of Physics*, 18.
- Scheuer, J., I. Schwartz, S. Muller, Q. Chen, I. Dhand, M. B. Plenio, B. Naydenov, and F. Jelezko. 2017. 'Robust techniques for polarization and detection of nuclear spin ensembles', *Physical Review B*, 96.
- Schmitt, S., T. Gefen, F. M. Stürner, T. Uden, G. Wolff, C. Müller, J. Scheuer, B. Naydenov, M. Markham, S. Pezzagna, J. Meijer, I. Schwarz, M. B. Plenio, A. Retzker, L. P. McGuinness, and F. Jelezko. 2017. 'Submillihertz magnetic spectroscopy performed with a nanoscale quantum sensor', *Science*, 356: 832-36.

# Diamond nanoneedles under high electric field and laser illumination: electrical, optical and thermal properties studied by ion and photon emission.

A. Vella<sup>1</sup>, L. Venturi<sup>1</sup>, M. Borz<sup>1</sup>, I. Blum<sup>1</sup>, J. Houard<sup>1</sup>, L. Arnoldi<sup>1</sup>, L. Rigutti<sup>1</sup>, A. Obraztsov<sup>2,3</sup>

1. GPM - UMR 6634 CNRS-INSU-Université de Rouen, Normandie Université, France.

2. M. V. Lomonosov Moscow State University, Department of Physics, Moscow, Russia

3. University of Eastern Finland, Department of Physics and Mathematics, Joensuu 80101, Finland

Corresponding author : [angela.vella@univ-rouen.fr](mailto:angela.vella@univ-rouen.fr)

Diamond nano-needles (NNds), elaborated by a combination of chemical vapor deposition growth and selective oxidation of polycrystalline films [1], are attractive samples for several applications such as light emitters, tensile stress sensor or electron sources so that the study of their physical properties becomes of great interest. In this work we report on new methods to study the optical, electrical and thermal properties of these NNds. The experimental set-up is schematically represented in Fig. 1 (a). The sample is introduced in a high vacuum chamber and is biased at high voltage in order to create a high electric field at its apex. Ultra-fast laser pulses are focused on the sample, the focus position can move along the sample axis and the laser wavelength can be changed from near infrared to ultraviolet light. Thanks to photon and ion spectrometers, the energy of the emitted photons and ions is analyzed as a function of the applied field and the illumination conditions.

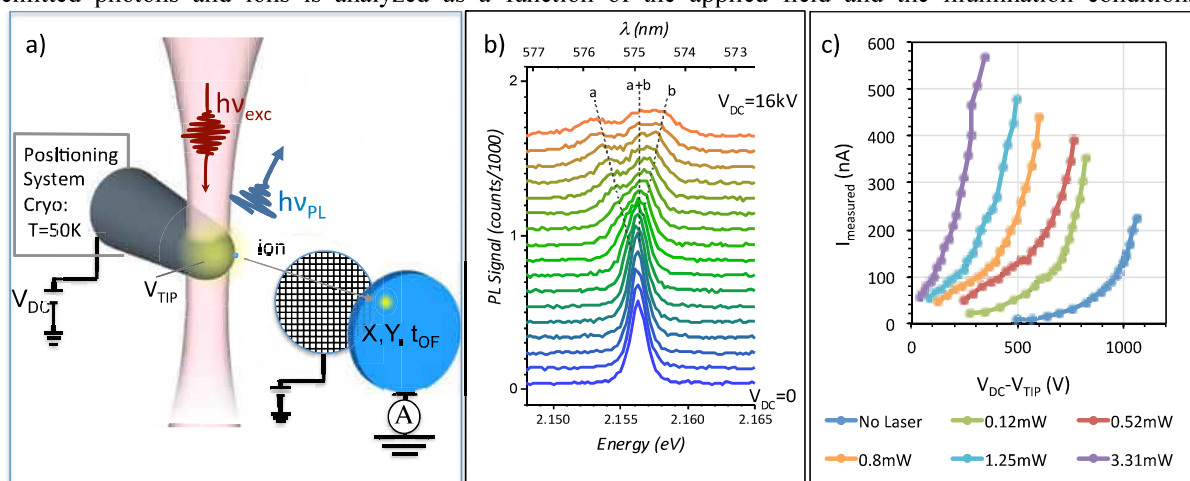


Figure 1. The needle specimen is inserted in a vacuum chamber equipped with an in situ photoluminescence bench, an ion spectrometer and a position and time sensitive detector. The high voltage applied to the tip leads to an intense electric field at the specimen's apex, which allows field evaporation of ions. Moreover, laser pulses can trigger ion evaporation and photon emission. (b) The photoluminescent signal acquired for different values of the applied voltage. (c) The current voltage characteristic of the diamond needle as a function of the laser illumination conditions.

Measuring the energy of the light emitted by the color centers inside the diamond NNds, we report the change of the emission's spectra as a function of the applied bias as reported in Fig. 1(b). The application of the electric field induces a large stress inside the sample. We perform the measurement of the stress in the NNds by contactless piezo-spectroscopy using electrostatic field regulation [2].

Measuring the energy of the emitted ions and their current, two different behaviours of electrical conduction have been reported on diamond NNds, as reported in Fig. 1(c). At low emission current, we report a Ohmic conduction and, at high emission current, a Poole-Frenkel (PF) conduction [3]. We discuss the transition between these two conduction mechanisms and its dependence as a function of the emitted current, the needle geometry and the illumination conditions.

[2] A. N. Obraztsov, G. M. Mikheev, Yu. P. Svirko, R. G. Zonov, A. P. Volkov, D. A. Lyashenko and K. Paivasaari, *Diamond and Related Materials*, **15**, 842 (2006).

[2] L. Rigutti, et al., Optical Contactless Measurement of Electric Field-Induced Tensile Stress in Diamond Nanoscale Needles. *Nano Lett.*, ACS Pub., 2017.

[3] V.I.Kleshch et al., "Single Crystal Diamond Needle as Point Electron Source", *Scientific Reports* **6**, Article number: 35260 (2016)



## GeV, SiV and NV color centers in single crystal diamond needles

S.A. Malykhin<sup>1,2,3</sup>, R.R. Ismagilov<sup>2</sup>, A.S. Orekhov<sup>4</sup>, E.A. Obraztsova<sup>5</sup>, A.N. Obraztsov<sup>1,2</sup>

<sup>1</sup>Department of Physics and Mathematics, University of Eastern Finland, Joensuu, Finland

<sup>2</sup>Department of Physics, Lomonosov Moscow State University, Moscow, Russia

<sup>3</sup>Lebedev Physical Institute, Russian Academy of Sciences, Moscow, Russia

<sup>4</sup>Russian Research Centre Kurchatov Institute, Moscow, Russia

<sup>5</sup>Shemyakin and Ovchinnikov Institute of Bioorganic Chemistry, Russian Academy of Sciences, Moscow, Russia  
sermal92@mail.ru

Single crystal diamond needles (SCDN) were produced by combination of chemical vapor deposition (CVD) and selective oxidation techniques. Necessary properties of fabricated film material are determined by parameters of the CVD process including substrate temperature gas mixture composition and direct plasma discharge glowing. Optimization of these parameters of the CVD process allows us to create carbon film consisting of SCDNs with different geometries [1]. Injection of nitrogen, silicon and germanium containing precursors into the CVD chamber and further optimization of the process parameters allows us creation of nitrogen-vacancy (NV), silicon-vacancy (SiV) and germanium-vacancy (GeV) color centers in SCDNs. Optical properties of obtained SCDNs with NV, SiV and GeV color centers were investigated using photo- and cathodoluminescence (PL and CL) techniques. Morphological properties were analyzed using scanning electron microscopy (SEM). PL spectra of NV<sup>0</sup>, SiV<sup>-</sup> and GeV color centers created in SCDNs presented in Fig.1.

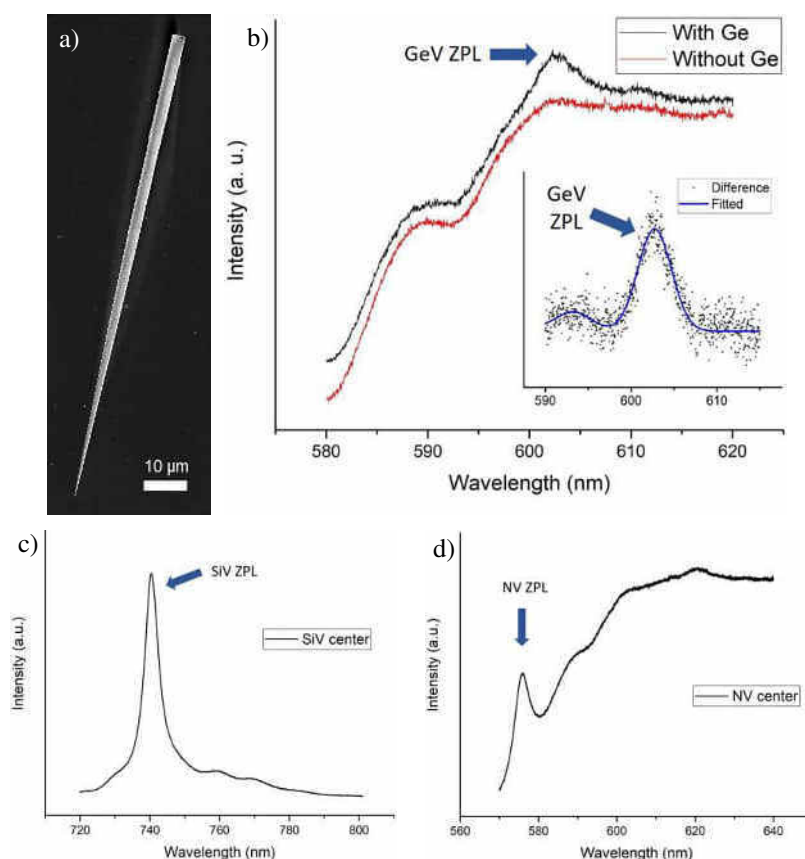


Fig. 1. SEM image of SCDN (a) and PL spectra of GeV (b), negative SiV (c), neutral NV (d) color centers in it. Zero phonon lines of these centers marked by blue arrows [2,3].

The PL bands of GeV are revealed via comparison of PL spectra detected for material obtained with and without Ge injection as it is demonstrated in Fig.1(b) presenting PL spectra of SCDNs containing GeV color centers, without GeV and their difference in the box for clarity.

This work was supported by Russian Foundation for Basic Research (grant # 18-02-00495) and by Academy of Finland (grant # 298298). SAM is a grantee of the Foundation for the advancement of theoretical physics and mathematics “BASIS”.

[1] A. A. Zolotukhin, M. A. Dolganov, A. M. Alekseev, A. N. Obraztsov, *Diamond and Related Materials*, **42**, 15 (2014)

[2] A. M. Zaitsev, *Optical Properties of Diamond. A Data Handbook*, (Springer Science & Business Media, 2001)

[3] B. Dischler, *Handbook of Spectral Lines in Diamond*, (Springer Science & Business Media, 2012)



# Meter-Scale Single-Wall Carbon Nanotube Films for the Use in Flexible and Transparent Integrated Circuits

Dong-Ming Sun, Bing-Wei Wang, Chang Liu, Hui-Ming Cheng

Shenyang National Laboratory for Materials Science, Institute of Metal Research, Chinese Academy of Sciences, 72 Wenhua Road, Shenyang, 110016, P. R. China

School of Material Science and Engineering, University of Science and Technology of China, 96 Jinzhai Road, Hefei, 230026, P. R. China  
dmsun@imr.ac.cn

## 1. Introduction

Thin films composed of single-wall carbon nanotubes (SWCNTs) have been demonstrated as transparent conductive film electrodes or semiconducting active channels in various flexible and transparent electronics.[1,2] However, two major obstacles remain for the research and development of macro-electronics based on SWCNT thin films. First, the size of fabricated SWCNT films is usually limited to the square centimeter scale, and the batch processing used is not scalable. SWCNT films, either deposited by a gas/liquid vacuum filtration or synthesized by chemical vapor deposition (CVD), are usually smaller than, or close to, the size of membrane filters and/or growth substrates. Second, the optoelectrical performance of SWCNT films remains unsatisfactory due to the introduction of impurities and structural defects during the solution processes of film fabrication, such as dispersion, purification and separation. In this study, we propose a continuous synthesis, deposition and transfer technique for the fabrication of high-quality SWCNT thin films of meter-scale dimension with excellent optoelectrical performance.

## 2. Results

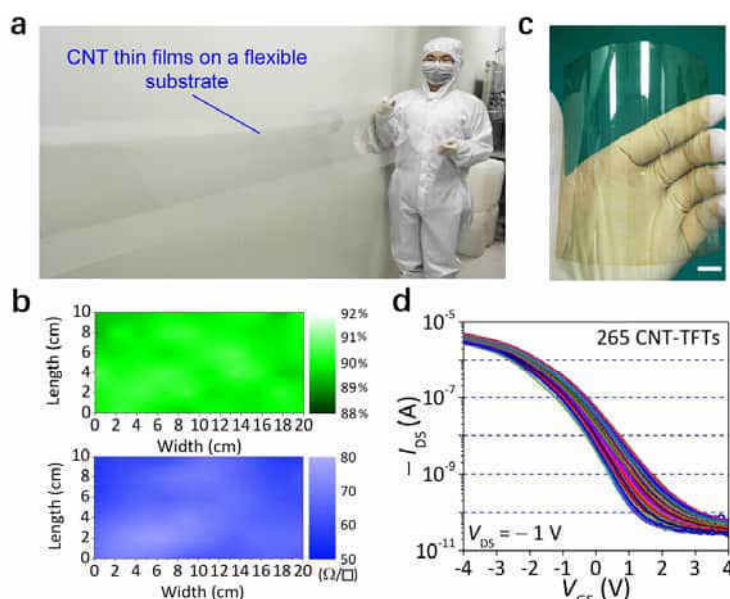


Fig. 1. (a) A SWCNT thin film transferred on a flexible PET substrate with a length of more than 2 m. (b) Transmittance (upper) and sheet resistance (lower) mapping of the as-prepared SWCNT thin films. (c) Photograph of all-CNT TFT device fabricated on a flexible PEN substrate with a size of  $100 \times 100 \text{ mm}^2$  (scale bar, 10 mm). (d) Transfer ( $I_{DS} - V_{GS}$ ) characteristics of 265 TFTs at  $V_{DS} = -1 \text{ V}$ .

The SWCNTs are continuously synthesized by a floating catalyst chemical vapor deposition (CVD) technique. The maximum width of the SWCNT thin films obtained is 0.5 m, and can be adjusted by selecting different filtration windows of various dimensions. The length of the film is unlimited, because the as-deposited film is transferred onto a flexible polyethylene terephthalate (PET) substrate with the aid of a roll-to-roll transfer system, and the filter can be repeatedly used for CNT film collection. The meter-scale SWCNT film deposited on the membrane filter can be easily transferred onto a target substrate, thus allowing us to construct large-area all-CNT devices. The good reproducibility and uniformity of the fabricated all-CNT TFTs allow us to construct logic ICs. A 101-stage ring oscillator with an output buffer, where 204 all-CNT

TFTs were integrated on a PEN substrate spontaneously begins oscillating at a  $V_{DD}$  of  $-3 \text{ V}$ . The successful operation of the ring oscillator indicates excellent uniformity of the SWCNT thin films and the all-CNT TFTs.

## 3. Acknowledgement

The authors sincerely thank Prof. Esko I. Kauppinen, Mr. S. Jiang, Dr. S. Qiu, Prof. Q. Li for their constructive advices.

## 4. References

- [1] Y. Chen, Y. Sun, Q. Zhu, B. Wang, X. Yan, S. Qiu, Q. Li, P. Hou, C. Liu, D. Sun and H. Cheng, *Advanced Science*, 1700965 (2018).
- [2] L. Zhang, D. Sun, P. Hou, C. Liu, T. Liu, J. Wen, N. Tang, J. Luan, C. Shi, J. Li, H. Cong and H. Cheng, *Advanced Materials*, **29**, 1652719 (2017).
- [3] X. Li, Z. Fan, P. Liu, M. Chen, X. Liu, C. Jia, D. Sun, X. Jiang, Z. Han, V. Bouchiat, J. Guo, J. Chen, Z. Zhang, *Nature Communications*, **8**, 970 (2017).

# Carbon nanotube-based analog circuits for wearable sensor applications: Device modeling, circuit design and fabrication

Yutaka Ohno

*Institute of Materials and Systems for Sustainability, Nagoya University, Furo-cho, Chikusa-ku, Nagoya 464-8603, Japan  
yohno@nagoya-u.jp*

## 1. Introduction

Wearable healthcare devices have the potential to revolutionize preventive medical care and health promotion technologies. Carbon nanotube (CNT) thin films are promising electronic materials for transistors and integrated circuits [1-3], biosensors [4,5], and other passive components to build flexible and stretchable devices with excellent wearability and performance because of the high-carrier mobility, mechanical flexibility, and biocompatibility. Recently, high-yield and reproducible fabrication of CNT TFTs became possible by using purified semiconducting CNTs, leading extensive study on circuit applications.

An integration of analog circuits with a sensor is essential for wearable sensor devices to amplify the sensing signal as preventing external noise. A differential amplifier is a fundamental analog amplification circuit used for various sensor devices. In this work, we are focusing on the analog circuit application of CNT TFTs. To design CNT-based analog circuits, circuit simulations have been performed by using a precise device model which has been built on the basis of electrical characterizations of CNT TFTs. We have realized differential amplifiers on a flexible and transparent plastic film.

## 2. Device modeling for circuit simulation

Device modelling is indispensable for circuit design. We built the RC-ladder device model based on the charge based model for CNT TFTs, where a correction of pinch off condition was taken into account, considering the contact resistances between CNTs. In order to fit the subthreshold current, the charge equation in weak inversion characteristics was modified. The proposed model well expresses the output characteristics. The frequency dependence of capacitance-voltage characteristic was also built by considering the non-quasi-static effect in the Mayer model.

## 3. Differential amplifier: circuit design and fabrication

CNT-based differential amplifiers were designed by using the circuit simulation with proposed device model. We also demonstrated the differential amplifiers on a flexible plastic film as shown in Fig. 1. Bottom-gate CNT TFTs with purified semiconducting CNTs were used as the active device. A differential output was obtained with respect to a differential input. Maximum voltage gain of 16.3 (24.3 dB) was achieved for a sinusoidal wave input of 100 mVpp at 100 Hz with a power source of -12 V. Figure 2 shows the gain as a function of frequency, exhibiting -20 dB/dec. The voltage gain cut-off frequency was 210 kHz.

## Acknowledgments

The semiconducting CNTs were provided by TASC. This work was partially supported by JST/CREST.

- [1] Q. Cao et al., Nature 454, 495 (2008).
- [2] D.-M. Sun et al., Nat. Nanotechnol. 6, 156 (2011).
- [3] D.-M. Sun et al., Nat. Commun. 4, 2302 (2013).
- [4] I. Dumitrescu et al., Chem. Commun. 45, 6886 (2009)
- [5] W. Harreither et al., Anal. Chem. 85, 7447 (2013)

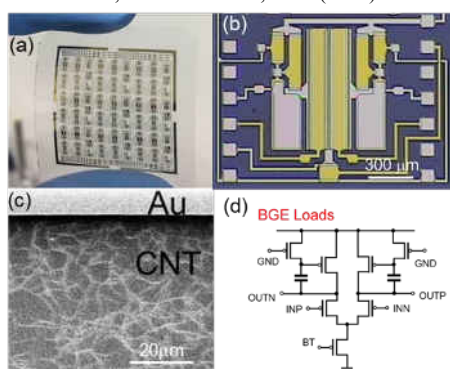


Fig. 1 CNT differential amplifier on plastic film. (a) Photograph of chip, (b) photograph of circuit, (c) SEM image of CNT thin film, (d) circuit diagram.

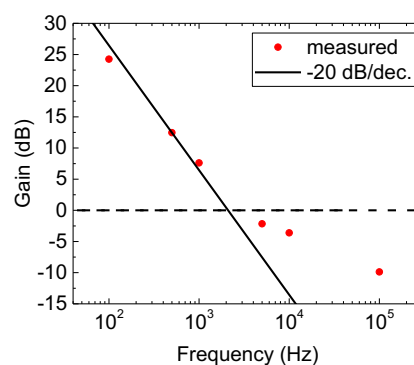


Fig. 2 Frequency dependence of voltage gain.

# Transport properties of semiconducting and metallic single-walled carbon nanotubes thin films

V.A. Eremina<sup>1,2</sup>, T. Matsui<sup>3</sup>, H. Fukuyama<sup>3,4</sup>, E.D. Obraztsova<sup>1,2</sup>

<sup>1</sup>Physics Department of M.V. Lomonosov Moscow State University, 1 Leninskie gori, Moscow, Russia

<sup>2</sup>A.M. Prokhorov General Physics Institute, RAS, 38 Vavilov street, 119991 Moscow, Russia

<sup>3</sup>Department of Physics, The University of Tokyo, 7-3-1 Hongo, Bunkyo-ku, Tokyo 113-0033, Japan

<sup>4</sup>Cryogenic Research Center, The University of Tokyo, 2-11-16 Yayoi, Bunkyo-ku, Tokyo 113-0032, Japan  
erjomina@physics.msu.ru

Understanding the conduction mechanisms in single-walled carbon nanotubes (SWCNTs) is crucial for their use in various applications, such as transistors and conductive films [1]. Furthermore, the interaction of charge carriers in SWCNTs is interesting from the fundamental point of view [2-4].

In this study, we used aqueous two-phase extraction technique [5,6] to achieve high purity separation of SWCNTs by type of conductivity. As parent material we used "Tuball" nanotubes with an average diameter of 1.8 nm. Thin films with different metallic/semiconducting ratios were prepared. Measurements of resistance were conducted in wide temperature range (from 300 K down to 1.6 K) (Fig.1). At low temperatures current-voltage characteristics were also measured.

We observed variable range hopping conductance mechanisms with different dimensionality for semiconducting films and for films with the presence of semiconducting nanotubes. For pure metallic SWCNTs and for SWCNTs doped with CuCl [7] we found the conduction mechanism is similar to Tomonaga-Luttinger behavior. For single-walled carbon nanotubes doped with copper chloride we observed power law behavior in transport with Luttinger parameter  $\alpha = 0.43$ .

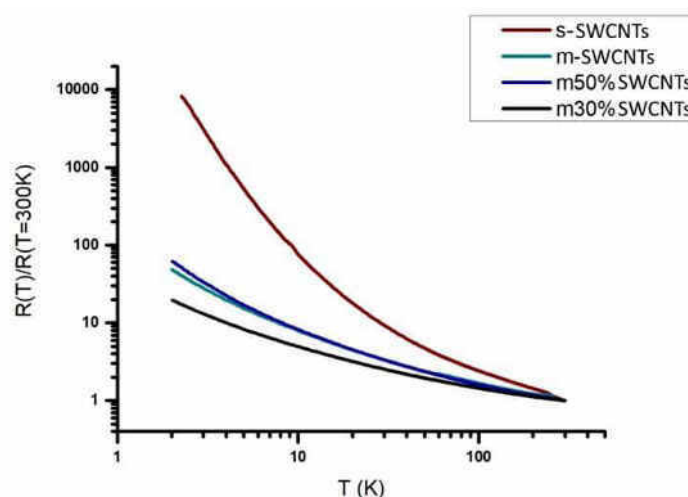


Fig.1. Normalized resistance of four different samples with different metallic/semiconducting ratios as a function of temperature, 98% semiconducting SWCNTs (brown), 98% metallic SWCNTs (light blue), 50% metallic SWCNTs (navy), 30% metallic – parent SWCNTs (black).

## Acknowledgements

The reported study was funded by RFBR according to the research project № 18-32-00998. The author is thankful to the STEPS program.

## References

- [1] Baughman, Ray H., Anvar A. Zakhidov, and Walt A. de Heer. "Carbon nanotubes-the route toward applications." *Science* 297.5582 (2002): 787-792.
- [2] Yosida, Y.; Oguro, I. "Variable Range Hopping Conduction in Bulk Samples Composed of Single-Walled Carbon Nanotubes." *J. Appl. Phys.* 1999, 86, 999–1003.
- [3] Takano, T.; Takenobu, T.; Iwasa, Y. "Enhancement of Carrier Hopping by Doping in Single Walled Carbon Nanotube Films." *J. Phys. Soc. Jpn.* 2008, 77, 124709–124713.
- [4] Bockrath, Marc, et al. "Luttinger-liquid behaviour in carbon nanotubes." *Nature* 397.6720 (1999): 598.
- [5] Khripin, Constantine Y., Jeffrey A. Fagan, and Ming Zheng. "Spontaneous partition of carbon nanotubes in polymer-modified aqueous phases." *Journal of the American Chemical Society* 135.18 (2013): 6822-6825.
- [6] Eremina, V.A., Obraztsov, P.A., et al. "Separation and optical identification of semiconducting and metallic single-walled carbon nanotubes." *Physica Status Solidi (b)* 254.5 (2017).
- [7] Eremina, Valentina A., Pavel V. Fedotov, and Elena D. Obraztsova. "Copper chloride functionalization of semiconducting and metallic fractions of single-walled carbon nanotubes." *Journal of Nanophotonics* 10.1 (2016): 012515-012515.

# Revealing floating-catalyst carbon nanotube quality by ultraclean individual CNT transistor array

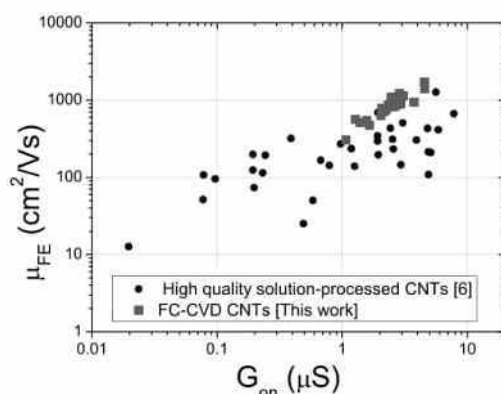
Nan Wei<sup>1</sup>, Patrik Laiho<sup>1</sup>, Saeed Ahmed<sup>1</sup>, Aqeel Hussain<sup>1</sup>, Qiang Zhang<sup>1</sup>, Taher Khan<sup>1</sup>, Yongping Liao<sup>1</sup>, Ying Tian<sup>1,3</sup>, Er-Xiong Ding<sup>1</sup>, Yutaka Ohno<sup>2</sup>, Esko I. Kauppinen<sup>1</sup>

<sup>1</sup> Department of Applied Physics, Aalto University School of Science, Puumiehenkuja 2, 00076 Aalto, Finland

<sup>2</sup> Institute of Materials and Systems for Sustainability, Nagoya University, Furo-cho, Chikusa-ku, Nagoya 464-8603, Japan

<sup>3</sup> Department of Physics, Dalian Maritime University, Dalian, Liaoning 116026, China

Corresponding Author: E. Kauppinen esko.kauppinen@aalto.fi



Carbon nanotubes (CNTs) grown by the floating-catalyst chemical vapor deposition (FC-CVD) are known to make fast thin-film transistors [1,2], however, the electronic quality of individual FC- CVD CNTs has not been clearly understood, as compared solution- processed and substrate-grown CNTs [3-5]. Here, we introduce a dry method for fabricating a statistically significant number of ultraclean single CNT field-effect transistors using FC-CVD CNTs, revealing the quality of FC-CVD CNTs with a mean field-effect mobility 3.3 times higher than that of

high- quality solution-processed CNTs [6], and on-off current ratios higher than 107.5. This method enables a fast, reliable and fine-grained inspection of FC-CVD CNT population, and provided a strong direct evidence about their near-perfect electronic quality[7]. This new understanding explains the good performance of FC-CVD CNT films and TFTs, and the obtained large number of ultraclean single-walled CNT transistors provide new possibilities to study the properties of pristine CNTs.

## Acknowledgement.

The research leading to these results has received partial funding from the European Union Seventh Framework Programme (FP7/2007-2013) under Grant Agreement No. 604472 (IRENA project) and the Aalto Energy Efficiency (AEF) Research Program through the MOPPI project. The research has also been partially supported by Academy of Finland via projects 286546 (DEMEC) and 292600 (SUPER) as well as by TEKES Finland via projects 3303/31/2015 (CNT-PV) and 1882/31/2016 (FEDOC). This work made use of the Aalto University Nanomicroscopy Center (Aalto-NMC) premises. Aalto NanoFab (Micronova) clean room resources are greatly appreciated.

## References

- [1] D. Sun *et al.* *Nat. Nanotechnol.* 6, 156 (2011).
- [2] D.-M. Sun *et al.* *Nat. Commun.* 4,2302 (2013).
- [3] A. E. Islam, J. A. Rogers, and M. A. Alam *Adv. Mater.* 27, 7908 (2015).
- [4] Q. Cao, S. Han, G. S. Tulevski, A. D. Franklin, and W. Haensch *ACS Nano* 6, 6471 (2012).
- [5] E. A. Laird *et al.* *Rev. Mod. Phys.* 87, 703 (2015).
- [6] P. Stokes and S. I. Khondaker *Appl. Phys. Lett.* 96, 83110 (2010).
- [7] X. Zhou, *et al.* *Phys. Rev. Lett.* 95,146805 (2005)

## Air-suspended carbon nanotubes for nanoscale quantum photonics

Yuichiro K. Kato

*Nanoscale Quantum Photonics Laboratory, RIKEN, Saitama 351-0198, Japan  
Quantum Optoelectronics Research Team, RIKEN Center for Advanced Photonics, Saitama 351-0198, Japan  
yuichiro.kato@riken.jp*

Single-walled carbon nanotubes have unique optical properties as a result of their one-dimensional structure. Reduced screening leads to large exciton binding energies which allow for room-temperature excitonic luminescence, while enhanced interactions give rise to a variety of exciton processes that may be utilized for modulating the emission properties. Furthermore, their luminescence is in the telecom-wavelengths and they can be directly synthesized on silicon substrates, providing new opportunities for nanoscale quantum photonics and optoelectronics.

Here we discuss the use of individual single-walled carbon nanotubes for generation and manipulation of photons on a chip. Strong exciton-exciton annihilation process leads to antibunching at room temperature [1], opening up a pathway to single photon sources. Specially-designed air-mode photonic crystal cavities allow for efficient coupling to nanotube emission [2], while the coupling can be readily tuned by large spectral shifts induced by molecular desorption [3]. Such spectral changes due to the adsorbed molecules give rise to optical bistability, which can be utilized for all-optical memory operations [4]. Gate control over carrier density can be used to generate trions that are also stable at room temperature [5], and efficient carrier-exciton interactions can be used to produce optical pulse trains [6]. Narrow linewidth electroluminescence can be obtained in split-gate devices [7]. Ultimately, these results may be combined to achieve further control over photons at the nanoscale.

Work partially supported by KAKENHI (JP16H05962, JP16K13613) as well as the Nanotechnology Platform and Photon Frontier Network Program of MEXT, Japan.

### References

- [1] A. Ishii, T. Uda, Y. K. Kato, "Room-temperature single photon emission from micron-long air-suspended carbon nanotubes," [Phys. Rev. Applied](#) **8**, 054039 (2017).
- [2] R. Miura, S. Imamura, R. Ohta, A. Ishii, X. Liu, T. Shimada, S. Iwamoto, Y. Arakawa, Y. K. Kato, "Ultralow mode-volume photonic crystal nanobeam cavities for high-efficiency coupling to individual carbon nanotube emitters," [Nature Commun.](#) **5**, 5580 (2014).
- [3] H. Machiya, T. Uda, A. Ishii, and Y. K. Kato, "Spectral tuning of optical coupling between air-mode nanobeam cavities and individual carbon nanotubes," [Appl. Phys. Lett.](#) **112**, 021101 (2018).
- [4] T. Uda, A. Ishii, Y. K. Kato, "Single carbon nanotubes as ultrasmall all-optical memories," [ACS Photonics](#) **5**, 559 (2018).
- [5] M. Yoshida, A. Popert, Y. K. Kato, "Gate-voltage induced trions in suspended carbon nanotubes," [Phys. Rev. B](#) **93**, 041402(R) (2016).
- [6] M. Jiang, Y. Kumamoto, A. Ishii, M. Yoshida, T. Shimada, Y. K. Kato, "Gate-controlled generation of optical pulse trains using individual carbon nanotubes," [Nature Commun.](#) **6**, 6335 (2015).
- [7] N. Higashide, M. Yoshida, T. Uda, A. Ishii, Y. K. Kato, [Appl. Phys. Lett.](#) **110**, 191101 (2017).



# Ultrafast field emission from carbon nanotubes

Chi Li<sup>1†</sup>, Xu Zhou<sup>2†</sup>, Feng Zhai<sup>3</sup>, Zhenjun Li<sup>1</sup>, Fengrui Yao<sup>2</sup>, Ruixi Qiao<sup>2</sup>, Ke Chen<sup>1</sup>, Dapeng Yu<sup>2</sup>, Zhipei Sun<sup>4\*</sup>, Kaihui Liu<sup>2\*</sup>, Qing Dai<sup>1\*</sup>

<sup>1</sup>Nanophotonics Research Division, CAS Center for Excellence in Nanoscience, National Center for Nanoscience and Technology, Beijing 100190, China.

<sup>2</sup>School of Physics, Academy for Advanced Interdisciplinary Studies, Collaborative Innovation Center of Quantum Matter, Peking University, Beijing 100871, China.

<sup>3</sup>Department of Physics, Zhejiang Normal University, Jinhua 321004, China.

<sup>4</sup>Department of Electronics and Nanoengineering, Aalto University, Tietotie 3, FI-02150 Espoo, Finland.

\*Correspondence: [daiq@nanocr.cn](mailto:daiq@nanocr.cn) (Q.D.), [khliu@pku.edu.cn](mailto:khliu@pku.edu.cn) (K.L.), [zhipei.sun@aalto.fi](mailto:zhipei.sun@aalto.fi) (Z.S.).

High brightness, ultra-fast electron sources with spatially structured emission from nanoscale solids are of fundamental interest for next-generation free-electron lasers, compact coherent X-ray sources, electron diffractive imaging, and attosecond science[1]. Due to their high aspect ratio, small tip radius, unique electronic structures, impressive structural stability, and high thermal conductivity; carbon nanotubes exhibit widely promising properties as mediators for enhanced electron sources, and as such have attracted tremendous attention in the past two decades. Here, we expanded the field of ultrafast optical field emission from metal nanostructures to carbon nanotubes.

Here, we study the performance of carbon nanotube as an optical field emitter and attempt to reach into strong field and sub-cycle regime in the visible (410 nm) and near-infrared (820 nm) fields. Three CNT emitters with different tip radius and morphology were studied, as shown in Fig. 1a, b, c. All samples consisted of vertically aligned arrays of few-walled CNTs (Fig. 1a, b, radius of  $\sim 3$  nm, high and medium  $\beta$ ) and multi-wall CNTs (Fig. 1c, radius of  $\sim 10$  nm, low  $\beta$ ) which were grown by chemical vapor deposition. In the present study, femtosecond pulses were focused onto the CNT arrays mounted in a cryogenically cooled ultra-high vacuum.

Fig.1(d, e, f) displays the photocurrent as a function of incident peak intensity for different tip radii. At similar laser intensity, the emission current from the CNTs with high  $\beta$  is two order of magnitude greater than that from the low  $\beta$  CNTs, and one order of magnitude from that of the medium  $\beta$  CNTs; results which are in good agreement with the predicted field-enhancement in Fig.1. The maximum emission current from a single CNT cluster in Fig. 1a (yellow circle) reached up to 40 nA, corresponding to a time average current density of a 4 A/cm<sup>2</sup> (estimated emission area of  $\sim 1 \mu\text{m}$ ), and a very high instantaneous current density of  $4 \times 10^6$  A/cm<sup>2</sup>. This is much higher than the current density obtained from CNT emitters during static field excitation, and is also much higher than that from metal emitters excited at optical frequencies[2].

The adiabatic electron emission at ultra-short periods and ultra-low temperatures may contribute to the extremely high current density. Though still largely unclear, we tentatively attribute the electron emission in this optical field to sub-nanometric localized fields, which are lattice enhanced by the ultra-low temperature across the ultra-short timescales, all of which make it possible to, for the first time, to empirically probe new mechanisms of field driven electron emission, which we hope will attract further study.

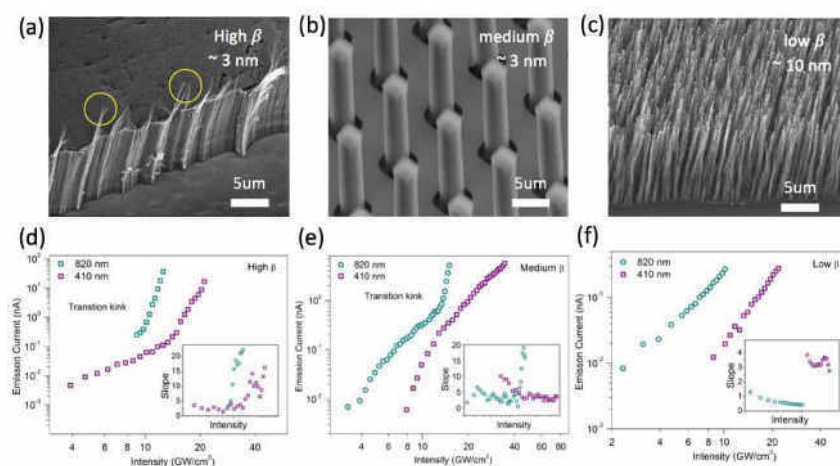


Fig.1 ultrafast field emission from three different carbon nanotube emitters.

[1] M.F. Ciappina, J. A. Pérez-Hernández, A. S. Landsman, et al., “Attosecond physics at the nanoscale”, Reports on Progress in Physics, **80**, 054401 (2017)

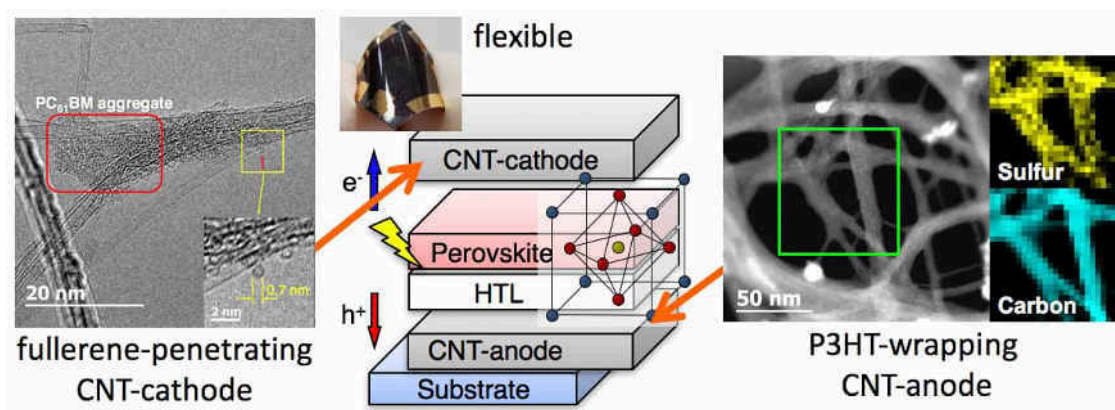
[2] G. Herink, D. R. Solli, M. Gulde, C. Ropers, “Field-driven photoemission from nanostructures quenches the quiver motion”, Nature, **483**, 190 (2012)

## Use of Carbon Nanotubes in Organic and Perovskite Solar Cells

Yutaka Matsuo<sup>1,2</sup>, Il Jeon<sup>1</sup>, Esko I. Kauppinen<sup>3</sup>, Shigeo Maruyama<sup>1,4</sup>

<sup>1</sup>The University of Tokyo, <sup>2</sup>University of Science and Technology of China, <sup>3</sup>Aalto University School of Science, <sup>4</sup>AIST  
matsuo@photon.t.u-tokyo.ac.jp

Carbon nanotubes (CNTs) have excellent charge carrier transport property and facilitates high flexibility of organic solar cells devices. In order to realize the use of CNTs in solar cells, we need to consider quality and electronic property of CNTs. We employ CNT transparent films made from aerosol CNTs which can be produced with floating iron catalysts prepared by thermal deposition of sublimated ferrocene. To obtain high electronic property of CNTs, we investigated Brønsted acid, Lewis acid, and electrophilic fullerenes for electronics application. We report CNTs-electrode-based flexible organic and perovskite solar cells.<sup>1</sup> With replacing metal or metal oxide electrodes by CNT transparent electrodes, rare or expensive metal-free, highly flexible, potentially low cost, low hysteresis solar cells are realized. CNT electrodes can usually become hole-collecting electrode with acid doping, while we also developed electron-collecting CNT electrodes with penetration of fullerene derivatives into CNTs spatial networks. Both CNT cathode and anode electrodes can also be possible to be fabricated by fully solution process without vacuum deposition.



### References

- [1] *J. Am. Chem. Soc.* **2015**, 137, 7982. [2] *Nano Lett.* **2015**, 15, 6665. [3] *Adv. Electron. Mater.* **2016**, 2, 1500341. [4] *Sci. Rep.* **2016**, 6, 31348. [5] *Adv. Energy Mater.* **2017**, 7, 1700449. [6] *Adv. Mater.* **2017**, 1702141. [7] *J. Phys. Chem. Lett.* **2017**, 8, 5395. [8] *J. Phys. Chem. C* **2017**, 121, 25743. [9] *J. Mater. Chem. A* **2018**, 6, 1382. [10] *J. Mater. Chem. A* **2018**, 6, 5746. [11] *Angew. Chem. Int. Ed.* **2018**, 57, 4607.

## Tailoring electronic structure of SWCNTs for transparent and conductive film applications

Alexey P. Tsapenko<sup>1</sup>, Daria S. Kopylova<sup>1</sup>, Fedor S. Fedorov<sup>1</sup>, Alena A. Alekseeva<sup>1</sup>, Evgenia P. Gilshteyn<sup>1</sup>, Pramod M. Rajanna<sup>1</sup>, Vsevolod Iakovlev<sup>1</sup> and Albert G. Nasibulin<sup>1,2</sup>

<sup>1</sup> Skolkovo Institute of Science and Technology, Nobel str. 3, Moscow, 143026, Russia

<sup>2</sup> Aalto University, Department of Applied Physics, 00076, Aalto, Finland

[a.nasibulin@skoltech.ru](mailto:a.nasibulin@skoltech.ru)

Single-walled carbon nanotubes (SWCNTs) are among the strongest candidates for the replacement of commonly used transparent and conductive films (TCFs) based on doped metal oxides, such as indium tin oxide (ITO). SWCNTs possess unique multifunctional nature, which is based on their outstanding combination of mechanical strength and flexibility, chemical stability, exceptional electrical conductivity and optical properties [1]. However, to fully utilize these properties in modern transparent electrode applications, SWCNT-based TCFs have to demonstrate the optoelectronic performance at the level of high-end ITO-based TCFs. This has not been achieved for SWCNT films yet and as a result limit their practical usage.

Using gold chloride as the most effective dopant for the SWCNTs (Table 1), we improve their optoelectrical characteristics by optimizing the doping solvent and conditions [2]. We examined various solvents to push the optoelectrical performance of the TCFs based on SWCNTs. As a result, we obtained the sheet resistance as low as 40  $\Omega/\square$  at the transmittance of 90% (at 550 nm) using 15 mM HAuCl<sub>4</sub> solution (Figure 1). This optoelectrical performance is better than that of ITO on PET substrates and satisfy most of the requirements for modern applications and relatively stable without additional protection over two years storing under ambient conditions.

**Table 1.** Work function of 80% and 65% transmittance SWCNT films before and after the doping by AuCl<sub>3</sub> and HAuCl<sub>4</sub> and measured by means of UPS technique.

Transmittance of the film at 550 nm (%)	Work function of pristine SWCNTs (eV)	Work function of AuCl <sub>3</sub> -doped SWCNTs (eV)	Work function of HAuCl <sub>4</sub> -doped SWCNTs (eV)
80	4.46	5.87	6.14
65	4.44	5.85	6.07

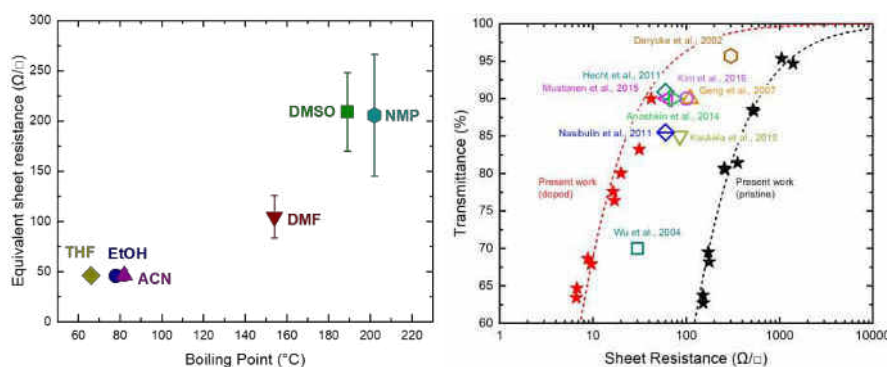


**Figure 1.** a) The resulting equivalent sheet resistance of the HAuCl<sub>4</sub>-doped samples at RT plotted vs. the boiling temperature of the solvents. b) Comparison of the performance of SWCNT-based TCFs after p-type doping: sheet resistance vs. optical transparency at 550 nm. Dashed lines indicated theoretical relationship between transmittance and sheet resistance of pristine (black) and HAuCl<sub>4</sub>-doped (using EtOH as a solvent) SWCNT films (red) obtained in this work.

Also, we examine the effect of ionic liquid gating on the electronic structure of the SWCNTs and their optical and electrical properties.

The effect of the presence of catalyst particles on the optoelectronic properties of the SWCNT films is also presented.

This work was supported by the Russian Science Foundation (Project identifier: 17-19-01787).

[1] A. L. Gorkina, A. P. Tsapenko, E. P. Gilshteyn, T. S. Koltsova, T. V. Larionova, A. Talyzin, A. S. Anisimov, I. V. Anoshkin, E. I. Kauppinen, O. V. Tolochko, A. G. Nasibulin, Carbon **100**, 501 (2016).

[2] A. P. Tsapenko, A. E. Goldt, E. Shulga, Z. I. Popov, K. I. Maslakov, A. S. Anisimov, E. P. Gilshteyn, P. B. Sorokin, A. G. Nasibulin, Carbon **130**, 448 (2018).



# Graphene Functionalized and Optically Forged by Femtosecond Laser

Andreas Johansson<sup>1,2</sup>, Pasi Myllyperkiö<sup>1</sup>, Pekka Koskinen<sup>2</sup>, Jukka Aumanen<sup>1</sup>, Juha Koivistoinen<sup>1</sup>, Hung-Chieh Tsai<sup>3</sup>, Chia-Hao Chen<sup>4</sup>, Lo-Yueh Chang<sup>4</sup>, Vesa-Matti Hiltunen<sup>2</sup>, Jyrki J. Manninen<sup>2</sup>, Kamila Mentel<sup>1</sup>, Wei Yen Woon<sup>3</sup>, Mika Pettersson<sup>1</sup>

<sup>1,2</sup>Nanoscience Center, Department of Chemistry<sup>1</sup>, and Physics<sup>2</sup>, P.O. Box 35, FI-40014, University of Jyväskylä, Finland

<sup>3</sup>Department of Physics, National Central University, Jungli, 32054, Taiwan, Republic of China

<sup>4</sup>National Synchrotron Radiation Research Center, Hsinchu, 30076, Taiwan, Republic of China

Corresponding author: andreas.johansson@jyu.fi

Laser irradiation can be used for modifying properties of graphene. As an example, we have found graphene can be functionalized with oxygen-containing groups through femtosecond pulse irradiation in air [1]. We have characterized the resulting graphene oxide, using  $\mu\text{m}$ -XPS, and found that the chemical composition can be controlled, with varying fractions of hydroxyl and epoxy groups strongly dominating [2]. The two-photon functionalization method therefore allows tailoring of local functionalization with a patterning line width of about 300 nm. It may be used for tuning electronic properties of graphene, e.g. resistivity over five orders of magnitude [1], or its chemical reactivity which may be used for creating complex graphene-based structures. An example of graphene patterning is shown in Fig. 1a and 1b.

When irradiation is performed in inert atmosphere such as nitrogen, an unexpected phenomenon occurs: graphene detaches from the substrate and forms stable, elevated plateaus at the irradiated areas. By controlling local irradiation dose, the height of the plateaus can be varied from about 1 nm to more than 100 nm enabling drawing of complex 3D shapes from graphene simply with a laser beam. This is demonstrated in Fig. 1c, which shows an AFM image of a pyramid made by laser irradiation of graphene. This method is termed optical forging in which a pulsed laser beam forges a graphene sheet into controlled 3D shapes in the nanoscale [3]. The forging mechanism is based on laser-induced local expansion of graphene, as suggested by computer simulations using thin sheet elasticity theory (see Fig. 1d). The expansion is presumably caused by laser irradiation induced formation of defects into the graphene lattice.

The optical functionalization and forging concepts presented here offers new methods for fabricating complex graphene structures, which may provide solutions for building integrated circuitry from layered materials.

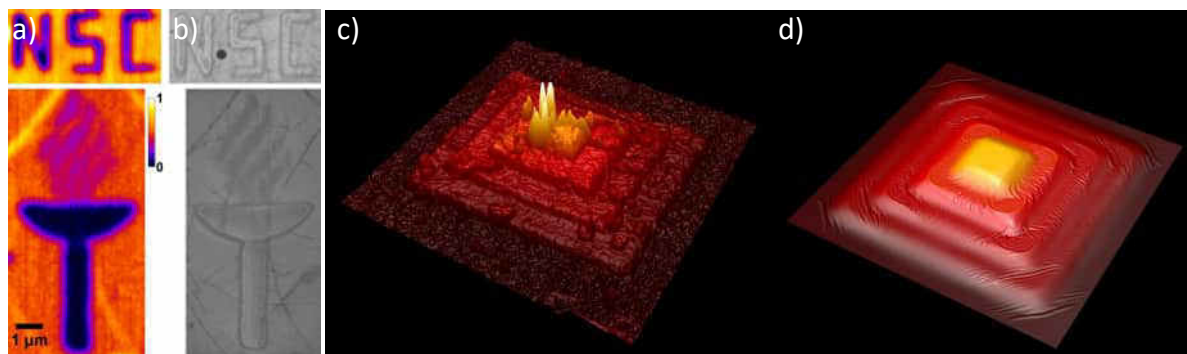


Figure 1. Monolayer CVD graphene on silicon chip. From left, two-photon oxidation patterning imaged with (a) four-wave mixing and (b) scanning electron microscopy. (c) AFM image of a pyramid shape fabricated by optical forging. The side is 11  $\mu\text{m}$  and the maximum height is  $\sim 60$  nm. (d) Simulation (elasticity modelling) of the same pyramid.

[1] J. Aumanen, A. Johansson, J. Koivistoinen, P. Myllyperkiö and M. Pettersson. *Nanoscale*, **7**, 2851 (2015).

[2] A. Johansson, H.-C. Tsai, J. Aumanen, J. Koivistoinen, P. Myllyperkiö, Y.-Z. Hung, M.-C. Chuang, C.-C. Chen, W.-Y. Woon and M. Pettersson, *Carbon*, **115**, 77 (2017).

[3] A. Johansson, P. Myllyperkiö, P. Koskinen, J. Aumanen, J. Koivistoinen, H.-C. Tsai, C.-H. Chen, L.-Y. Chang, V.-M. Hiltunen, J. J. Manninen, W. Y. Woon and M. Pettersson, *Nano Letters*, **17**, 6469 (2017).

# High Aspect Ratio Laser Cutting of CFRP using Nanosecond UV Laser Pulses

Junji Yumoto

*Inst. for Photon Sci. and Tech., The Univ. of Tokyo, 7-3-1, Hongo Bunkyo-ku, Tokyo 113-0033 Japan  
Corresponding author e-mail (8-point type, centered, italicized)*

Carbon Fiber Reinforced Plastics (CFRPs) are expanding their applications in various fields including the aviation and automobile industries because CFRPs are lightweight, strong, and durable. Machining and water jets are used for CFRP cutting, but there are problems with machining accuracy and running costs. Recently, laser processing has been researched as an alternative technology to CFRP cutting [1-3], but the heat-affected zone (HAZ) deteriorated by the irradiation of laser light is an unavoidable problem, and is a major obstacle to using laser-cutting as a standard process.

In this study, we aim to develop high quality laser processing technology applicable to CFRPs designed for aircraft using a pulsed laser at a wavelength of 258nm[4].

The samples are unidirectional CFRPs for Aircraft (supplied by Toray Industries, Inc.), with a thickness of 1.6 mm. Laser pulses have a duration of 7ns and a repetition rate of 10kHz. Laser light with average power of 1W was focused on the CFRP with a diameter of 20 $\mu$ m, and the stage on which the CFRP was placed was moved once at a speed of 0.05-1mm/s orthogonal to the orientation of the carbon fibers. Fig. 1 is a microscope photograph of the cross-section of a laser-cut groove when the stage was moved at a speed of 0.1mm/s and 0.2 mm/s. The moving speed of 0.05 mm/s realizes separation of the 1.6-mm CFRP with a cutting width of 20  $\mu$ m which corresponds to the left edge of the CFRP in Fig. 1. This gives an aspect ratio of more than 80.

EDX analysis was performed on the surface and cross-section of the laser-cut groove. In Fig. 2(a), it is clearly observed that the vertical position of each laser-cut carbon fiber is almost aligned but they are covered with a thin layer. Fig.2 (b) shows the result of sulfur analysis for the same area as Fig. 2(a). Sulfur is just one of the components included in the resin, and the carbon concentration of the layer is around the middle of the resin and CFs. This implies that the layer formed after the CFRP was laser-cut, and that the layer is a mixture of resin and particles of carbon fiber. This imply is also supported by Raman Spectroscopy of the thin layer. The observed Raman spectrum as shown in Fig.2 (c) have peaks due to D and G bands in graphite[5].

We believe this to be the first report of high aspect ratio laser cutting of more than 80 on CFRPs, and it is expected to meet the requirements of industries.

This research is supported by the Center of Innovation Program from the Japan Science and Technology Agency, JST.

[1] H. Niino et al., 2D/3D laser cutting of carbon fiber reinforced plastic (CFRP) by fiber laser irradiation, Proc. of SPIE, Vol. 9353, pp. 935303, (2015).

[2] J. Finger, M. Weinand, and D. Wortmann, Ablation and cutting of carbon-fiber reinforced plastics using picosecond pulsed laser radiation with high average power, J. Laser Appl., Vol. 25, No. 4, pp. 042007, (2013).

[3] Y. Sato, et al., Thermal effect on CFRP ablation with a 100-W class pulse fiber laser using a PCF amplifier, Appl. Surface Sci., Vol. 417, pp.250-255 (2017)

[4] M. Moriyama, et al., The Third Smart Laser Processing Conference 2018, SLPC 9-5, Yokohama, (2018).

[5] I. Pocsika, et al., J. Non-Crystalline Solids 227-230, 1083 (1998).

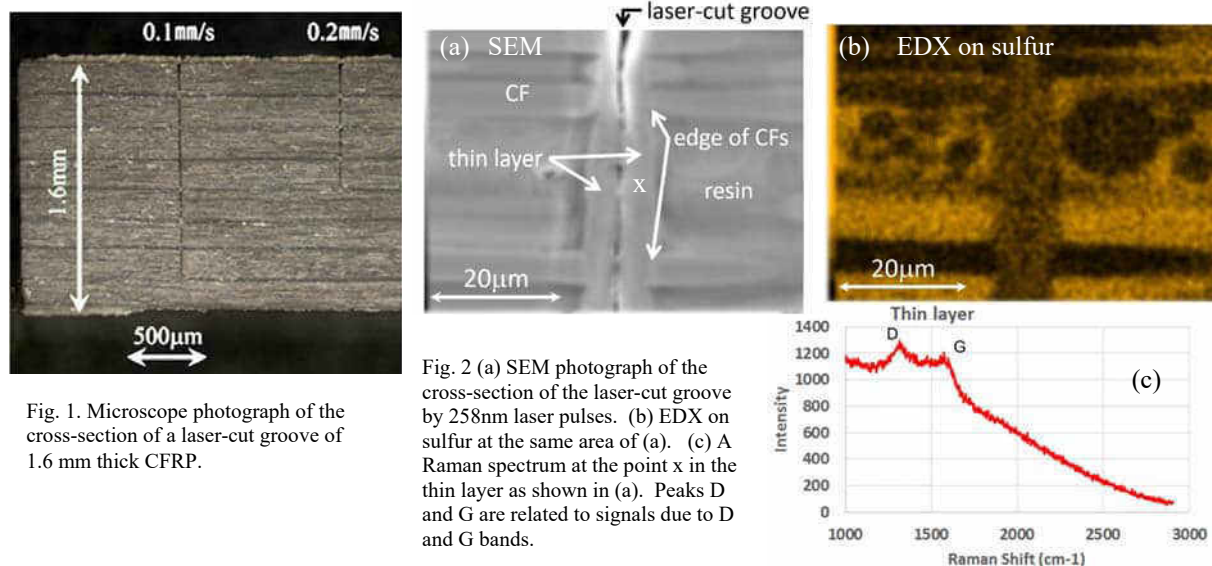


Fig. 1. Microscope photograph of the cross-section of a laser-cut groove of 1.6 mm thick CFRP.

Fig. 2 (a) SEM photograph of the cross-section of the laser-cut groove by 258nm laser pulses. (b) EDX on sulfur at the same area of (a). (c) A Raman spectrum at the point x in the thin layer as shown in (a). Peaks D and G are related to signals due to D and G bands.



## Poster session II



©G. Lepehin



## **Floating catalyst CVD synthesis of single walled carbon nanotubes using ethylene as carbon precursor for transparent electrode**

**Aqeel Hussain, Yongping Liao centered, Qiang Zhang, Er-Xiong Ding, Patrik Laiho, Saeed Ahmad, Hua Jiang, Esko I. Kauppinen**

*Department of Applied Physics, Aalto University School of Science, P.O Box 15100, FI-00076 Aalto, Finland*

*Corresponding author: [esko.kauppinen@aalto.fi](mailto:esko.kauppinen@aalto.fi)*

Transparent conducting films (TCFs) are critical components of many optoelectronic devices that pervade modern technology. Due to their excellent optoelectronic properties and flexibility, single-walled carbon nanotube (SWNT) films are regarded as an important alternative to the conventional transparent conducting material, i.e the brittle indium tin oxide. Herein, we have developed aerosol synthesis of SWCNTs using C<sub>2</sub>H<sub>4</sub>-H<sub>2</sub>-N<sub>2</sub> system for high performance thin SWNT film fabrication. For the first time, ethylene has been used as the only carbon source for high-quality SWNT synthesis in FCCVD with N<sub>2</sub> as the main carrier gas, which makes the growth process economical, safe and environmental friendly. The electron diffraction (ED) analysis indicates that chirality of the SWNT randomly distributes between armchair and zigzag structures and the proportion of metallic SWNTs is around 38%. High-performance TCFs of SWNTs are directly fabricated with deposition of SWCNT aerosol on the filters at room temperature. Specifically, CNT TCFs exhibit improved performance up to 51 Ω/sq. at 90 % transmittance after HNO<sub>3</sub> doping with the optimized synthesis process. The excellent conductivity of the SWNT TCFs is attributed to long tubes (mean length 13 μm) and low bundling with 29 % of individual tubes. This high-performance SWCNT TCFs have great potential in flexible electronics, photovoltaic [1] and electrochemistry [2]. Moreover, the addition of water vapors produced very small diameter SWCNTs.

[1] Aitola, K, et al. *Energy & Environmental Science* 9.2 (2016): 461-466.

[2] Tavakkoli, M, et al. *Angewandte Chemie* 127.15 (2015): 4618-4621



## Influence of the carbon nanoparticles structure on their lithium storage capacity

**L.L. Lapteva,<sup>1,2</sup> Yu.V. Fedoseeva,<sup>1,2</sup> E.V. Shlyakhova,<sup>1,2</sup> L.G. Bulusheva,<sup>1,2</sup> A.V. Okotrub<sup>1,2</sup>**

<sup>1</sup>*Nikolaev Institute of Inorganic Chemistry SB RAS, 3 Acad. Lavrentiev Avenue, 630090 Novosibirsk, Russia*

<sup>2</sup>*Novosibirsk State University, 2 Pirogova Street, 630090 Novosibirsk, Russia*

*lapteva.l.l@yandex.ru*

Investigation of carbon/lithium interface is an urgent task for energy storage devices such as lithium-ion batteries and supercapacitors. It has been shown that single-walled carbon nanotubes (SWCNTs) and porous carbon materials are successful for electrochemical applications. We used commercial SWCNTs by OCSiAl and porous carbon grown via CVD from ethanol, toluene and acetonitrile. To characterize the samples high-resolution transmission electron microscopy, scanning electron microscopy, Raman spectroscopy and optical absorption spectroscopy were applied. The SWCNT sample is a mixture of semiconducting and metallic single-walled nanotubes of different diameters. The average diameter of SWNTs was estimated to be 1.7 nm. In addition, we found that porous carbons synthesized from ethanol and acetonitrile have thin-layered sponge-like structure, while porous carbon grown with toluene is enriched by hollow capsules of 10 nm thickness.

We have studied the effect of vacuum thermal vapor deposition of lithium on SWCNTs and porous carbon by in situ X-ray photoelectron spectroscopy (XPS) and near-edge X-ray absorption fine structure spectroscopy. The low ratio between lithium and carbon materials means that carbon materials are incompletely covered by Li. In case of SWCNTs, two types of carbon atoms, which are located close to and away from Li atoms were emerged clearly. Quantum-chemical modeling of XPS spectra and calculation of atomic charges and molecular electrostatic potential maps showed that carbon atoms located near Li atoms are in strong positive electric field from Li, whereas Li-free regions have negative electrostatic potential. Similar effects should be for porous carbon but they can not be separated because of a large amount of defects.

Electrochemical studies were carried out in half cells, using lithium metal foil as anode and porous carbon as cathode. The cells were galvanostatically charged and discharged over the potential range from 0.01 to 2.50 V versus Li/Li<sup>+</sup> at various current densities. The charge-discharge voltage curve revealed different behavior for fast and slow cycling which is explained by various conductivity, pore size and surface area of the samples.

The work was financially supported by Russian Science Foundation (grant 17-73-10226).

## Electrochemical properties of carbon nanostructures modified by oxygen containing groups

Fedorovskaya E.O.<sup>1,2</sup>, Kurenaya A.G.<sup>2</sup>, Asanov I.P.<sup>1,2</sup>, Bulusheva L.G.<sup>1,2</sup>, Okotrub A.V.<sup>1,2</sup>

<sup>1</sup>Novosibirsk State University, 630090, Novosibirsk, 1, Pirogova str., Russia

<sup>2</sup>Nikolaev Institute of Inorganic Chemistry, SB RAS, 630090, Novosibirsk, 3, Acad. Lavrentiev Ave., Russia

e.fedorovskaia@nsu.ru

Carbon nanomaterials (graphene, nanotubes, etc.) are promising for use in electronics, energy storage devices, sensors, catalytic systems, etc. due to high conductivity, large surface area, chemical inertness and physical stability. Functional groups on the carbon surface are able to accumulate additional energy due to oxidation-reduction processes in the electrodes of supercapacitors, by increasing of the hydrophilicity and changing the mesoporous structure of the carbon nanomaterial. In addition, oxygen-containing functional groups can be used to attach more complex macromolecules. The cyclic voltammetry method is used to study of the oxidation-reduction processes in the electrode material and this method clearly demonstrates the ongoing reactions. However, despite the importance of studying of the functionalization processes of the carbon nanostructures surface and studying the behavior of oxygen-containing functional groups during electrochemical cycling, this issue has not been studied sufficiently

The methods for oxidizing of the carbon nanostructures surface (double-layered carbon nanotubes, multiwall carbon nanotubes [1], and reduced graphite oxide) were investigated. Nanostructures were functionalized with oxygen-containing functional groups in the process of hydrothermal treatment, heat treatment and chemical modification of the surface. Morphology and functional composition of the surface were studied using SEM and TEM microscopy and IR, Raman spectroscopy, and X-ray photoelectron spectroscopy. The electrochemical behavior of the initial and modified materials was studied using cyclic voltammetry and electrochemical impedance spectroscopy

Using the method of cyclic voltammetry, half-reaction potentials were obtained and correlated with the reactions occurring on the nanotube or graphene surface. When the concentration of functional groups on the surface increases, the capacity increases due to the contribution of the pseudo-capacity. In addition, the relationship between the morphology of the material, its conductivity and the features of the diffusion processes was demonstrated using the method of spectroscopy of electrochemical impedance.

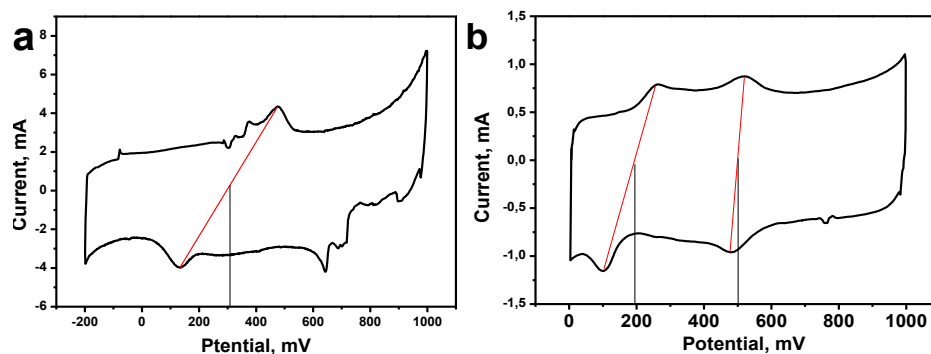


**Fig. 1.** Cyclic voltammograms of double-layered carbon nanotubes after oxidative treatment with mineral acids (a) and multiwall carbon nanotubes after hydrothermal treatment (b). The peaks on the CV curves correspond to the oxidation and reduction processes of oxygen-containing functional groups



## Carbon nanotube buckypaper, reduced graphene oxide and polypyrrole nanocomposites for supercapacitor applications.

Iurchenkova A. A.<sup>1</sup>, Popov K. M.<sup>2</sup>, Fedorovskaya E. O.<sup>1,2</sup>, Bulusheva L. G.<sup>1,2</sup>, Okotrub A. V.<sup>1,2</sup>

<sup>1</sup>Novosibirsk State University, 630090, Novosibirsk, 1, Pirogova str., Russia

<sup>2</sup>Nikolaev Institute of Inorganic Chemistry, SB RAS, 630090, Novosibirsk, 3, Acad. Lavrentiev Ave., Russia  
anna.yurchenkova@yandex.ru

Due to their high power, charging rate, low weight and durability supercapacitors have become effective devices for energy storage. Through these advantages they can be widely used in pulse electronics, such as photoflash tubes, pulse lasers, etc., as well as electric vehicle supply systems. Charge accumulation in supercapacitors is accounted for two processes: double electric layer formation, formed on the electrode surface–electrolyte interface, and redox (reduction – oxidation, so called Faraday) reactions procedure. Typically, carbon materials, conducting polymers, transition metals oxides and composites based on them are the materials for supercapacitors. Carbon materials mainly accumulate energy due to the double electric layer foundation. Thus, their advantages are large surface area, high conductivity and cycling stability. Conducting polymers and transition metals oxides basically accumulate energy through the Faraday reactions, they possess more capacities, but lower chemical stability in comparison with carbon materials. Thus, derivatization of the composites that combine the carbon template and electrically active conducting polymers properties has shown the promising applications in high-effective electrode supercapacitor materials production.

In our work we synthesized buckypaper based on multiwall carbon nanotubes and reduced graphite oxide, later used as carbon template. Further, chemical and electrochemical deposition of polypyrrole was carried out on the carbon material electrodes. To study the morphology and functional composition of obtained products we used SEM, IR-spectroscopy, XPS and Raman spectroscopy methods. Cyclic voltammetry and electrochemical impedance spectroscopy methods were used to investigate electrochemical behavior of the samples.

We also studied the influence of carbon template and polypyrrole deposition methods on their morphology and electrochemical properties. Carbon nanostructures specific capacity was shown to increase after polypyrrole deposition, reaching 200 F/g, since the materials demonstrated high stability during the cycling process.

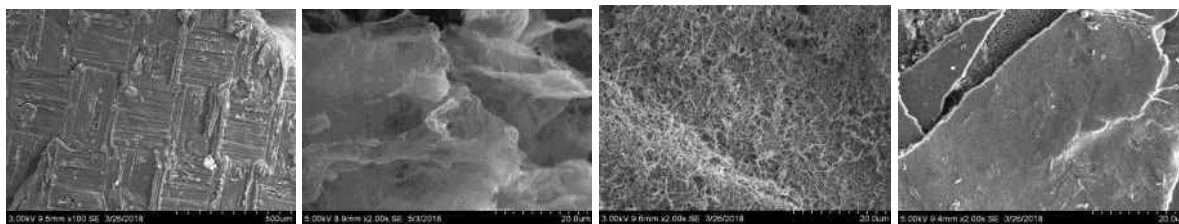


**Fig 1.** SEM images of carbon material and their composite with carbon material: a) carbon nanotube buckypaper; b) reduced graphene oxide; c) composite of buckypaper with chemical precipitated polypyrrole; d) composite of buckypaper with electrochemical precipitated polypyrrole.

The work was supported by Russian Foundation for Basic Research (project 18-43-543018 r\_mol\_a)

## Purification of single-wall carbon nanotubes by magnetic separation

O.A. Gurova<sup>1\*</sup>, V.E. Arhipov<sup>1</sup>, E.N. Vostretsova<sup>2</sup>, V.O. Koroteev<sup>1</sup>, O.V. Sedelnikova,<sup>1</sup> A.V. Okotrub<sup>1</sup>

<sup>1</sup>Nikolaev Institute of Inorganic Chemistry SB RAS, 3, Acad. Lavrentiev ave., Novosibirsk, 630090, Russia

<sup>2</sup> Tomsk State University, 36 Lenin ave., Tomsk, 634050, Russia

Corresponding author e-mail: olga.gurov@gmail.com

Carbon nanotubes have attractive optical, electronic, thermal and mechanical properties for various area of application [1]. However, one of the problems preventing useful application of CNTs is getting metal free nanotubes. The major impurities present in produced CNTs is metallic catalyst particles (e.g. iron, nickel, cobalt) remaining from the synthesis. The most common purification methods are the oxidation by different techniques [2], treatment with different acids [3], ultracentrifugation [4], etc.

In this work, we offer combination method of CNTs purification by HCl acid and magnetic separation. We use single-wall carbon nanotubes (SWCNT) provided by OCSiAl company. Tubes average diameter was 1.7 nm. SWCNT had a purity of 75%. According to atomic-absorption spectroscopy, the amount of Fe catalytic particles in the SWCNT data was ~ 7 mass%. In addition, TEM image confirms a large amount of Fe particles (fig. 1(a)).

In the first stage of purification, SWCNTs were treated with HCl acid in an ultrasonic bath. After HCl treatment, the amount of Fe decreased to 2%. SWCNTs dispersion containing surfactant was prepared for a second stage of purification. The SWCNT dispersion was passed through magnetic installation. The magnetic separation was carried out using silicone tube placed in a magnetic field. SWCNT dispersion was pumped by a slow flow through the tube. It was shown that the amount of iron is reduced to 0.3%. This method could be combined with other dispersion based techniques, which allow separation of SWCNT by transport properties and chirality.

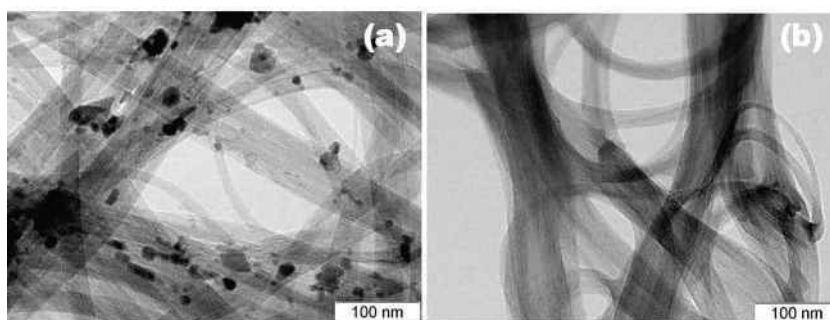


Fig.1 TEM images of (a) initial SWCNT and (b) after HCl treatment and magnetic separation.

This work was partially supported by and the Russian Science Foundation (Project 18-72-00017).

[1] J.G. Park, J. Louis, Q. Cheng, J. Bao, J. Smithyman, R. Liang, B. Wang, C. Zhang, J.S. Brooks, L. Kramer, P. Fanchasis and D. Dorrough, *Nanotechnology*, **20**, 1 (2009).

[2] N. Dementev, S. Osswald, Yu. Gogotsi and E. Borguet, *J. Mater. Chem.*, **19**, 7904 (2009).

[3] E.R. Edwards, E.F. Antunes, E.C. Botelho, M.R. Baldan and E.J. Corat, *Appl. Surf. Sci.*, **258**, 2 (2011).

[4] Y. Matsuzawa, Y. Takada, T. Kodaira, H. Kihara, H. Kataura, and M. Yoshida, *J. Phys. Chem. C*, **118**, 9, (2014).

# FCCVD growth of SWCNTs by spark discharge based metallic and bimetallic catalysts particles

Saeed Ahmad, Aqeel Hussain, Yongping Liao, Er-Xiong Ding, Qiang Zhang, Esko I. Kauppinen \*

*Department of Applied Physics, Aalto University School of Science, P.O. Box 15100, FI-00076 Aalto, Finland.*

*Corresponding author: esko.kauppinen@aalto.fi*

## Abstract

Floating catalyst chemical vapor deposition (FCCVD) is one of the most widely used technique for CNT synthesis. The catalysts for CNT synthesis in FCCVD are strongly tied with the CNT yield, morphology, and chirality. However, the catalyst aerosol in conventional FCCVD, is made with the pyrolysis of volatile organometallic compounds, e.g. ferrocene. This conventional process of catalyst fabrication in FCCVD, not only limits the composition of the catalyst but also hinders to regulate the concentration and configuration of the catalyst. Here, we introduce a novel rod to tube type spark discharge generator (R-T SDG) to synthesize time stable metallic and bimetallic catalyst nanoparticles for the FCCVD growth of SWCNTs. Based on the physical evaporation-nucleation-condensation process, spark discharge generation of nanoparticles is a low-cost and scalable gas phase method that can produce variety of highly pure metal or alloy nanoparticles with controllable number concentration and particle size distribution [1,2]. We synthesized monometallic Fe and Co as well as bimetallic Co-Ni catalyst particles from R-T SDG. These particles were introduced inside a vertical FCCVD reactor along with ethylene as carbon source to grow high quality SWCNT. At the outlet of the reactor SWCNTs were deposited in gas phase on membrane filter to form CNT films which can be applied in high-performance transparent electrodes. The sheet resistance of 90% transparent CNT films at 550 nm wavelength after doping with 16 mM  $\text{AuCl}_3$  varies in the range  $180\text{--}240\ \Omega\ \text{sq}^{-1}$  as shown in the Fig.1. This novel technique has great potential in academic and industrial fields of CNT synthesis and their applications.

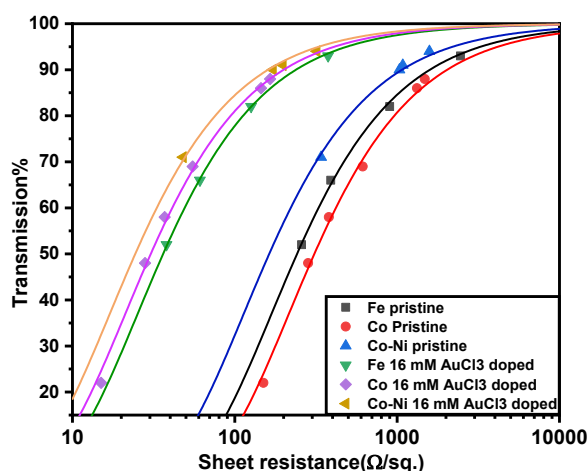


**Fig. 1.** Optoelectronic performance of SWCNTs synthesized in gas phase inside a vertical FCCVD reactor using spark produced Fe, Co and Co-Ni catalyst nanoparticles.

## References

- [1] Chae, S., Lee, D., Kim, M.-C., Kim, D. S., & Choi, M, Aerosol Science and Technology, 49(7), 463–471 (2015).
- [2] Mustonen, K., Laiho, P., Kaskela, A., Zhu, Z., Reynaud, O., Houbenov, N., ... Kauppinen, E. I, Applied Physics Letters, 107(1) (2015).

# Compact chemical vapor deposition system with embedded scanning probe microscope for in-situ study of material growth

A.B. Loginov, R.R. Ismagilov, A.N. Obratsov

Lomonosov Moscow State University, Department of Physics, Moscow 119991, Russia  
loginov.ab15@physics.msu.ru

The chemical vapor deposition (CVD) setup combining reactor and scanning probe microscope (SPM) was developed using principles described earlier [1,2]. Exceptional feature of the created setup is its ability to provide *in-situ* measurements during deposition process.

A key problem solved in this work is construction of sample holder providing ability for isolation of the SPM body from the heated up to 1200 °C sample. The holder was made as a cylinder of aerogel (SiO<sub>2</sub> with extremely high porosity). The sample temperature was ensured by Joule heating of a chip produced from standard 500µm thick Si wafer with two molybdenum wires used as electrodes to supply electric current. The whole system was attached to the sample holder made from quartz plate. The photo images of the CVD reactor chamber and its reactive zone are shown in Fig.1. Thin Ni substrate was located on the heater and supported by molybdenum wire (see Fig.1a). Moreover, besides fixation this wire simultaneously plays a second important role – it supplies tunnel voltage to the substrate.

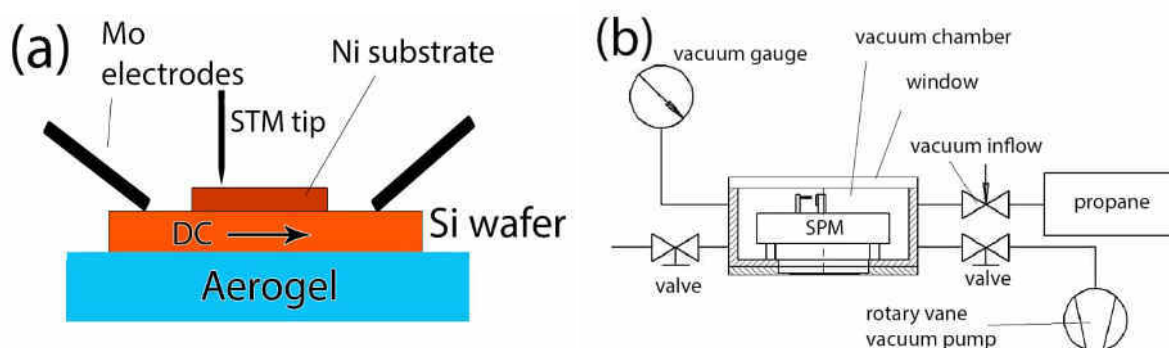


Fig. 1. (a) – scheme of the sample holder with embedded heating system ; (b) – scheme of the CVD system with embedded STM

Preliminary results of *in-situ* measurements demonstrate ability of the system for detection carbon deposits formed on substrate. Typical examples of the STM images obtained during *in-situ* measurements are presented in Fig. 2. The STM images of nickel substrate were obtained from the same regions of the substrate before and after 3 min CVD process. Thermal CVD process was realized by heating Ni substrate up to 700-800 °C in propane gas atmosphere at 6 mbar pressure.

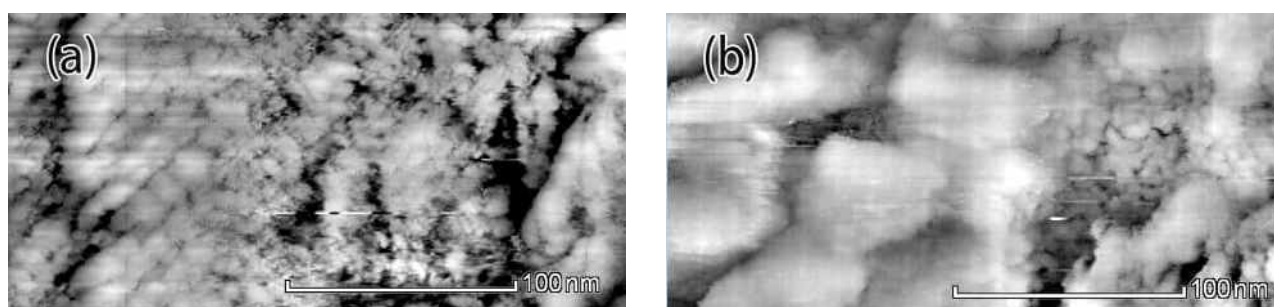


Fig. 2.(a) – STM image of Ni sample before heating; (b) – STM image of Ni sample in a same place after 3 min heating in propane

This work was supported by RSF project 17-72-10173

[1] A. B. Loginov, R. R. Ismagilov. Designing a scanning probe microscope for in situ study of carbon materials growth processes during chemical vapor deposition. *Journal of Nanophotonics*, 11(2017)032509.

[2] A.N. Obratsov, A.A. Zolotukhin, A.O. Ustinov, A.P. Volkov, Yu.P. Svirko. Chemical vapor deposition of carbon films: in-situ plasma diagnostics. *Carbon* 41 (2003) 836. If you wish you may include an acknowledgment of grants support at the end of the main text.

## Single-crystal diamond pyramids formation by hot filament chemical vapor deposition

I. P. Kudarenko<sup>\*1</sup>, R. R. Ismagilov<sup>1</sup>, S. A. Malykhin<sup>1,2</sup>, A. N. Obraztsov<sup>1,2</sup>

<sup>1</sup>Department of Physics, Lomonosov Moscow State University, Moscow 119991, Russia

<sup>2</sup>Department of Physics and Mathematics, University of Eastern Finland, Joensuu 80101, Finland

\*kudarenko@polly.phys.msu.ru

Chemical vapor deposition (CVD) allows fabrication of different types of thin film carbon materials. Recently it was demonstrated in our works that combination of CVD and selective oxidation might be used for synthesis single-crystal diamond crystallites with numerous attractive characteristics [1-3]. Plasma enhanced CVD has been used in these previous studies, which limits capacity of its productivity.

In this study we demonstrate possibility of production of similar polycrystalline films and single crystal diamonds by using hot filament CVD (HFCVD). Usage in this work industrial HF CVD system "SP3 Diamond Technologies Inc." potentially allows fabrication of large area polycrystalline films with total surface area of about 0.5 m<sup>2</sup>. Obtained results confirm ability of used HFCVD method to provide synthesis of polycrystalline diamond films with characteristics allowing obtaining single crystal diamonds using selective oxidation. SEM images presented in Fig. 1 demonstrate the diamond crystallites obtained by HF CVD. The analysis of the methodology will be presented in this report.

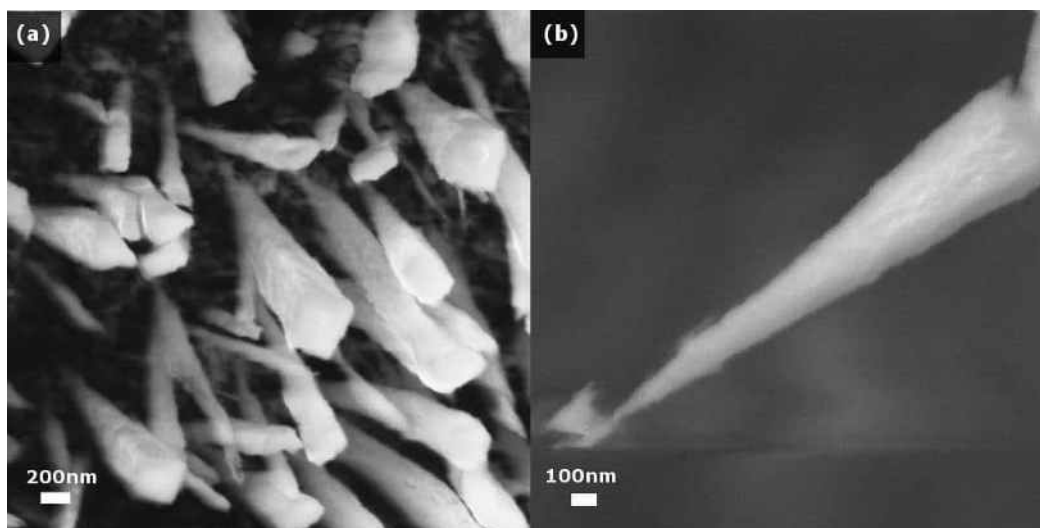


Fig. 1. (a,b) – typical SEM images of the diamond needles, which were obtained by selective oxidation of polycrystalline films produced using industrial HFCVD reactor

This work was supported by RSF project 17-72-10173.

- [1] Feruza T. Tuyakova, Ekaterina A. Obraztsova, and Rinat R. Ismagilov. Single-crystal diamond pyramids: synthesis and application for atomic force microscopy. *Journal of Nanophotonics*, 10(1):012517, 2016.
- [2] Feruza T. Tuyakova, Ekaterina A. Obraztsova, Evgeny V. Korostylev, Dmitry V. Klinov, Kirill A. Prusakov, Andrey A. Alekseev, Rinat R. Ismagilov, and Alexander N. Obraztsov. Photo-and cathodo-luminescence of needle-like single crystal diamonds. *Journal of Luminescence*, 179:539–544, 2016.
- [3] L. Arnoldi, M. Spies, J. Houard, I. Blum, A. Etienne, R. Ismagilov, A. Obraztsov, and A. Vella. Thermal diffusivity of diamond nanowires studied by laser assisted atom probe tomography. *Applied Physics Letters*, 112:143104, 2018

# Continuous direct production of carbon nanotube films and fibers by floating-catalyst CVD

Qiang Zhang<sup>1\*</sup>, Weiya Zhou<sup>2</sup>, Sishen Xie<sup>2</sup>, Esko I. Kauppinen<sup>1\*</sup>,

*<sup>1</sup>Department of Applied Physics, Aalto University School of Science, P.O. Box 15100, FI-00076, Aalto, Finland*

*<sup>2</sup>Beijing National Laboratory for Condensed Matter Physics, Institute of Physics, Chinese Academy of Sciences, Beijing, 100190 (P.R. China)*

*Corresponding author: qiang.zhang@aalto.fi, esko.kauppinen@aalto.fi*

Macroscale carbon nanotube (CNT) architectures, especially films and fibers, are desired for both fundamental research and potential applications [1]. Here, continuous CNT films and fibers are directly produced by floating-catalyst chemical vapor deposition (FCCVD). Based on the hydrocarbon-FeCp<sub>2</sub> FCCVD system, the tubular CNT films can be directly and continuously fabricated with transformation from CNT aerosol into CNT aerogel in the process of CNT synthesis. The optimized synthesis process manifests a high carbon efficiency (~ 60%), high extrusion yield (hundreds of meters per hour), and stable controllability in the fabrication of freestanding films. Specially, this continuous CNT films have excellent transparent and conductive performance (Fig.1). The sheet resistance of as-synthesized film is around 180  $\Omega/\text{sq}$  for transmittance of 90%. The film conductivity can be improved by 3~4 times with chloroauric acid doping (sheet resistance / transmittance, ~50  $\Omega/\text{sq}$  / 90%). Moreover, the continuous CNT fibers can be directly fabricated by shrinking tubular CNT films with liquid [2]. For performance improvement, as-prepared fibers are further post-treated by acid resulting in the compaction and surface modification of the CNTs in fibers, which are beneficial for the electron and load transfer. Compared to the HNO<sub>3</sub> treatment, HClSO<sub>3</sub> or H<sub>2</sub>SO<sub>4</sub> treatment is more effective for the improvement of the fibers' properties. After HClSO<sub>3</sub> treatment for 2 h, the fibers' strength and electrical conductivity reach up to ~2 GPa and ~4.3 MS/m, which are promoted by ~200% and almost one order of magnitude than those without acid treatment, respectively. The load-bearing status of the CNT fibers are analyzed based on the downshifts of the G' band and the strain transfer factor of the fibers under tension. The results reveal that acid treatment could greatly enhance the load transfer and inter-bundle strength. With the HClSO<sub>3</sub> treatment, the strain transfer factor is enhanced from ~3.9% to ~53.6%. Because of its low set-up cost and high production yield, scalability, and degree of control, this advanced FCCVD has potential in the fabrication of CNT-based transparent electrodes and high-performance fibers.

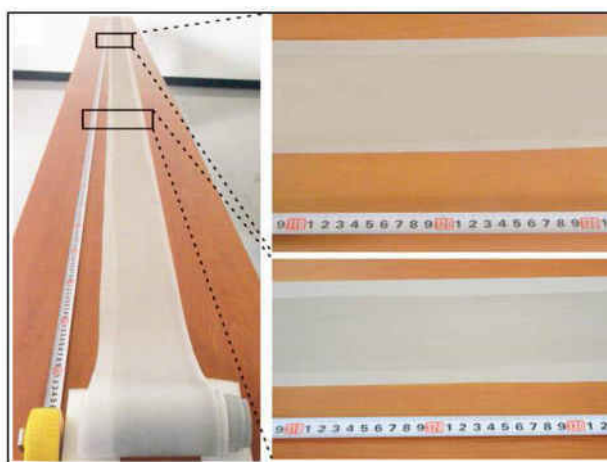


Fig.1 The continuous CNT film from FCCVD

[1]. Nasibulin A G, Kaskela A, Mustonen K, et al. ACS nano, 2011, 5(4): 3214-3221.

[2]. Zhang Q, Li K, Fan Q, et al. Chinese Physics B, 2017, 26(2): 028802.

## Temperature dependence of aqueous two-phase extraction of single-walled carbon nanotubes

D.A. Musatov<sup>1</sup>, V.A. Eremina<sup>2</sup>, E.D. Obraztsova<sup>2</sup>

<sup>1</sup>Department of Problems of Physics and Energetics, Moscow Institute of Physics and Technology (State University), 7 Institutskiy per., Dolgoprudny, Moscow Region, Russia

<sup>2</sup>A.M. Prokhorov General Physics Institute, RAS, 38 Vavilov street, 119991 Moscow, Russia  
dima.musatov97@gmail.com

Single-walled carbon nanotubes (SWCNTs) are considered as one of the most promising nanomaterials because of their extraordinary mechanical, thermal and electrical properties. SWCNTs have an exceptional feature that they can be either metallic or semiconducting with varying band gaps, depending on their diameter and chirality. Semiconducting single-walled carbon nanotubes can be useful for photonic device applications, while metallic are particularly promising for a variety of electronic applications such as nanocircuit components [1]. Most of the currently known SWCNT synthetic techniques produce SWCNTs in a mixture of both types of conductivities. Therefore, the problem of extraction either semiconducting or metallic SWCNTs becomes important. In this work, we considered a spontaneous partition of SWCNTs in polymer-modified aqueous phases [2,3] and studied the temperature dependence of metallic/semiconductor separation of SWCNTs.

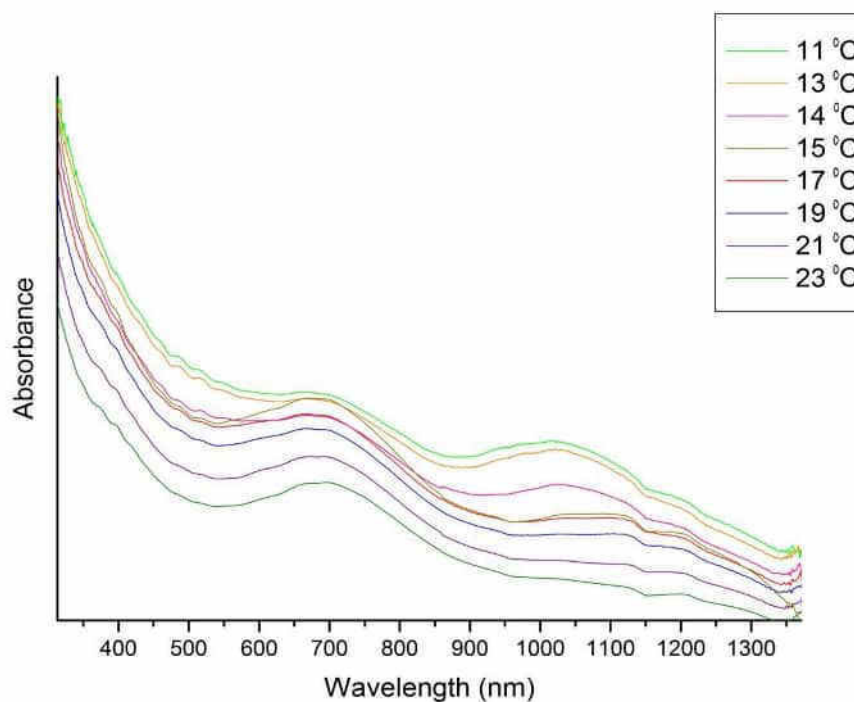


Fig. 1. UV-vis-NIR absorption spectra from the bottom (metallic) phase depending on the temperature.

### Acknowledgements

The reported study was funded by RFBR according to the research project № 18-32-00998.

### References

- [1] Vajtai R. Springer Handbook of Nanomaterials. Springer, 2013.
- [2] Khripin, Constantine Y., Jeffrey A. Fagan, and Ming Zheng. "Spontaneous partition of carbon nanotubes in polymer-modified aqueous phases." *Journal of the American Chemical Society* 135.18 (2013): 6822-6825.
- [3] Eremina, V.A., Obraztsov, P.A., et al. "Separation and optical identification of semiconducting and metallic single-walled carbon nanotubes." *Physica Status Solidi (b)* 254.5 (2017).



## Morphology and transport properties of B, N and BN-doped carbon materials synthesized using arc discharge procedure

O.V. Sedelnikova,<sup>1,2\*</sup> Yu. V. Fedoseeva, A.I. Romanenko, D.S. Bychanok,<sup>3</sup> L.G. Bulusheva,<sup>1,2</sup> A.V. Okotrub<sup>1,2</sup>

<sup>1</sup>Nikolaev Institute of Inorganic Chemistry SB RAS, 3 Academician Lavrentiev Av., Novosibirsk 630090, Russian Federation

<sup>2</sup>Novosibirsk State University, 2 Pirogov Str., Novosibirsk 630090, Russian Federation

<sup>3</sup>Research Institute for Nuclear Problems, Belarusian State University, 220030 Minsk, Belarus  
o.sedelnikova@gmail.com

Arc discharge is a capable route for mass production of metal-free multi-walled carbon nanotubes (MWCNTs). The doping of carbon nanostructures with heteroatoms, such as boron or nitrogen, is one of the effective ways to change their properties as required by the application. Taking into account diversity of morphologies of carbon nanostructures produced by arc discharge method, finding how transport properties depend on doping and the structure of the material can make transport measurement a useful characterization tool. Here, we report the effect of introduction of nitrogen and boron species in an electric arc on composition of cathode deposits and analyze their transport properties.

The pure carbon and doped carbon materials were synthesized in an electric arc using apparatus described elsewhere [1]. The doping of carbon material with nitrogen and/or boron was achieved by a vaporization of graphitic electrode in nitrogen atmosphere and boron-filled electrode in nitrogen or helium atmosphere. The samples were examined by transmission electron microscopy, Raman spectroscopy, and Near-edge X-ray absorption fine structure (NEXAFS) spectroscopy and X-ray photoelectron spectroscopy (XPS, spectra were measured at the BESSY II using radiation from the Russian-German beamline). Temperature dependence of the samples' conductivity was measured at zero magnetic field from the liquid helium to room temperature. The Hall coefficient and magnetoresistance (MR) were determined for the same specimen in a helium atmosphere.

It was noticed that the addition of nitrogen and boron in arc discharge process changes the composition, atomic ordering, charge carrier density, and in effect – transport properties of arc discharge product. A comprehensive characterization confirms a successful nitrogen and boron substitution in graphite lattice, corresponding to *n*- and *p*-type conducting N-doped composite and B- and BN-doped composites, respectively. Even at low impurity content, incorporation of boron in carbon network is accompanied with formation of structural defects that endows the arc discharge composite with transport properties of disordered electronic system governed by the weak localization and diffusive scattering effects. In the presence of nitrogen, we obtained the well-graphitized arc discharge product, which, among other nanocarbons, includes submicron-sized graphite plates. N-doped composite exhibits low-field (<3000 G) negative MR which arises from disordered nature of nano-sized structures crossovers to positive MR at higher field. We attribute this effect to compensation from ordinary positive MR in big graphite plates.

This work was done with the support of Russian Foundation for Basic Research (Project 17-52-04077). O.V. Sedelnikova thanks the Scholarship of the President of the Russian Federation (SP-3530.2016.1).

[1] A. V. Okotrub, Yu. V. Shevtsov, L. I. Nasonova, D. E. Sinyakov, O. A. Novoseltsev, S. V. Trubin, V. S. Kravchenko, L. N. Mazalov.. *Pribory i Tekhnika Experimenta* **1**, 193 (1995).



# Highly conductive and transparent single-walled carbon nanotube film fabricated by floating catalyst chemical vapor deposition using liquid carbon source

**Er-Xiong Ding, Hua Jiang, Qiang Zhang, Yongping Liao, Aqeel Hussain, Esko I. Kauppinen\***

*Department of Applied Physics, Aalto University School of Science, Puumiehenkuja 2, 00076 Aalto, Espoo, Finland  
esko.kauppinen@aalto.fi*

Single-walled carbon nanotube (SWCNT) films have a great potential to replace indium tin oxide films for the applications in transparent and conductive electronics. Here we report SWCNT transparent conducting films (TCFs) fabricated by floating catalyst chemical vapor deposition (FCCVD) method using liquid carbon source. Ethanol [1,2] and toluene [3] are separately selected as carbon sources since neither of them has been employed for the direct fabrication of SWCNT TCFs from a FCCVD reactor. Utilizing ethanol as carbon source, the fabricated SWCNT TCFs exhibit low sheet resistances of 78  $\Omega/\text{sq.}$  at 90% transmittance at 550 nm. The sheet resistance value decreases to 63  $\Omega/\text{sq.}$  at the same transmittance when toluene is adopted. Meanwhile, various characterizations, including diameter and length of SWCNT bundles, are performed to elucidate the causes of the excellent optoelectronic performance of our SWCNT TCFs. It turns out that long and narrow bundled SWCNTs with large diameters are synthesized. Depicting chirality maps of SWCNTs by analyzing statistically counted electron diffraction patterns is the most significant part, which fills the gap in chirality distribution of SWCNTs. With ethanol as carbon source, the majority SWCNTs are close to armchair type with 77% semiconducting species. As for those SWCNTs obtained from toluene, a bimodal chirality distribution of both near zigzag and armchair types are found. Our studies provide fundamental basis to SWCNT research, and highlight the potential of SWCNT TCFs to be extensively applied in high performance flexible electronics.

[1] E.-X. Ding, H. Jiang, Q. Zhang, Y. Tian, P. Laiho, A. Hussain, Y. Liao, N. Wei and E. I. Kauppinen, *Nanoscale*, **9**, 17601 (2017).

[2] E.-X. Ding, Q. Zhang, N. Wei, A. T. Khan and E. I. Kauppinen. Accepted by Royal Society Open Science on 4<sup>th</sup> May, 2018.

[3] E.-X. Ding, *et al.* In preparation, 2018.

## Controlled graphene synthesis from solid carbon sources

Kondrashov Ivan, Rybin Maxim and Elena Obraztsova

*A.M. Prokhorov General Physics Institute, Vavilov str. 38, Moscow, Russia, 119991  
navi.soul@gmail.com*

Graphene with its extraordinary electronic and mechanical properties can be used in various applications. One of the popular methods of synthesizing large area graphene is atmospheric or low pressure CVD technique using hydrogen as a balancing gas and methane or acetylene as primary carbon source gas. But it is difficult to apply the technology to a some of potential applications, because CVD method is limited to the use of gaseous raw materials. Growth from solid carbon sources is not only an alternative route for graphene synthesis as well as a way to avoid the use of dangerous carbon-containing gases and make the synthesis process less expensive.

In this work we present the investigation of controllable growth of large area high quality graphene from different solid carbon sources. We used a CVD configuration from our previous works to grow graphene on Cu foils [1,2], adopting solid hydrocarbon sources. With solid poly(methyl methacrylate) (PMMA) and poly(ethylene) precursors, monolayer graphene films were synthesized at a growth temperature about 850 C and under low pressure conditions. We can control the amount of carbon involved in the synthesis by changing the thickness of the spin-coated PMMA or the amount of poly(ethylene). Raman Spectroscopy has been used for characterization of the layers in graphene films.

### Acknowledgement

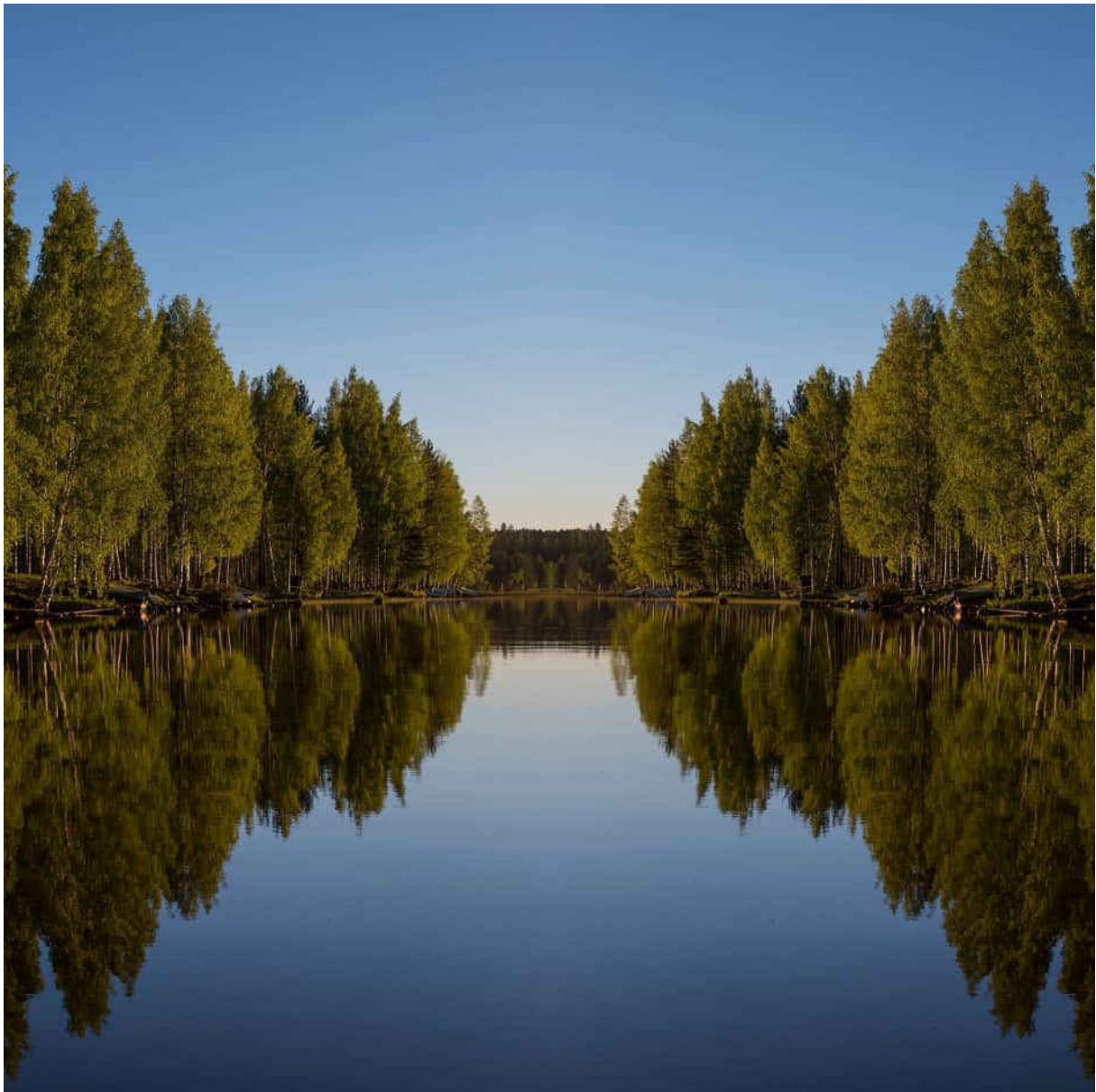
The reported study was funded by RFBR according to the research project № 18-32-00998.

### References

- [1] I. I. Kondrashov, P. S. Rusakov, M. G. Rybin, A. S. Pozharov and E. D. Obraztsova, Journal of nanoelectronics and optoelectronics, **8**, 1 (2013) 83-86.
- [2] M. G. Rybin, I. I. Kondrashov, A. S. Pozharov, V.C. Nguyen, N.M. Phan and E. D. Obraztsova, Phys. Status Solidi B, **255**,1, (2018)



## Friday, August 10



©G. Lepehin



# Graphdiyne: A new member of carbon family

Jin ZHANG

Center for Nanochemistry, College of Chemistry and Molecular Engineering,  
Peking University, Beijing 100871, China.

Email: [jinzhang@pku.edu.cn](mailto:jinzhang@pku.edu.cn)

Graphdiyne (GDY) is an ordered two-dimensional (2D) carbon allotrope comprising  $sp$  and  $sp^2$  hybridized carbon atoms with high degrees of  $\pi$ -conjugation, which features a natural bandgap and superior electric properties. However, the synthesis of well-defined GDY remains challenging due to the free rotation around alkyne-aryl single bonds and the lack of thickness control. Herein, we developed several rational approaches to synthesize high-quality structure-controlled GDY. We first demonstrated that the morphology of GDY could be finely controlled by using a modified Hay-Glaser coupling reaction under optimized reaction conditions. Unique vertically grown  $\gamma$ -GDY nanowalls ( $\sim 200$  nm) were fabricated on either copper foils or foams<sup>[1,2]</sup>.  $\beta$ -GDY, another new member of graphyne family, was also explored using similar method with tetraethynylethene monomers<sup>[3]</sup>. Notably, we recently reported a facile synthetic route to synthesize ultrathin single-crystalline GDY, through a solution phase van der Waals (vdW) epitaxial strategy<sup>[4]</sup>. The as-grown GDY film has a tri-layer structure with a ABC stacking order as directly observed by electron microscopy. The high quality of the as-grown GDY film and the graphene-enhanced Raman scattering (GERS) effect ensure the predicted Raman fingerprints belonging to a perfectly ordered 2D GDY structure<sup>[5]</sup> are experimentally observed. Finally, encouraged by the intriguing properties of such 2D acetylenic carbon allotropes, we designed various GDY-based hierarchical architectures and composites towards practical applications. As one example, a three-dimensional (3D) GDY foam was synthesized and further used for oil/water separation, exhibiting both high efficiency and good recyclability<sup>[2]</sup>. Considering the intriguing physicochemical properties of GDY, it also shows promise in various applications, such as water splitting cell<sup>[7]</sup> and solar steam generation<sup>[8]</sup>.

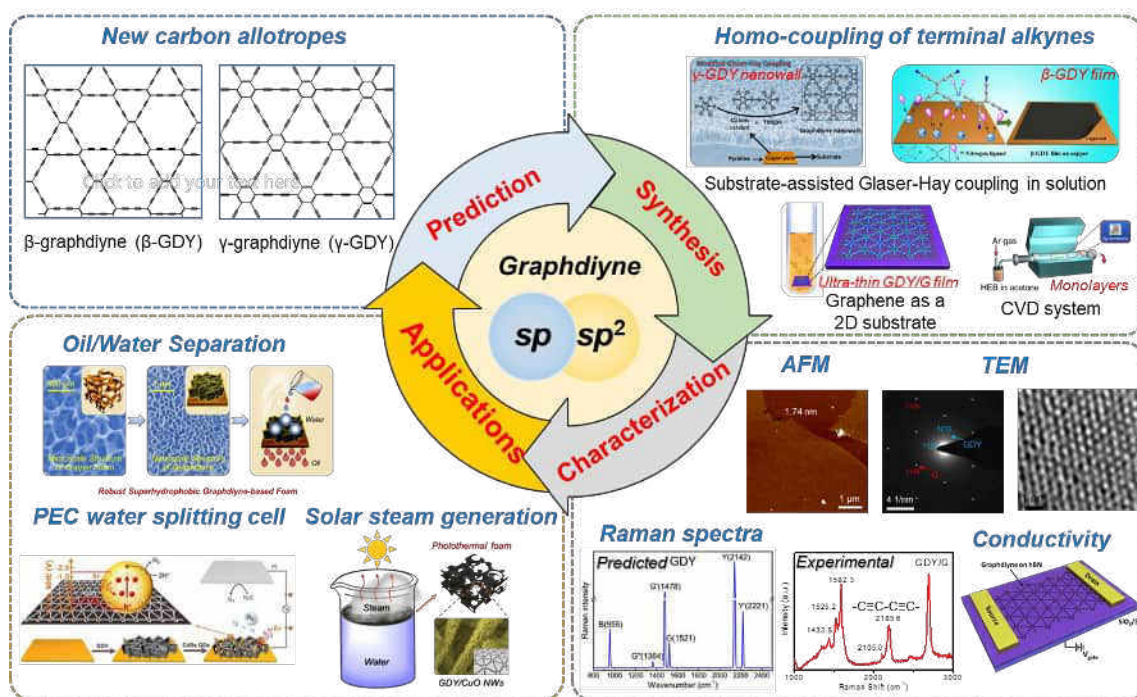


Fig. 1. The synthesis and applications of graphdiyne.

## References

- [1] J. Zhang *et al.*, J. Am. Chem. Soc. **137**, 24 (2015).
- [2] J. Zhang *et al.*, Adv. Mater. **28**, 1 (2016).
- [3] J. Zhang *et al.*, Adv. Mater. **29**, 19 (2017).
- [4] J. Zhang *et al.*, Submitted, 2018
- [5] J. Zhang *et al.*, J. Phys. Chem. C **120**, 19 (2016).
- [6] J. Zhang *et al.*, Adv. Mater. **29**, 18 (2017).
- [7] J. Zhang *et al.*, J. Am. Chem. Soc. **138**, 12 (2016).
- [8] J. Zhang *et al.*, Chem. Mater. **29**, 14 (2017).

# The chemistry and physics of carbon from first-principles, multiscale simulations, and experiments

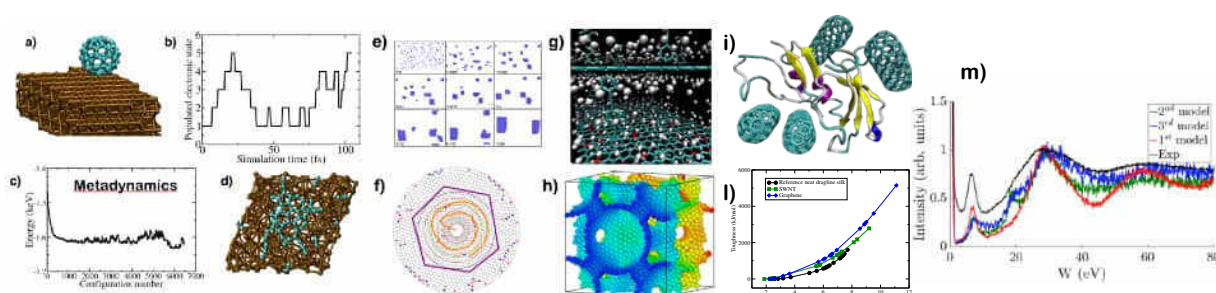
Simone Taioli

European Centre for Theoretical Studies in Nuclear Physics and Related Areas (ECT\*), Trento, Italy & Faculty of Mathematics and Physics,  
Charles University, Prague, Czech Republic  
[taioli@ectstar.eu](mailto:taioli@ectstar.eu)

In this talk I will first discuss the processes leading to the room-temperature growth of carbon-based materials, notably silicon carbide (SiC) [1,2] and graphene [3,4], by supersonic molecular beam epitaxy. In particular, I will present both experiments and computational modelling of fullerene impacts on silicon and copper surfaces (Fig. a)) at intermediate-energy regimes (few tens of eV). This collision induces strong chemical-physical perturbations in the system and, for sufficient  $C_{60}$  translational energy, disruption of molecular bonds and cage breaking. Characterization of the epitaxial grown materials by a variety of experimental techniques, such as XPS, UPS, Auger, LEED, TEM, and Raman after the collision, demonstrates the potentiality of our approach to grow nanostructured and 2D materials at low temperature. On the theoretical side, we show that in these out-of-equilibrium conditions it is necessary to go beyond the standard implementation of ab-initio molecular dynamics based on the Born-Oppenheimer approximation, which fails to capture the excited-state dynamics. In particular, we analyse the Si- and Cu- $C_{60}$  collision within the non-adiabatic nuclear dynamics framework (Fig. b)), where stochastic hops occur between adiabatic surfaces calculated via time-dependent density functional theory. The theoretical description of  $C_{60}$  impacts on metallic and semiconductor substrates will be further analysed by multiscale techniques based on metadynamics (Fig. c), d)) and Kinetic Monte Carlo (Fig. e)).

Furthermore, the discovery of novel energetically stable carbon structures shaped as Beltrami pseudospheres (Fig. f)) for investigating the physics of curved spacetimes [5], the mechanical and gas-sieving properties of pillared graphene oxides [6] and foams [7,8] will be shown (Fig. g, h)). Moreover, we report the observations of silk mechanical properties increment, up to a fracture strength  $\sim 5.4$  GPa and to a toughness modulus  $\sim 1570$  J g $^{-1}$ , by incorporating graphene and carbon nanotubes (Figs. i, l)) via spider spinning, after feeding spiders with aqueous dispersions [9].

Finally, Monte Carlo simulations of Reflection Electron Energy Loss spectra (REELS) of diamond and HOP graphite in order to investigate the role of the anisotropic structure in plasmon excitations will be discussed [10]. In our model, elastic scattering between electrons and target atoms is treated via the Mott theory, which is based on the solution of the Dirac equation in a central field. Inelastic interactions between primary beam electrons and the target electron cloud, resulting in bulk excitation and surface plasma oscillations, are described by the dielectric theory developed by Ritchie. In this model, the key quantity for the calculation of the inelastic cross section is the momentum- and energy-dependent dielectric function, which is calculated via a full ab initio approach (Fig. m)).



- [1] R. Verucchi, L. Aversa, M.V. Nardi, S. Taioli, S. a Beccara, D. Alfè, L. Nasi, F. Rossi, G. Salvati, S. Iannotta, J. Am. Chem. Soc.: Communications, **134**, 17400 (2012)
- [2] S. Taioli, G. Garberoglio, S. Simonucci, S. a Beccara, L. Aversa, M.V. Nardi, R. Verucchi, S. Iannotta, D. Alfè, J.Chem. Phys., **138**, 044701 (2013) selected as JOURNAL COVER
- [3] S. Taioli, J. Mol. Mod., **20**, 1 (2014)
- [4] R. Tatti, L. Aversa, R. Verucchi, E. Cavaliere, G. Garberoglio, N. Pugno, G. Speranza, S. Taioli, RSC Advances, **6**, 37982 (2016)
- [5] S. Taioli, R. Gabbriellini, S. Simonucci, N. Pugno, A. Iorio, J. Phys.: Cond Mat., **28**, 13LT01 (2016)
- [6] G. Garberoglio, N. Pugno, S. Taioli, J. Phys. Chem. C, **119**, 1980 (2016)
- [7] A. Pedrielli, S. Taioli, G. Garberoglio, N. Pugno, Mic. Mes. Mat., 2017, in press
- [8] A. Pedrielli, S. Taioli, G. Garberoglio, N. Pugno, Carbon, **111**, 796 (2017)
- [9] E. Lepore et al., 2D Materials, **4**, 031013 (2017)
- [10] M. Azzolini et al., Carbon, **118**, 299 (2017)



## Polybromide formation in carbons

O.V. Sedelnikova,<sup>1,2\*</sup> C.P. Ewels,<sup>3</sup> G.N. Chekhova,<sup>1</sup> D.V. Pinakov,<sup>1,2</sup> E. Flahaut,<sup>4,5</sup> L.G. Bulusheva,<sup>1,2</sup> and A.V. Okotrub<sup>1,2</sup>

<sup>1</sup>Nikolaev Institute of Inorganic Chemistry SB RAS, 3 Academician Lavrentiev Av., Novosibirsk 630090, Russian Federation

<sup>2</sup>Novosibirsk State University, 2 Pirogov Str., Novosibirsk 630090, Russian Federation

<sup>3</sup>Institut des Matériaux Jean Rouxel, CNRS-Université de Nantes, UMR6502, Nantes, France

<sup>4</sup>Université de Toulouse; UPS, INP; Institut Carnot Cirimat; 118, route de Narbonne, F-31062 Toulouse cedex 9, France

<sup>5</sup>CNRS, Institut Carnot Cirimat, F-31062 Toulouse, France

*o.sedelnikova@gmail.com*

Bromination of carbon materials is the effective route to control work function and to enhance conductivity of carbon materials because bromine acts as a *p*-dopant to graphite and carbon nanotubes. Intercalation of bromine into carbon material is successfully investigated by Raman spectroscopy. The most pronounced low-frequency bromine feature is the strong broad peak at  $\sim 230$ - $240$   $\text{cm}^{-1}$  which is significantly downshifted from its position in gaseous and solid bromine ( $\sim 305$   $\text{cm}^{-1}$ ). The spectrum in the vicinity of this peak is broad and complicated, therefore, interpretation of Raman bands for intercalation compounds of graphite and carbon nanotubes with bromine will be helpful in understanding bromine intercalation process.

In the present work, we synthesized bromine-intercalated natural graphite, graphite fluorides with different fluorination content and double-walled carbon nanotubes. Vibrational properties of bromine intercalated in carbon nanomaterials has been investigated by Raman spectroscopy accompanied with density-functional theory (DFT) calculations. The calculations were performed within the local density approximation using the AIMPRO software package [1-3]. This software contains basis sets of atomic orbitals in the form of localized Gaussian based functions (22 and 50 independent functions for carbon, fluoride and bromine, respectively) with angular momenta up to  $l = 3$ .

The spectra of pristine graphite and highly fluorinated graphites were found to be featureless in the region  $100$ - $550$   $\text{cm}^{-1}$ . For other carbon samples, the presence of bromine causes distinct features in Raman spectrum dominated by two main peaks around  $154$ - $161$   $\text{cm}^{-1}$  and  $229$ - $237$   $\text{cm}^{-1}$ . In order to gain insight into the origin of peaks observed in the Raman spectra, we calculated normal vibration frequencies of bromides adsorbed on graphene and graphene fluoride. Our results suggest preferable formation of polybromides on graphene and fluorinated graphene surface. Nudged elastic band calculations show that this reaction could be exothermic with small energetic barrier.

This work was partially supported by and the Russian Foundation for Basic Research (Project 16-53-150003). O.V. Sedelnikova thanks the Scholarship of the President of the Russian Federation (SP-3530.2016.1). Some of these results were obtained using the CCIPL, "Centre de Calculs Intensif Pays de la Loire".

[1] R. Jones, P. Briddon. *Semiconductors and Semimetals*, **51**, 287 (1998).

[2] M. Rayson, P. Briddon. *Computer Physics Communications*, **178**, 128 (2008).

[3] M. J. Rayson, P. R. Briddon. *Physical Review. B*, **80**, 205104 (2009).



## **Radiative tolerance of graphene: THz components for space applications**

**Alesia Paddubskaya<sup>1</sup>, Polina Kuzhir<sup>1,2</sup>, A. Stepanov<sup>2</sup>, G. Remnev<sup>2</sup>, Tommi Kaplas<sup>3</sup>, Yuri Svirko<sup>3</sup>**

<sup>1</sup>*Institute for Nuclear Problems of Belarusian State University, Minsk Belarus*

<sup>2</sup>*Tomsk Polytechnic University, Lenin Ave, 30, Tomsk, Tomskaya oblast', Russia, 634050*

<sup>3</sup>*Institute of Photonics, University of Eastern Finland, Joensuu, Finland*

*polina.kuzhir@gmail.com*

The possibility to utilize graphene as a basic absorptive element in passive Terahertz devices (shields, filters, polarizers, collimators, bolometric-type detectors) for space applications has been investigated by 80 ns 300 keV ions beam comprising 30% of hydrogen and 70% of carbon ions at density of  $1.5 \cdot 10^{12}$  ions per  $\text{cm}^2$ . In order to estimate the ionizing losses and other processes leading to the radiative modification of the graphene based devices the modelling of the ion scattering using SRIM-2013 package (<http://www.srim.org/>) has been performed. Along with THz as well as Raman characterizations, the modeling proves the outstanding radiative resistance of graphene. However, graphene/polymer/ $\text{SiO}_2$  heterostructures shows a relatively low tolerance against ionizing radiation due to (i) destructive contribution of low-energy recoil atoms coming back to graphene from the side of dielectric supports and (ii) gas bubbles formation on the graphene/substrate interface leading to snapping off upper graphene layers.

### **Acknowledgement**

The reported study was supported by RFBR, research project No. 17-38-50050 mol\_nr, H2020 Project ID 644076 MSCA-RISE-2014 Programme CoExAN. The experiment on irradiation of graphene/polymer sandwiches are carried out at Tomsk Polytechnic University within the framework of Tomsk Polytechnic University Competitiveness Enhancement Program grant.

## Wafer-scale transfer of CVD graphene for flexible electronics

**Harri Lipsanen**

*Department of Electronics and Nanoengineering, Aalto University, Tietotie 3, 02150 Espoo, Finland  
harri.lipsanen@aalto.fi*

Flexible electronics is expected to be the ubiquitous platform for the next-generation life science, environmental monitoring, display, and energy conversion applications. Outstanding multifunctional mechanical, thermal, electrical, and chemical properties of graphene combined with transparency and flexibility solidifies it as ideal for these applications. Although chemical vapor deposition (CVD) enables cost-effective fabrication of high-quality large-area graphene films, one critical bottleneck is an efficient and reproducible transfer of graphene to flexible substrates.

We explore and describe a direct transfer method of 6-inch monolayer CVD graphene onto transparent and flexible substrate based on direct vapor phase deposition of conformal parylene on an as-grown graphene/copper film. [1] The method is straightforward, scalable, cost-effective and reproducible. The transferred film shows high uniformity, lack of mechanical defects and sheet resistance for doped graphene as low as 18 ohm/sq and 96.5% transparency at 550 nm while withstanding high strain in bending. To underline that the introduced technique is capable of delivering graphene films for next-generation flexible applications we demonstrate a wearable capacitive controller, a heater, and a self-powered triboelectric sensor.

[1] Maria Kim, Ali Shah, Changfeng Li, Petri Mustonen, Jannatul Susoma, Farshid Manoocheri, Juha Riikonen and Harri Lipsanen, 2D Materials, **4**, 035004 (2017).

# Multifunctional polymer film in graphene transfer

Tommi Kaplas, Arijit Bera and Pertti Pääkkönen

*Institute of Photonics, University of Eastern Finland, Yliopistokatu 7, 80101 Joensuu, Finland*

*Corresponding author: [tommi.kaplas@uef.fi](mailto:tommi.kaplas@uef.fi)*

Chemical vapour deposition (CVD) of graphene has been recognized a key technology for large are graphene production [1]. By CVD, graphene is grown on a transient metal substrate and thereafter transferred on a dielectric substrate. During the transfer process, a graphene film is conventionally supported by a layer of poly(methyl methacrylate) (PMMA) which is then removed after the transfer [1]. Since PMMA is a widely used electron-beam resist material, it offers an interesting idea to use this resist layer for graphene transfer and patterning simultaneously.

In our experiment, we synthesized graphene on a copper foil by a conventional CVD technique [2]. The copper foil/graphene was spin coated with a long chained PMMA based resist and the Cu foil was removed by wet etching. We transferred then the graphene/PMMA film on an oxidized silicon. Thereafter, the supporting PMMA was patterned by electron-beam writer and developed in methyl isobutyl ketone. The PMMA resist mask was then coated by an evaporated 80 nm thick Cu film. By removing PMMA in acetone, we performed a lift-off and obtained a metallic mask on graphene. The metallic mask protected graphene during oxygen dry etching. Finally, the metallic mask was removed by wet etching revealing the patterned graphene on the oxidized silicon substrate. The process is described illustrated in Fig. 1.

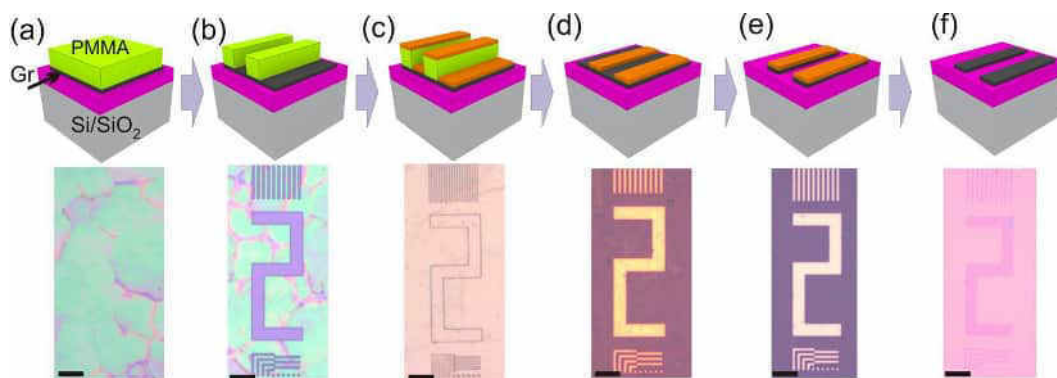


Figure 1. Schematic illustration (and corresponding optical microscope images) of the graphene transferring and patterning by using the one and same PMMA film on both processes. (a) At first graphene/PMMA is transferred on a substrate and (b) the PMMA support is patterned by electron-beam lithography. (c) The patterned PMMA is coated by a thin copper film. (d) The PMMA is removed resulting a Cu mask for (e) graphene patterning by reactive ion etching. (f) At the end, Cu mask is removed by wet etching. (Scale bar is 20  $\mu\text{m}$ .)

In summary, we have presented a simple and straightforward technique to pattern graphene by using the same PMMA film in graphene transfer and patterning. Despite, the graphene film was exposed to focused electron beam and relatively high doses we did not observe any damage or defects in graphene proving the technique to be safe for graphene [2]. Thus, we believe, this method could provide a nice technological platform for graphene post-processing.

## Acknowledgement.

This work was financially supported by the Academy of Finland (project no. 287886).

## References

- [1] C. Mattevi, H. Kim, and M. Chhowalla, *J. Mater. Chem.* **21**, 3324–3334 (2011).
- [2] X. Li, Y. Zhu, W. Cai, M. Borysiak, B. Han, D. Chen, R. D. Piner, L. Colombo, and R. S. Ruoff, *Nano Lett.* **9**, 4359–4363 (2009).
- [3] T. Kaplas, A. Bera, A. Matikainen, P. Pääkkönen, and H. Lipsanen, *Appl. Phys. Lett.* **112**, 073107 (2018).

## Stacking-dependent Interlayer Couplings in 2D Materials

Kaihui Liu

*School of Physics, Peking University, Beijing 100871, China*

When the characteristic length of a material shrinks to 1 nm scale, many distinct physical phenomena, such as quantum confinement, enhanced many-body interactions, strong van der Waals inter-material couplings and ultrafast charge separation, will appear. To investigate the related fascinating low-dimensional physics, we need a tool to quantitatively link the atomic structures to the physical properties of these very small nano-materials. In this talk, I will introduce our recently developed in-situ TEM + ultrafast nano-optical spectroscopy technique, which combines capability of structural characterization in TEM and property characterization in nano-optic spectroscopy on the same individual nano-materials. Several examples of using this technique to study the mechanical/electronic couplings and ultrafast charge transfer in 2D bilayer systems will be demonstrated [1-4].

### References:

- [1] Kaihui Liu, Liming Zhang, Ting Cao, Chenhao Jin, Diana Qiu, Qin Zhou, Alex Zettl, Peidong Yang, Steven Louie, and Feng Wang\*. "Evolution of Interlayer Coupling in Twisted MoS<sub>2</sub> Bilayers", **Nature Communications** **2014**, 5, 4966
- [2] Xu Zhou, Jingxin Cheng, Yubing Zhou, Shiwei Wu\*, Hailin Peng\*, Kaihui Liu\* and et al., "Strong Second-Harmonic Generation in Atomic Layered GaSe", **JACS** **2015**, 137, 7994-7997.
- [3] Jing Liang, Jin Zhang, Zhenzhu Li, Hao Hong, Peng Gao, Zhirong Liu, Zhongfan Liu, Zhipei Sun\*, Sheng Meng\*, Kaihui Liu\*, and et al. "Monitoring Local Strain Vector in Atomic-Layered MoSe<sub>2</sub> by Second-Harmonic Generation", **Nano Letters** **2017**, 17, 7539
- [4] Ziheng Ji, Hao Hong, Jin Zhang, Chuanhong Jin\*, Liying Jiao, Kebin Shi\*, Sheng Meng and Kaihui Liu\* and et al. "Robust Stacking-Independent Ultrafast Charge Transfer in MoS<sub>2</sub>/WS<sub>2</sub> Bilayers", **ACS Nano** **2017**, 11, 12020

## Aberration-Corrected TEM/ETEM-Based Research on Single-Walled Carbon Nanotubes

Hua Jiang<sup>1</sup>, Ying Tian<sup>1,2</sup>, Yongping Liao<sup>1</sup>, Qiang Zhang<sup>1</sup>, Nan Wei<sup>1</sup> and Esko Kauppinen<sup>1</sup>

<sup>1</sup> Department of Physics, Aalto University School of Science, Espoo, Finland

<sup>2</sup> Department of Physics, Dalian Maritime University, Dalian, Liaoning 116026, China

[hua.jiang@aalto.fi](mailto:hua.jiang@aalto.fi)

In this contribution, we will review methods of chiral structure analysis of single-walled carbon nanotubes (SWCNTs) with the aid of electron diffraction (ED) technique [1]. On the basis of this, we have established an approach using ED as a means to evaluate the validity of Raman spectroscopy for quantification of concentrations of metallic SWNTs (M%) or of semi-conducting tubes (S-SWNT%) [2]. Chirality distribution maps of SWNTs produced by CVD methods with Fe nanoparticles as catalysts at various synthesis conditions have been analyzed. As a recent advance [3], we have successfully achieved direct synthesis of single-walled carbon nanotube thin films with various colors using a novel floating-catalyst-CVD process with ferrocene-based iron catalyst particles and CO as the carbon source. The color is tunable by adjusting the reactor conditions, i.e. the temperature and especially the addition of CO<sub>2</sub>. Based on electron diffraction analysis of individual SWCNTs in our colorful SWCNT thin films, we were able to attribute the colors of the SWCNT thin films to their narrow diameter in certain ranges which give rise to absorption peaks in the visible region. It is demonstrated that the narrow (*n*, *m*) chirality distribution also accounts for the display of certain color of a SWCNT thin film.

We also demonstrate that structural control of SWNTs is achievable by fabricating nanoparticle catalysts with a defined structure on crystalline substrates via controlled growth techniques. *In situ* time-resolved environmental transmission electron microscope (ETEM) observation at atomic resolution of nanoparticle formation and SWNT growth are accomplished.

### References

- [1] H. Jiang, et. al, Carbon, **45** (2016), 662.
- [2] Y. Tian, et. al, Anal. Chem. **90** (2018), 2517.
- [3] Y.P. Liao, et. al, Submitted to JACS, 2018.

## Tailoring the morphology and properties of carbon-based materials by *in situ* TEM

Simona Moldovan<sup>1,2\*</sup>, Georgian Melinte<sup>1</sup>, Walid Baaziz<sup>1</sup>, Cuong Pham-Huu<sup>3</sup>, Ovidiu Ersen<sup>1</sup>

1. Institut de Physique et Chimie des Matériaux de Strasbourg, CNRS-Université de Strasbourg, 23 rue du Loess 67000, Strasbourg, France

2. Groupe de Physique des Matériaux, CNRS-INSA Rouen, avenue de l'Université, Rouen, France

3. Institut de Chimie et Procédés pour l'Energie, l'Environnement et la Santé (ICPEES), CNRS, ECPM, Université de Strasbourg 25, rue Becquerel, 67087 Strasbourg, France

simona.moldovan@univ-rouen.fr

In the actual context of the fast development of nanotechnologies, the industry is confronted with the production of materials and structures with well-defined sizes, geometries and morphologies. The carbon-based structures like graphene, carbon nanotubes (CNTs) and nanofibers (CNFs) are promising candidates for the development of nanodevices which strongly demand for a close control of materials properties at the nanoscale at each step of synthesis, manipulation and further implementation in the process. Owing to the high resolutions developed achieved by transmission Electron Microscopy (TEM), the recent development of the associated *in-situ* methodologies allow to follow the evolution of nanomaterials from the early synthesis stages up to their functioning under operation conditions. In this work, two *in-situ* TEM methodologies are employed. The first one, the gas assisted environmental approach is employed for the controlled “synthesis” of CNFs by nanopatterning of Few Layer Graphene (FLG) sheets, whereas the STM-TEM *in-situ* approach permits to take advantage of the CNTs conduction properties to design an original methodology for a nano-printing/erasing experiments.

The *in-situ* Environmental TEM as developed in an adapted closed cell (E-cell) allows to perform real time observations of materials evolution under gaseous environments in the high temperature/pressure ranges at with the atomic resolution. The nanopatterning of FLG has the potential of creating nanosheets with well-defined shapes and edge configurations which can be transformed in single-layer GNRs by simple techniques as for instance the chemical exfoliation. To initially characterize the channeling process and the obtained nanostructures we used a system consisting in Fe<sub>3</sub>O<sub>4</sub> nanoparticles dispersed onto FLG sheets, which has undergone an *ex-situ* heating treatment (800°C) in H<sub>2</sub> atmosphere. The TEM-based results give extensive 2D and 3D insights on both the cutting process and the properties of the nanostructures obtained by catalytic nanopatterning [1]. The *in-situ* E-TEM methodology was further employed to re-create the very same nanopatterning conditions in an effort to accede to finer patterning characteristics such as the cutting speed or the correlation between the channels directions and the catalysts crystallographic orientations [2]. Indeed, the possibility of building up appropriate experimental conditions allowed to advance the cutting mechanisms by considering the behavior of a complex NPs/FLG support system in the high temperature/pressure conditions and a hydrogen environment.

The scanning tunneling microscope (STM) is an attractive alternative to move single atoms with incredible precision, but this approach is not adapted for assembling nanodevices with thousands of atoms. The use of CNTs as “nanopipetts” able to transport femtograms of mass to predefined spots can be envisaged, an approach based on the Joule assisted electromigration phenomenon, when a high current pass through a metal phase encapsulated inside a CNT. We propose here a highly precise method for delivering nanoparticles (NPs) to the graphene and few-layer graphene (FLG) edges and surfaces using a CNT filled with Fe<sub>3-x</sub>O<sub>4</sub> NPs as a nanopipette. The experiment is realized inside a TEM by using a STM-TEM holder allowing high precision sub-nanometer movement and high voltage supply. A nanoprinting-like experiment highlights the possibility to deposit NPs on the surface of a FLG sheet with a radial distribution relative to the CNT/FLG contact point, or to control the NPs deposition at the FLG edge. The *in-situ* TEM observation of the experiment has made possible a real time analysis of the structural and chemical properties of both the NPs and the supporting CNT.

The STM-TEM approach can be extended to the CNFs synthesized by the E-TEM methodology in order to get a complete and close control of the sizes, morphologies, NPs distribution and location within the composite systems to be utilized for specific nanodevices.

[1] G. Melinte, I. Florea, S. Moldovan, I. Janowska, W. Baaziz, R. Arenal, A. Wisnet, C. Scheu, S. Begin-Colin, D. Begin, C. Pham-Huu and O. Ersen, *Nature Communications*, **5**, 4109 (2014).

[2] G. Melinte, S. Moldovan, C. Hirlimann, W. Baaziz, S. Begin-Colin, C. Pham-Huu and O. Ersen, *ACS Catalysis*, **7**, 5941 (2017).

[3] G. Melinte, S. Moldovan, C. Hirlimann, X. Liu, S. Begin-Colin, D. Begin, F. Banhart, C. Pham-Huu and O. Ersen, *Nature Communications*, **6**, 8071 (2015).

## Carbon nanotube saturable absorber with electrical gating for control over pulse generation regime.

Yu. Gladush<sup>1</sup>, A. Mkrtchyan<sup>1</sup>, V. Iakovlev<sup>1</sup>, D. Kopylova<sup>1</sup>, A. Khegay<sup>2</sup>, M. Melkumov<sup>2</sup>, A. Nasibulin<sup>1,3</sup>

<sup>1</sup> Skolkovo Institute of Science and Technology, Nobel str. 3, Moscow, 143026, Russia

<sup>2</sup> Fiber optics research center, Vavilov str. 38, Moscow, Russia

<sup>3</sup> Aalto University, Department of Applied Physics, 00076, Aalto, Finland

y.gladush@skoltech.ru

### Abstract

Passive mode-locking is a method to produce ultra-short (from picosecond to femtosecond) pulses in laser. For its implementation one should simply insert the material with saturable absorption on laser working wavelength inside the laser resonator. It is well known that single walled carbon nanotubes (SWCNT) work perfectly as a saturable absorber for fiber laser. Conventional methods imply mixing of SWCNTs with polymer to produce a composite tabled that is clamped between two connectors. This method has a drawback of a small thermal damage threshold of a hosting polymer compared to SWCNTs. Another approach is to deposit a SWCNTs from the liquid directly on the surface of the fiber – facet, side-polished surface or tapered fiber – by thermosdiffusion or any other method. In this case one have to do additional steps SWCNT solution preparation.

In our work we use a dry transfer technic to deposit SWCNTs on a side-polished fiber [1]. For this we use SWCNTs grown by aerosol synthesis and collected on the filter. Produced SWCNT film do not have any contamination nor polymer support. This result in high stability towards thermal damage due to heating by the short pulse train propagating through the SA in laser resonator.

Another advantage is possibility of control of the absorbance of SWCNT film by ionic liquid gating. For this we have prepared an electrochemical cell in three electrode scheme where working electrode covers the surface of side-polished fiber. By applying on a working electrode voltage below 1 V we can reduce the SWCNT absorbance up to 2dB. Control over absorbance of SA allows to switch between different generation regimes [2]. We show switching of the pulse generation regimes for both anomalous and normal net dispersion laser resonators. In anomalous net dispersion regime we can change between 400 fs pulses in mode-lock regime to 2 um pulses in Q-switch regime. To take advantage of high thermal stability of SA on the side-polished fiber we also investigate pulse generation switching in normal net dispersion regime. Dissipative solitons in resonators with high normal net dispersion can have much higher energy per pulse compared to conservative soliton. We show that in this regime pulse generation can also undergo switching between mode-locking and Q-switch by changing absorption of the saturable absorber. We attribute the mechanism of the switching to change of the modulation depth of the saturable absorber: when voltage is applied the transmission of the SWCNT film increases mostly due to the saturable part of the absorption.

[1] S Kobtsev et. al., Ultrafast all-fibre laser mode-locked by polymer-free carbon nanotube film Optics Express **24**, 28768 (2016)

[2] Lee E. J. et al., Active control of all-fibre graphene devices with electrical gating. Nature Communications **6**, 6851 (2015)



## Electronic properties and electrochemical applications of UV irradiated fluorinated graphene films

A.V. Okotrub, V.I. Sysoev, K.M. Popov, V.E. Arkhipov, D.V. Gorodetskii, L.G. Bulusheva

*Nikolaev Institute of Inorganic Chemistry SB RAS, pr. Lavrenteva, 3, Novosibirsk, 630090, Russia  
spectrum@niic.nsc.ru*

The development of electronic devices has increased necessity of high power micro-supercapacitors. Graphene materials have been ideal material platform for constructing flexible electronic; its 2D structure, high specific area and good conductivity are attractive for energy storage devices. The fluorinated graphenes with composition  $C_2F$  were synthesized using low temperature fluorination by  $BrF_3$  from natural graphite. Suspension of fluorinated graphite in toluene was used to produce films having a thickness of 1 - 10  $\mu m$ . The UV radiation treatment of film surface performed local conversion of fluorinated graphene to graphene. Depending on irradiation conditions, it is possible to vary functionalization degree of the resulted graphene material. The almost complete defunctionalization (98 % of carbon) of surface layer of films was achieved using focusing radiation of low power laser ( $\lambda = 380$  nm). Produced electrode material with high electrical conductivity and flexibility is useful for energy storage devices without binders or conductive additives. We reveal an influence of structural features and functional composition of graphene material on electrochemical performance of in-plane microsupercapacitors. Pattern of microelectrodes was drawing by UV laser and supercapacitors properties of these elements were measured for different acid electrolytes (Fig. 1). Obtained materials showed tunable electrochemical performance, which reaches  $1.5\text{ mF/cm}^2$  at rate  $0.8\text{ mV/s}$ . The change of chemical states of capacitor surface under electrical charging was controlled by XPS and NEXAFS *in situ* measurements. We reveal an influence of structural features and functional composition of graphene material on electrochemical performance of in-plane micro supercapacitors.

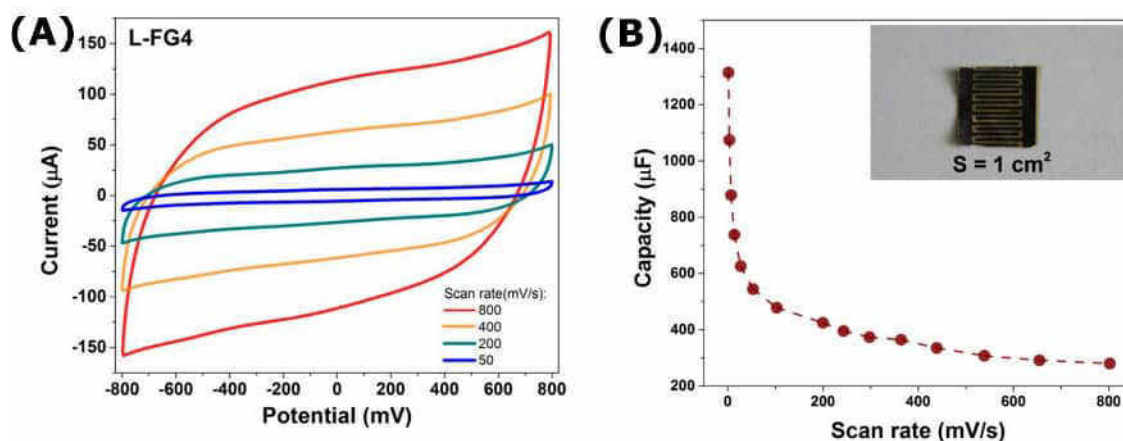


Fig. 1. Electrochemical characterization of LFG-MSC with interdigitated electrodes. (A) CV curves obtained at different scan rates. (B) Evolution of area capacitance versus scan rate. Inset shows optical photography of device.

## Fluorinated and chlorinated double-walled carbon nanotubes for gas sensing

L. G. Bulusheva<sup>1,\*</sup>, V. I. Sysoev<sup>1</sup>, E. V. Lobiak<sup>1</sup>, A. V. Okotrub<sup>1</sup>, E. Flahaut<sup>2</sup>

<sup>1</sup>Nikolaev Institute of Inorganic Chemistry, SB RAS, 630090 Novosibirsk, Russia

<sup>2</sup>CNRS, Institut Carnot Cirimat, F-31062 Toulouse, France

\*Corresponding author, e-mail: bul@niic.nsc.ru

Carbon nanotubes (CNTs), possessing a high surface area and electrical conductivity, are very sensitive to surface adsorbates. This makes them attractive for development of gas sensors. Detection of NO<sub>2</sub> and H<sub>2</sub>O molecules is important for industrial purposes and ordinary people environment. Double-walled CNTs (DWCNTs) consisting of two cylindrical tubes have been shown to be a good sensor material, where the inner nanotube transfers a signal from the outer nanotube electrostatically interacting with adsorbates. In this work, we demonstrate that covalent functionalization of DWCNTs by fluorine or chlorine allows substantially increase performance of the DWCNT-based sensor.

DWCNTs, purified from the synthesis by-products, have been fluorinated using a mixture of BrF<sub>3</sub> and Br<sub>2</sub> at room temperature. Chlorination of DWCNTs and holey-DWCNTs (produced by sample boiling in concentrated sulfuric acid) has been carried out using CCl<sub>4</sub> vapor at 650°C. The films of initial DWCNTs and halogenated DWCNTs were deposited on SiO<sub>2</sub>/Si substrates, which were used for device fabrication. Two silver electrodes of a width 5 mm were formed by a silver glue on the top of the film at a distance of ~ 1 mm from each other. The device was mounted in a test chamber and investigation of gas sensor properties was carried out under

nearly practical conditions (atmospheric pressure and room temperature) against NO<sub>2</sub> or H<sub>2</sub>O diluted by argon. A change in electrical resistance of the device was monitored when the sensor was periodically exposed to an analyte gas and pure Ar.

Covalent attachment of chlorine to the DWCNTs allowed preparing more uniform and thin film for gas sensing as compared to non-modified DWCNTs. This provided a higher change in electrical resistivity of the chlorinated holey-DWCNT sample under exposure to H<sub>2</sub>O vapor. Moreover, we showed that this sensor fully recovers after the heating at 115°C in argon flow. A comparative study of initial DWCNTs and fluorinated DWCNTs against to 100 ppm of NO<sub>2</sub> detected a higher relative response for the former sensor and better recovery of the latter sensor. The response and recovery of the fluorinated DWCNTs increased with a rise of the sensor temperature (see Fig.1).

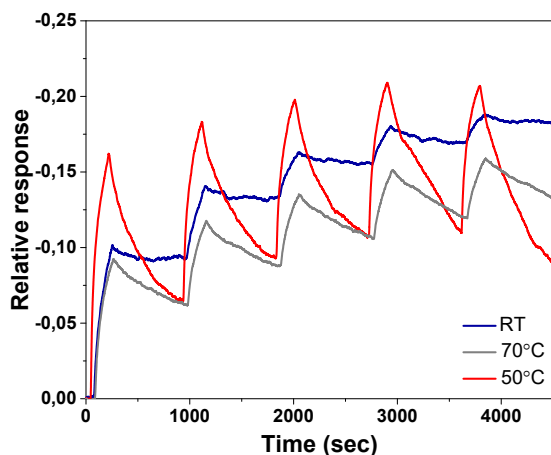


Fig. 1. Cycle-by-cycle response of fluorinated DWCNTs against 100 ppm of NO<sub>2</sub>, measured at room temperature (RT) and enhanced temperatures.

The work was supported by the Russian Foundation for Basic Research, grant 16-53-150003.

# Carbon nanotubes as promising materials to design a new class of high-performance electrocatalysts

Mohammad Tavakkoli\*, Tanja Kallio, Albert G. Nasibulin, Esko I. Kauppinen, and Kari Laasonen

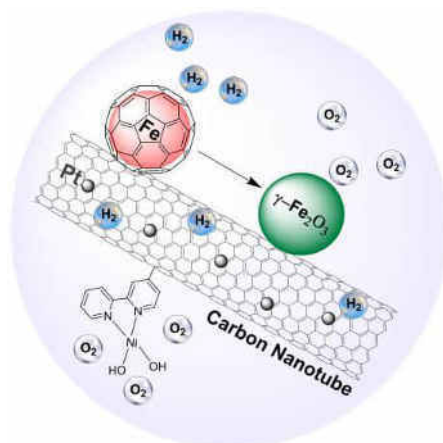
Aalto University, Espoo, Finland  
[mohammad.tavakkoli@aalto.fi](mailto:mohammad.tavakkoli@aalto.fi)

The development of efficient and low-cost electrocatalysts in electrocatalytic reactions plays an essential role because the catalyst determines not only the overall reaction efficiency but also the cost. We have developed a few synthesis methods to synthesize novel and low-cost electrocatalysts developed by carbon nanotubes (CNTs). CNTs are known for their exceptional properties in various applications. Here, I will further show that CNTs can be also utilized to create highly active and durable electrocatalysts [1-5]. In this talk, the focus is to design active catalysts for electrochemical water splitting by which highly pure hydrogen (as a clean energy carrier) and oxygen are produced from water. However, a new class of highly active and cost-effective electrocatalysts presenting in this talk can be also utilized in other electrochemical energy devices.

We have developed a one-step chemical vapor deposition synthesis process to grow carbon-encapsulated iron nanoparticles (CEINs) supported on CNTs, as efficient electrocatalysts for catalyzing hydrogen production through electrochemical hydrogen evolution reaction [1]. The structure of CEINs can be also electrochemically modified to make them active for catalyzing another half-reaction in water electrolysis devices which is oxygen evolution reaction [2].

I further introduce single-walled CNTs (SWNTs) as promising supports to stabilize individual atoms or subnano clusters of Pt in order to produce much cheaper Pt catalysts with almost a similar activity to that of bulk Pt for electrochemical hydrogen production. I show how Pt atoms can be strongly immobilized on pristine small diameter SWNTs, suggesting SWNTs as promising candidates for the synthesis of single-atom catalysts [3].

Finally, I remark the promising performance of multi-walled CNTs (MWNTs) for the covalent functionalization with organometallic compounds to produce stable materials for catalyzing reactions occurring under harsh oxidizing conditions. I show how MWNTs can be utilized to immobilize organometallic Ni complexes, in order to significantly improve their electrocatalytic activity toward oxygen evolution reaction as a critical reaction limiting the efficiency of water splitting devices [4].



[1] M. Tavakkoli, T. Kallio, O. Reynaud, A.G. Nasibulin, C. Johans, J. Sainio, H. Jiang, E.I. Kauppinen, K. Laasonen, Single-Shell Carbon-Encapsulated Iron Nanoparticles: Synthesis and High Electrocatalytic Activity for Hydrogen Evolution Reaction, *Angewandte Chemie International Edition*, 54 (2015) 4535-4538.

[2] M. Tavakkoli, T. Kallio, O. Reynaud, A.G. Nasibulin, J. Sainio, H. Jiang, E.I. Kauppinen, K. Laasonen, Maghemite nanoparticles decorated on carbon nanotubes as efficient electrocatalysts for the oxygen evolution reaction, *Journal of Materials Chemistry A*, 4 (2016) 5216-5222.

[3] M. Tavakkoli, N. Holmberg, R. Kronberg, H. Jiang, J. Sainio, E.I. Kauppinen, T. Kallio, K. Laasonen, Electrochemical Activation of Single-Walled Carbon Nanotubes with Pseudo-Atomic-Scale Platinum for the Hydrogen Evolution Reaction, *ACS Catalysis*, 7 (2017) 3121-3130.

[4] M. Tavakkoli, M. Nosek, J. Sainio, F. Davodi, T. Kallio, P.M. Joensuu, K. Laasonen, Functionalized Carbon Nanotubes with Ni(II) Bipyridine Complexes as Efficient Catalysts for the Alkaline Oxygen Evolution Reaction, *ACS Catalysis*, (2017) 8033-8041.

[5] F. Davodi, M. Tavakkoli, J. Lahtinen, T. Kallio, Straightforward synthesis of nitrogen-doped carbon nanotubes as highly active bifunctional electrocatalysts for full water splitting, *Journal of Catalysis*, 353 (2017) 19-27.

# Author index

- Ahmad, S., 53, 63, 68  
 Alekseeva, A. A., 57  
 Alexandrovich, E. V., 37  
 Arkhipov, V. E., 67, 89  
 Arnoldi, L., 48  
 Arutyunyan, N. R., 14  
 Asanov, I. P., 65  
 Aumanen, J., 58  
 Avramenko, M. V., 28  
  
 Baaziz, W., 87  
 Bai, Y., 5, 22  
 Banerjee, K., 3  
 Batrakov, K., 34  
 Bechstedt, F., 18  
 Bera, A., 84  
 Blum, I., 48  
 Borz, M., 48  
 Bukin, V. V., 35  
 Bulusheva, L. G., 64–66, 73, 81, 89, 90  
 Bychanok, D. S., 73  
  
 Callard, S., 6  
 Chang, L., 58  
 Chekhova, G. N., 81  
 Chen, Ang, 5, 8  
 Chen, C., 58  
 Chen, Ke, 55  
 Cheng, H., 50  
 Chiashi, S., 26  
 Cho, S., 32  
 Chuviln, A. L., 42  
 Conte, A. M., 18  
  
 Dai, Q., 7, 55  
 Dai, Y., 5, 8  
 Demongodin, P., 6  
 Ding, E., 53, 63, 68, 74  
 Dolmatov, T. V., 35  
 Downing, C. A., 9  
 Durnev, M. V., 10  
  
 Egorova, M. N., 36  
 Eremin, T. V., 19, 39  
 Eremina, V. A., 42, 52, 72  
 Ersen, O., 87  
 Evariste, L., 4  
 Ewels, C. P., 81  
  
 Fedorov, F. S., 57  
 Fedorovskaya, E. O., 65, 66  
 Fedoseeva, Yu. V., 64, 73  
 Flahaut, E., 4, 81, 90  
 Fu, Yao, 43  
 Fukuyama, H., 52  
  
 Galibert, A., 4  
 Ganichev, S. D., 10  
 Garacci, M., 4  
 Gauthier, L., 4  
 Ghimbeu, C. M., 4  
 Gilshteyn, E. P., 57  
 Gladush, Yu., 88  
 Glazov, M. M., 13  
 Gorodetskii, D. V., 89  
 Grassano, D., 18  
 Guan, F., 5, 8  
 Guo, Jia, 26  
 Guo, X., 7  
 Gurova, O. A., 67  
  
 Heo, C., 31  
 Hiltunen, V., 58  
 Hofer, C., 21  
 Houard, J., 48  
 Hu, Hai, 7  
 Hussain, A., 21, 53, 63, 68, 74  
  
 Iakovlev, V., 57, 88  
 Im, H. S., 31  
 Inoue, T., 26  
 Ismagilov, R. R., 49, 69, 70  
 Iurchekova, A. A., 66  
 Ivchenko, E. L., 17  
  
 Jelezko, F., 47  
 Jeon, Il, 56  
 Jeong, C., 31  
 Ji, B., 32  
 Jiang, Hua, 63, 74, 86  
 Jiang, Tao, 5  
 Johansson, A., 58  
  
 Kallio, T., 91  
 Kamynin, V. A., 35  
 Kaplas, T., 82, 84  
 Kato, Y. K., 54

- Kauppinen, E. I., 21, 42, 53, 56, 63, 68, 71, 74, 86, 91  
 Kawano, Y., 33  
 Kemiche, M., 6  
 Khan, T., 53  
 Kheday, A., 88  
 Kim, J., 12  
 Kim, T., 31  
 Koivistoinen, J., 58  
 Kondrashov, I., 75  
 Kondrashov, I. I., 42  
 Kopylova, D. S., 57, 88  
 Koroteev, V. O., 67  
 Koskinen, P., 58  
 Kotakoski, J., 21  
 Krivenkov, R. Yu., 41  
 Kudarenko, I. P., 70  
 Kurennya, A. G., 65  
 Kuzhir, P., 34, 82  
  
 Laasonen, K., 91  
 Lagier, L., 4  
 Laiho, P., 53, 63  
 Lapteva, L. L., 64  
 Larue, C., 4  
 Lee, J., 32  
 Lee, Y. Hee, 12, 32  
 Levshov, D. I., 28  
 Lhuillier, J., 6  
 Li, Chi, 55  
 Li, K., 33  
 Li, Yan, 26, 27  
 Li, Z., 55  
 Liao, Y., 63, 68, 74, 86  
 Line, C., 4  
 Lipsanen, H., 83  
 Liu, C., 50  
 Liu, K., 55, 85  
 Liu, M., 26  
 Liu, W., 11  
 Liu, X., 5, 8  
 Lobiak, E. V., 90  
 Loginov, A. B., 69  
 Luo, X., 43  
  
 Malykhin, S. A., 49, 70  
 Manninen, J. J., 58  
 Maruyama, S., 26, 56  
 Matsui, T., 52  
 Matsuo, Y., 56  
 Melinte, G., 87  
 Melkumov, M., 88  
 Mentel, K., 58  
 Meyer, J. C., 21  
 Mikheev, G. M., 37, 38, 41  
 Mikheev, K. G., 41  
 Mirzayev, R., 21  
  
 Mkrtchyan, A., 88  
 Mogileva, T. N., 41  
 Moldovan, S., 87  
 Monat, C., 6  
 Monazam, M., 21  
 Mottier, A., 4  
 Mouchet, F., 4  
 Musatov, D. A., 72  
 Mustonen, K., 21  
 Myllyperkiö, P., 58  
  
 Nasibulin, A. G., 57, 88, 91  
 Nunn, N., 41  
  
 Obratsov, A. N., 48, 49, 69, 70  
 Obratsov, P. A., 19, 35  
 Obratsova, E., 75  
 Obratsova, E. A., 14, 42, 49  
 Obratsova, E. D., 14, 19, 39, 42, 52, 72  
 Ochiai, Y., 33  
 Ohno, Y., 51, 53  
 Okhrimchuk, A. G., 35  
 Okotrub, A. V., 64–67, 73, 81, 89, 90  
 Orekhov, A. S., 42, 49  
  
 Pääkkönen, P., 84  
 Paddubskaya, A., 82  
 Paillet, M., 28  
 Pettersson, M., 58  
 Pham-Huu, C., 87  
 Pinakov, D. V., 81  
 Pinelli, E., 4  
 Plank, H., 10  
 Ponarina, M. V., 35  
 Popov, K. M., 66, 89  
 Portnoi, M. E., 9  
 Pulci, O., 18  
  
 Qiao, R., 55  
  
 Rajanna, P. M., 57  
 Remnev, G., 82  
 Rigutti, L., 48  
 Rojo-Romeo, P., 6  
 Romanenko, A. I., 73  
 Rybin, M., 75  
 Rybin, M. G., 35  
 Rybkovsky, D. V., 14  
  
 Sarrieu, C., 4  
 Saushin, A. S., 37, 38  
 Sauvajol, J. -L., 28  
 Sedelnikova, O. V., 73, 81  
 Semenova, A. A., 40  
 Seok, J., 32  
 Shen, B., 22  
 Shenderova, O. A., 41

- Shi, Lei, 5, 8  
Shlyakhova, E. V., 64  
Shubina, T. V., 19  
Smagulova, S. A., 36, 40  
Son, Y., 32  
Stepanov, A., 82  
Styapshin, V. M., 37, 38  
Sun, D., 50  
Sun, M., 33  
Sun, Z., 24, 55  
Susi, T., 21  
Suzuki, D., 33  
Svirko, Y. P., 38, 82  
Sysoev, V. I., 89, 90  
  
Taioli, S., 80  
Tan, P., 20  
Tarakanovsky, A. A., 35  
Tarasenko, S. A., 10  
Tavakkoli, M., 91  
Tian, Y., 43, 86  
Tian, Y. L., 53  
Tomskaya, A. E., 36  
Tonkikh, A. A., 42  
Tsai, H. C., 58  
Tsapenko, A. P., 57  
Tsebro, V. I., 42  
  
Velikanov, V. A., 19, 39  
Vella, A., 48  
Venturi, L., 48  
Verneuil, L., 4  
Vilquin, B., 6  
Vinokurov, P. V., 40  
Vostretsova, E. N., 67  
  
Wang, B., 50  
Wang, Bo, 8  
Wang, H., 43  
Wei, Fei, 22  
Wei, Nan, 53, 86  
Wood, T., 6  
Woon, Wei Yen, 58  
Wu, S., 5, 25  
  
Xia, C., 27  
Xia, Y., 5, 8  
Xiang, R., 26  
Xie, H., 22  
Xie, S., 71  
Xing, M., 43  
  
Yamashita, S., 23  
Yang, H., 32  
Yang, J., 27  
Yang, X., 7  
Yao, F., 55  
  
Yin, X., 43  
Yu, D., 55  
Yumoto, J., 59  
  
Zakharkina, E. I., 40  
Zhai, F., 55  
Zhang, D., 27  
Zhang, J., 22  
Zhang, Jin, 79  
Zhang, Q., 53, 63, 68, 71, 74, 86  
Zhang, Y., 5, 8  
Zheng, Y., 26  
Zhukhtova, I. V., 35  
Zhou, W., 71  
Zhou, Xu, 55  
Zhu, Z., 22  
Zi, J., 5, 8  
Zonov, R. G., 37